

Spring 2019

Manipulation of Noncovalent Interactions for the Synthesis and Use of Natural Product Synthons

Alison P. Hart
University of Southern Mississippi

Follow this and additional works at: <https://aquila.usm.edu/dissertations>

 Part of the [Medicinal-Pharmaceutical Chemistry Commons](#), and the [Organic Chemistry Commons](#)

Recommended Citation

Hart, Alison P., "Manipulation of Noncovalent Interactions for the Synthesis and Use of Natural Product Synthons" (2019). *Dissertations*. 1628.
<https://aquila.usm.edu/dissertations/1628>

This Dissertation is brought to you for free and open access by The Aquila Digital Community. It has been accepted for inclusion in Dissertations by an authorized administrator of The Aquila Digital Community. For more information, please contact Joshua.Cromwell@usm.edu.

MANIPULATION OF NONCOVALENT INTERACTIONS FOR THE
SYNTHESIS AND USE OF NATURAL PRODUCT SYNTHONS

by

Alison Patricia Hart

A Dissertation
Submitted to the Graduate School,
the College of Arts and Sciences
and the School of Mathematics and Natural Sciences
at The University of Southern Mississippi
in Partial Fulfillment of the Requirements
for the Degree of Doctor of Philosophy

Approved by:

Dr. Julie A. Pigza, Committee Chair
Dr. Matthew G. Donahue
Dr. Douglas S. Masterson
Dr. Gopinath Subramanian
Dr. J. Paige Buchanan

Dr. Julie A. Pigza
Committee Chair

Dr. Bernd Schroeder
Director of School

Dr. Karen S. Coats
Dean of the Graduate School

May 2019

COPYRIGHT BY

Alison Patricia Hart

2019

Published by the Graduate School



ABSTRACT

Natural products are widely used in the pharmaceutical industry, in agriculture, and as specialty chemicals. Methodology development focuses on optimizing the key organic reactions to access these natural products while trying to limit the overall number of synthetic steps. Key bond forming strategies are sought to provide new ways to address carbon-carbon or carbon-heteroatom bonds. The advancement of new asymmetric reactions to generate enantiopure products from achiral starting materials is a vital area of research. The objectives addressed in this dissertation include: 1) the development of a general reductive conversion of esters to ethers with a broad substrate scope accessing both aromatic and non-aromatic esters as well as accessing challenging α -substituted ethers, 2) the development of synthetic strategies for the preparation of trisubstituted biaryl quinoline scaffolds and subsequent derivatization to produce a library of heterocyclic substrates for the inhibition of HIV-1 integrase, and 3) the use of organocatalysis to explore new reactions and, through π - π and H- π bonding interactions between catalysts and substrates, to result in improved enantioselection as compared to transition-metal catalyzed reactions.

ACKNOWLEDGMENTS

I would like to acknowledge the individuals who have provided vital advice, guidance and support during the past five years. First, I would like to thank my academic advisor and research mentor, Dr. Julie Pigza for her profound investment in my development as a researcher and professional, as well as the many years of advice which has prepared me for the next stage in my career. Additionally, I would like to extend my appreciation to Dr. Matthew Donahue who has also invested his time and effort whenever I requested guidance or assistance. Also, I would like to thank Dr. Jacques Kessl for starting a collaborative project to make the work described in Chapter III possible. I would also like to thank Dr. Derek Patton and Dr. Sarah Morgan for their involvement with the NSF NRT INTERFACE for providing me with funding for my second year of graduate study, as well as awarding me with a NRT SEED research grant that funded the work presented in Chapter IV. Next, I would like to thank Dr. Stephen Wheeler and his research team for opening their lab to me during the summer of 2017 and 2018 training me to perform computational methods that were invaluable for my development in interdisciplinary research. Finally, I would like to thank my mother and father, Judi and Chris Hart as well as my sister Katie Hart for their love and support throughout my academic career. Your words of encouragement have enabled me to achieve every piece of work presented in this dissertation.

DEDICATION

This body of work is dedicated to my grandmother Dorothy M. Middlemiss, who always encouraged my enthusiasm towards academia. At the age of 84 she took in a 16-year-old girl so that she could obtain her A-levels in England. Her actions started me on the path to obtain my Ph.D. in Chemistry. Your love and support during one of the most crucial times in a young woman's life will never be forgotten. You are immensely missed, and I will always remember your love and devotion to your family.



TABLE OF CONTENTS

ABSTRACT	ii
ACKNOWLEDGMENTS	iii
DEDICATION	iv
LIST OF TABLES	xi
LIST OF FIGURES	xii
LIST OF SCHEMES.....	xiv
LIST OF ABBREVIATIONS.....	xvi
CHAPTER I – INTRODUCTION	1
1.1 Natural Product Isolation	1
1.2 Noncovalent Interactions in Organic Chemistry.....	2
CHAPTER II –Conservative Reduction of Esters to Ethers via an Oxonium Ion	
Intermediate	3
2.1 Introduction.....	3
2.1.1 The Importance of Ethers in Natural Product Synthesis.....	3
2.1.2 The General Synthesis of Ethers.....	4
2.1.3 Reduction of Esters	4
2.1.4 Historical Conversion of Esters to Ethers.....	6
2.1.5 Rychnovsky’s Work on the Conversion of Esters to Ethers.....	7
2.1.6 Interception of Oxonium Ion Intermediate by Nucleophiles	8

2.2 Research Hypothesis	9
2.3 Research Design and Methods.....	10
2.3.1 Ester Substrate Scope.....	10
2.3.2 In Situ Monitoring by ReactIR	11
2.3.3 Reduction of Non-Aromatic Esters to Ethers	12
2.3.4 Reduction of Aromatic Esters via One-Pot Reductive Method and Synthesis of α -Substituted Ethers.....	13
2.4 Results and Discussion	15
2.4.1 Synthesis of Esters to Fulfill Substrate Scope	15
2.4.2 Conversion of Esters to Acetals Using Non-Aromatic Esters	18
2.4.3 Conversion of Esters to Acetals Using Aromatic Esters	24
2.4.4 Reduction of the TMS-Protected Acetal to the Ether Product.....	27
2.4.5 Bifurcation Determination of TMS-Acetal Conversion to Ethers	34
2.4.6 One-Pot Conversion and Addition of Nucleophiles to the Oxonium Ion Intermediate	36
2.5 Summary and Conclusion	41
2.6 Experimental	42
2.6.1 General Methods	42
2.6.1.1 Experimental Techniques.....	42
2.6.1.2 Characterization	43

2.6.1.3 NMR Parameters.....	43
2.6.2 Synthesis of Intermediates	44
CHAPTER III - SYNTHESIS AND DERIVITIZATION OF QUINOLINE SCAFFOLDS FOR THE USE AS SMALL MOLECULE HIV-1 INTEGRASE INHIBITORS.....	
61	
3.1 Introduction.....	61
3.1.1 The Global Impact of HIV/AIDS – An Introduction to HIV-1	61
3.1.2 Current Modes of Treatment for HIV-1.....	62
3.1.3 HIV-1 Lifecycle and Mechanism of Attack.....	64
3.1.4 HIV-1 Inhibition of the Catalytic Core Domain	65
3.1.5 Quinoline Scaffolds as HIV-1 Inhibitors	66
3.1.6 Synthesis of the Quinoline Scaffold	67
3.2 Research Hypothesis	68
3.3 Research Design and Methods.....	69
3.3.1 Precursors for the Quinoline Scaffold.....	69
3.4 Results and Discussion	70
3.4.1 Forward Synthesis of the 4-Substituted Quinolines.....	70
3.4.2 Structural Elucidation of Biaryl Quinoline Scaffolds	76
3.4.3 Multimerization Assay	81
3.4.4 Structure Activity Relationships of Quinoline Substrates	82
3.5 Summary and Conclusion	86

3.6 Experimental	87
3.6.1 General Methods	87
3.6.1.1 Experimental Techniques.....	87
3.6.1.2 Characterization	88
3.6.1.3 NMR Parameters.....	89
3.6.2 Synthesis of Intermediates	89
3.6.2.1 General Procedure for the Preparation of 4-Aryl Quinolines (3.25-3.28):	89
3.6.2.2 General Procedure for Ethyl Ester Hydrolysis (3.21-3.24).....	101
3.6.2.3 Recombinant Proteins and IN Multimerization Assay.	110
CHAPTER IV – A Foray into Organocatalyzed Carbon-Carbon Bond Forming Reactions	
.....	112
4.1 Introduction.....	112
4.1.1 Catalysis in Chemistry	112
4.1.2 Rise of Organocatalysis	112
4.1.3 Hydrogen Bonding and Chiral Anion Organocatalysts	113
4.1.4 Structure Activity Relationships of Thiourea and Squaramide Subunits	115
4.2 Research Hypothesis.....	117
4.3 Research Design and Methods.....	118
4.3.1 Probing New Organocatalyzed Reactions	118
4.4 Results and Discussion	118

4.4.1 Reaction Screen for Enantioselective Additions.....	118
4.4.2 Enantioselective Addition of Masked Acyl Cyanides to β -Nitrostyrenes	121
4.4.2.1 Synthesis of β -Nitrostyrenes to Fulfill Substrate Scope	121
4.4.2.2 Enantioselective Addition of Masked Acyl Cyanide to β -Nitrostyrenes	123
4.4.2.3 Derivatization of Nitro-MAC Analogs	130
4.5 Summary and Conclusion	132
4.6 Experimental	133
4.6.1 General Methods	133
4.6.1.1 Experimental Techniques.....	133
4.6.1.2 Characterization	134
4.6.1.3 NMR Parameters.....	134
4.6.1.4 General Procedures for the Synthesis of β -Nitrostyrene Derivatives	135
4.6.1.5 General Procedure for the Synthesis of TBS protected Masked Acyl Cyanide	137
4.6.1.6 General Procedure for the Racemic Base Catalyzed Addition of Masked Acyl Cyanides to β -Nitrostyrenes.....	138
4.6.1.7 General Procedure for the Organocatalyzed addition of Masked Acyl Cyanides to β -Nitrostyrenes.....	139
CHAPTER V - CONCLUSION	149
APPENDIX A	152

APPENDIX B	153
APPENDIX C	154

LIST OF TABLES

Table 2.1 TMS trapping reagent screen where base additives used are indicated	20
Table 2.2 Substrate scope for the synthesis of TMS-protected non-aromatic acetals.....	22
Table 2.3 Solvent screen for the reduction of aromatic ester 2.5u	26
Table 2.4 Lewis acid and hydride screen for the conversion of TMS-protected acetals to ethers.	29
Table 2.5 Substrate scope for the reduction of TMS-protected acetals to ethers	31
Table 2.6 One-pot reduction of esters to ethers	38
Table 2.7 One-pot nucleophile addition for the synthesis of α -substituted ethers	40
Table 3.1 List of common HAART HIV-1 treatments	64
Table 3.2 Summary of phenyl-substituted biaryl quinolines yields	73
Table 3.3 Summary of heterocyclic and bicyclic biaryl quinoline yields	74
Table 3.4 ^1H and ^{13}C NMR Data of 3.21c and 3.23c	80
Table 3.5 SAR for substituted aromatic biaryl quinolines	83
Table 3.6 SAR data of heterocyclic biaryl quinoline substrates	86
Table 4.1 Reaction screening for enantioselective Michael addition to β -nitrostyrene.	120
Table 4.2 Organocatalyst Screen.....	125
Table 4.3 Solvent screen with organocatalyst 4.38f	127
Table 4.4 Enantioselective substrate scope	129
Table 4.5 Racemic synthesis of the MAC addition to β -nitrostyrenes	139

LIST OF FIGURES

Figure 2.1 A selection of natural products with ether functional groups	4
Figure 2.2 Classification of aromatic and non-aromatic esters.....	6
Figure 2.3 Substrate scope for the reduction of esters to ethers	10
Figure 2.4 React IR 3D plot	12
Figure 2.5 Comparison stabilized aromatic aluminate acetal intermediates.....	14
Figure 2.6 Substrate scope of esters synthesized by EDC/DCC or thionyl/oxalyl chloride	16
Figure 2.7 React IR surface of the reduction of non-aromatic ester 2.5a depicting the loss of the carbonyl stretch at 1728 cm^{-1}	18
Figure 2.8 ReactIR surface depicting the reduction of aromatic ester 2.5u by decrease of the carbonyl stretch at 1708 cm^{-1}	25
Figure 3.1 Map of HIV prevalence in adults ⁸¹	62
Figure 3.2 Common components in HAART HIV-1 treatments	63
Figure 3.3 HIV lifecycle ⁸⁷	65
Figure 3.4 Trisubstituted biaryl quinoline scaffolds with quinoline structure notation...	66
Figure 3.5 Ribbon representation of the IN CCD dimer with quinoline 3.7	67
Figure 3.6 ^1H and ^{13}C assignments with HMBC and COSY correlations for 3.21c	77
Figure 3.7 Comparison of 3.21c and 3.23c-1 and 3.23c-2 ^{13}C NMR spectral regions	78
Figure 3.8 ^1H and ^{13}C assignments with HMBC and COSY correlations for 3.23c	79
Figure 3.9 Carbon-fluorine couplings	81
Figure 3.10 Ribbon representation of 3.21c with the target IN binding pocket.	84
Figure 3.11 SAR trends of the phenyl substitutions	85

Figure 4.1 Some examples of organocatalysts	113
Figure 4.2 General structure of squaramide and thiourea organocatalysts	114
Figure 4.3 Competing conformations of thiourea catalysts	116
Figure 4.4 Comparison of pK_a values of common squaramide organocatalysts.....	117
Figure 4.5 Substrate scope of β -nitrostyrenes via aldehyde condensation with nitromethane	123
Figure 4.6 pK_a comparison of organocatalysts.....	124

LIST OF SCHEMES

Scheme 2.1 Considerations during ester reduction	5
Scheme 2.2 Rychnovsky's method for the reduction of esters to ethers	8
Scheme 2.3 Synthesis of α -substituted ethers by adding nucleophiles to the oxonium ion.	9
Scheme 2.4 Considerations for the reduction of esters to ethers.....	12
Scheme 2.5 Planned α -substituted ether scope with carbon nucleophiles	15
Scheme 2.6 Complications using DCC or EDC coupling procedures	17
Scheme 2.7 DIBAL-H reduction of aromatic ester 2.43	25
Scheme 2.8 Two routes for Lewis acid complexation with the protected acetal	27
Scheme 2.9 Proposed mechanism for the formation of the symmetric ether byproduct..	33
Scheme 2.10 Post transition state bifurcation to desired A and undesired B products	34
Scheme 2.11 One-pot reduction with aluminate acetal intermediate	37
Scheme 2.12 Proposed mechanism for the synthesis of secondary allyl alcohols.	39
Scheme 3.1 A variety of synthetic strategies for the synthesis of quinolines	68
Scheme 3.2 Synthetic analysis of quinoline scaffold 3.17	70
Scheme 3.3 Synthesis of trisubstituted biaryl quinolines	71
Scheme 3.4 Grignard addition with byproduct formation.....	71
Scheme 3.5 Synthesis of quinoline atropisomers, and their naming convention	75
Scheme 4.1 Examples of squaramide catalyzed organic reactions	115
Scheme 4.2 Enantioselective addition of MAC to π -bonds	121
Scheme 4.3 Synthesis of β -nitrostyrenes with byproduct formation.....	122
Scheme 4.4 Catalytic cycle for the addition of MAC to β -nitrostyrene.....	130

Scheme 4.5 Derivatization of β -nitrostyrenes to for desirable natural product synthons

..... 131

LIST OF ABBREVIATIONS

DIBAL-H	Diisobutylaluminum hydride
RED-AL	Sodium bis(2-methoxyethoxy) aluminum hydride
SDBBA	Sodium diisobutyl tert-butoxy aluminum hydride
LDBBA	Lithium diisobutyl tert-butoxy aluminum hydride
OAc	Acetate
TMS	Trimethylsilyl
TMS-Cl	Trimethylsilyl chloride
TMS-Imid	Trimethylsilyl imidazole
DCM	Dichloromethane
DCE	Dichloroethane
MTBE	Methyl tert-butyl ether
EtOAc	Ethyl acetate
MeOH	Methanol
DCC	N,N-Dicyclohexylcarbodiimide
EDC	1-Ethyl-3-(3-dimethylaminopropyl) carbodiimide
TMSOTf	Trimethylsilyl triflate
TEA	Triethylamine
THF	Tetrahydrofuran

DMF	Dimethylformamide
TMDS	1,1,3,3-Tetramethyldisilazane
PHMS	Polymethylhydrosiloxane
MsCl	Mesyl chloride
KOH	Potassium hydroxide
AIBN	Azobisisobutyronitrile
React IR	Mettler-Toledo React IR
TLC	Thin layer chromatography
IR	Infrared spectroscopy
FTIR	Fourier transform infrared spectroscopy
NMR	Nuclear magnetic resonance
R_f	Retention factor
MS	Mass spectrometry
HRMS	High resolution mass spectrometry
UV	Ultraviolet
HIV	Human Immunodeficiency Virus
LAV	Lymphadenopathy Associated Virus
HAART	Highly Active Antiretroviral Therapy
NRTI	Nucleoside Reverse Transcriptase Inhibitor
nNRTI	non-NRTI
IN	Integrase
INSTI	Integrase Strand Transfer Inhibitor
DVG	Dolutegravir

EVG	Elvitegravir
RGV	Raltegravir
AZT	azidothymidine
RNA	Ribonucleic acid
DNA	Deoxyribonucleic acid
PIC	Pre-integrated complex
vDNA	Viral deoxyribonucleic acid
NTD	n-Terminal domain
CCD	Catalytic core domain
CTD	c-Terminal domain
LEDGF	Lens epithelium-derived growth factor
IBD	Integrase binding domain
NBS	N-Bromosuccinimide
SAR	Structure activity relationship
DEPT	Distortionless enhancement by polarization transfer
COSY	Correlation spectroscopy
HSQC	Heteronuclear single-quantum correlation spectroscopy
HMBC	Heteronuclear multiple-bond correlation spectroscopy
HTRF	Homogeneous time resolved fluorescence
FRET	Förster resonance energy transfer

DFT	Density functional theory
MAC	Masked acyl cyanide
SOMO	Singly occupied molecular orbital
HBD	Hydrogen bond donating
SQ-OC	Squaramide organocatalyst
TBAF	Tetrabutylammonium fluoride
AARON	An Automated Reaction Optimizer for New Catalysts
TS	Transition state

CHAPTER I – INTRODUCTION

1.1 Natural Product Isolation

Herbal remedies have been used throughout human history to treat a variety of medical ailments encompassing acute, chronic, and terminal illnesses. The source of these herbal remedies typically originates from a small molecule that has been produced by its biological counterpart, otherwise known as a natural product. Medicinally, these natural products have been an extremely productive source for new therapeutics and provide continual inspiration for the development of even more potent treatments. However, isolation of these natural products is complicated two-fold. First, isolation of natural products can be extremely difficult and typically requires extensive isolation procedures, destroying the natural source in the process. Second, the percentage of the desired natural product within the plant is often extremely low. Natural product total synthesis enables chemists to provide the desired compound in abundant quantities and allows the synthesis of more potent derivatives.

Of specific interest in the vast library of natural products are the alkaloids. This subset contains extensive and structurally intriguing heterocyclic substructures encompassing fused, bicyclic, and spirocyclic ring systems. These heterocyclic moieties are of great synthetic interest to chemists as they pose challenges in forming carbon-carbon, carbon-oxygen, and carbon-nitrogen bonds within unique architectures. Although, total synthesis can increase the yield of the natural product versus the extraction from plants, there are often specific synthetic steps that are difficult and drastically decrease the total yield. New methodology must continually be developed to overcome these processes in natural product total synthesis.

1.2 Noncovalent Interactions in Organic Chemistry

Manipulation of noncovalent interactions is a key tool for organic chemists to enhance the desired product and/or introduce selectivity for one stereoisomer by reducing the energy barrier to access that product. While minute in impact alone, the collective of all these interactions ultimately dictate the outcome of the reaction. Some examples of noncovalent interactions in organic chemistry include: 1) transition-state manipulation of bifurcated reactions, 2) small molecule interactions within an enzyme binding site and, 3) organocatalyzed enantioselective C-C bond forming reactions. Noncovalent interactions include ionic or hydrogen bonding, Van der Waals forces, π -effects, as well as hydrophobic effects. An investigation of the contributions of noncovalent interactions present in asymmetric organocatalyzed reactions will enable the rational design of new catalysts.

The ultimate goal of this dissertation is to understand and exploit the subtle noncovalent interactions between two molecules to design effective and enantioselective bond forming methodologies for the synthesis of substructures found within natural products. In the following chapters, three individual projects will be presented. Each chapter presents a unique concept regarding noncovalent interactions and their use in organic methodology as it relates to natural product and synthon synthesis.

2.1 Introduction

2.1.1 The Importance of Ethers in Natural Product Synthesis

The development of a predictable method for the interconversion of common organic functional groups is highly sought in the field of organic chemistry. Ethers are a common functional group that can be found within a plethora of organic compounds and natural products. Some examples of ether containing natural products are non-small cell growth inhibitor trichoethers,¹ cholesterol blocking cyclic terpendoles,² and anti-inflammatory flavonolignans.³ Ethers can also be used as stabilizing agents for Grignard reagents and boron-containing compounds due to their capacity to form coordinate covalent bonds, as well as in crown ethers as phase transfer catalysts for increased solubility.⁴ Ethers are also found in cosmetics,⁵ as constituents in essential oils,⁶⁻⁷ and as organic solvents due to their generally inert properties such as tetrahydrofuran (THF), diethyl ether (Et₂O), and dioxane.

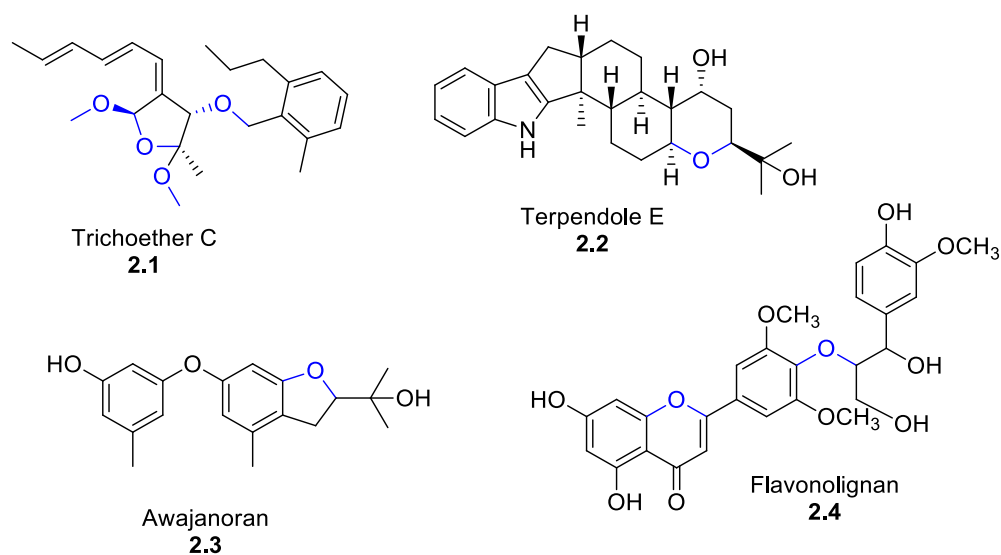


Figure 2.1 A selection of natural products with ether functional groups

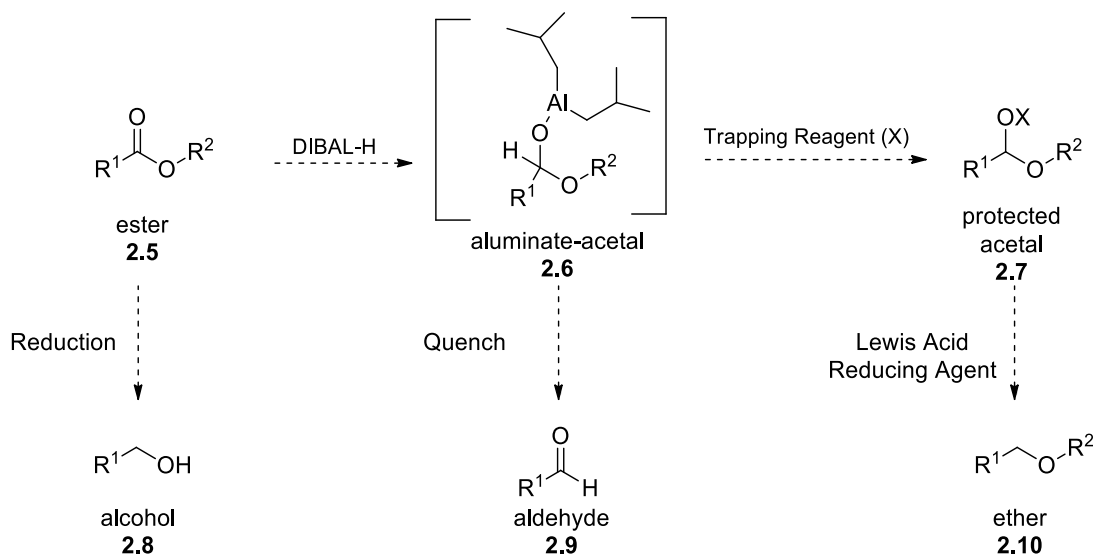
2.1.2 The General Synthesis of Ethers

The most common method to form ethers is the Williamson ether synthesis between alkyl halides and alkoxides.⁴ The reaction works best with primary alkyl halides and non-bulky alkoxides. Due to the S_N2 reaction mechanism, tertiary or bulky alkyl halides do not react at all or undergo an E2 elimination. Other general synthetic methods to form ethers include acid-catalyzed condensation of alcohols,⁸⁻¹² which is limited to forming symmetric ethers of primary alcohols, or alkoxymercuration-demercuration of alkenes,¹³ which uses toxic mercury compounds. None of these methods are stereoselective and often fail in reactions with increased alcohol substitution.

2.1.3 Reduction of Esters

Esters are fairly easy to synthesize by either using a coupling reaction with a carboxylic acid and alcohol¹⁴⁻¹⁵ or by converting the carboxylic acid to an acid chloride

before reaction with the alcohol.¹⁶ The standard ester reduction schemes and consideration are shown in Scheme 2.1. The typical loss of oxidation state moves from ester **2.5** to aldehyde **2.9** or alternatively from ester **2.5** directly to alcohol **2.8**. Early work with complete reduction of esters to primary alcohols began by reducing with either lithium aluminum hydride,¹⁷ sodium borohydride¹⁸, or a derivative¹⁹⁻²⁰ thereof in the presence of an expensive metal catalyst or a Lewis acid.²¹⁻²³ Recent literature has shown that ester **2.5** can be reduced to aldehyde **2.9** by using special reducing agents such as diisobutyl aluminium hydride (DIBAL-H),²⁴ or other similar aluminum reducing agents,²⁵⁻²⁸ which prevents over-reduction by forming an aluminate-acetal intermediate, such as **2.6**. Intermediate **2.6** is stable at cold temperatures and, after quenching with an aqueous solution, can form the desired aldehyde **2.9**. Hence this is a conservative reduction moving from an oxidation state of 3 (ester) to 2 (aldehyde).



Scheme 2.1 Considerations during ester reduction

2.1.4 Historical Conversion of Esters to Ethers

Alternatively, the formation of an ether from an ester can be envisioned by capturing the aluminate-acetal intermediate **2.6** with a trapping reagent. This would form the protected acetal **2.7** or ether **2.10**, the latter via a one-pot reduction. These applications have been most widely applied to non-aromatic esters in comparison to aromatic esters.²⁹⁻³⁴ Aromatic esters have the carbonyl group in conjugation with the aromatic ring, making it more difficult for the initial reduction and less stable during the intermediate stages, leading to low conversions or more side products (Figure 2.2).

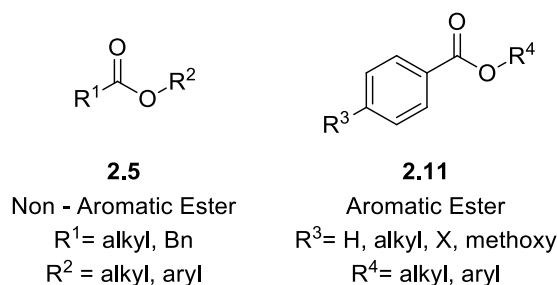


Figure 2.2 Classification of aromatic and non-aromatic esters.

Early attempts for ester to ether conversion were completed by Pettit in the 1960s.³⁵⁻³⁷ His group focused on reacting steroid natural products with $\text{BF}_3 \cdot \text{OEt}_2$, then adding the solution to lithium aluminum hydride (LAH) in an ice bath before refluxing to achieve moderate to low yields. An advancement in the conversion of esters to ethers utilized Lawesson's reagent to convert lactones to thiolactones, and then reduce the carbon-sulfur bond in a second step.³⁸ This was initially done by Baxter utilizing Raney nickel as the reducing agent,²⁹ followed by Nicolaou and Jang who both used a combination of diphenylsilane with an organotin hydride to form a tin-protected thioacetal, which then went through a radical cleavage using AIBN to produce the

ether.^{34, 39-40} In these examples, cyclic thiolactams were typically used but in some instances, non-aromatic and more importantly aromatic thioesters were also present.

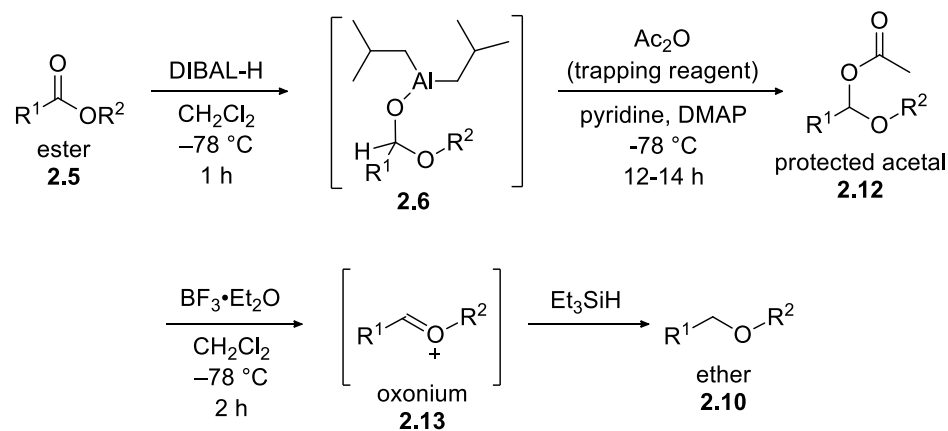
Another area of ester to ether conversion focuses on the use of transition metal or Lewis acid catalysts. Beller et al. utilized 10% mol loading of a $\text{Fe}_3(\text{CO})_{12}$ catalyst in the presence of tetramethyldisiloxane (TMDS) for the conversion of non-aromatic esters and lactones to their respective ether counterparts.³² The Buchwald group used a titanocene diphenoxide and difluoride catalyst in the presence of polymethylhydrosiloxane (PMHS) to convert five- and six-membered lactones to cyclic ethers in moderate to excellent yields.³¹ Sakai and coworkers also used PMHS with an indium tribromide catalyst for a one pot conversion of carboxylic acids and alcohols to ethers, however all instances were using non-aromatic with moderate to good yields.^{33, 41} Additionally, silanes in the presence of a Lewis acid were also used in the conversion of esters to ethers. Tsurugi developed two methods, the first of which used Et_3SiH in the presence of NiCl_3 and the second used Cl_3SiH . Both reactions were exposed to γ -radiation to produce only non-aromatic ethers in good to excellent yields.⁴²

Homma and Pagenkopf both created a 'super' Lewis acid by initially reacting TMSOTf with either TiCl_4 or $\text{BF}_3 \cdot \text{OEt}_2$, respectively, before adding Et_3SiH .⁴³⁻⁴⁴ However in both instances, only non-aromatic esters were used and the ethers were obtained in low to moderate yields due to over-reduction to the alcohol or the formation of silyl ether.

2.1.5 Rychnovsky's Work on the Conversion of Esters to Ethers

Current research has focused on the reduction of ester **2.5** to ether **2.10** utilizing aluminate-acetal intermediate **2.6** (Scheme 2.2).⁴⁵ At the forefront is the work done by the

Rychnovsky group.⁴⁶⁻⁴⁹ His group established a two-step protocol for ester to ether conversion in which the intermediate is trapped as an acetoxy-protected acetal **2.12**. This intermediate is prepared by the addition of DIBAL to the ester at -78 °C to initially form the aluminate **2.6** (Scheme 2). This intermediate (**2.6**) is stable at -78 °C, but if it is quenched with an aqueous workup, it will form aldehyde **2.9**. To prevent this, **2.6** can be trapped *in situ* with acetic anhydride in the presence of pyridine and DMAP to form acetal **2.12**.⁴⁶ This stable acetal can be isolated and purified by chromatography. Alternatively, if it is exposed to a Lewis acid and hydride source, the desired ether **2.10** is obtained via oxonium ion **2.13**. Although excellent yields are obtained, these reactions take a combined 16-20 hours at cold temperatures and have not been shown to work with aromatic esters or α,β -unsaturated esters.

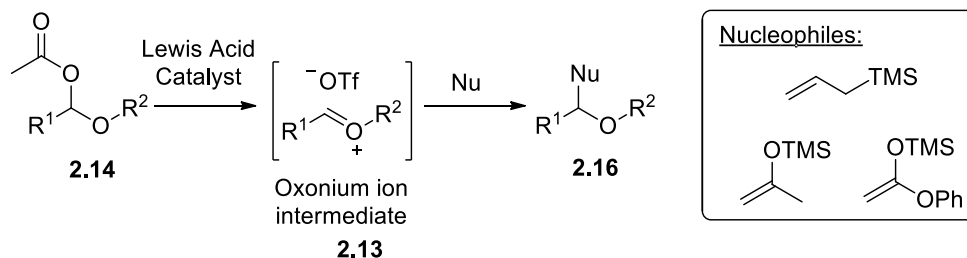


Scheme 2.2 Rychnovsky's method for the reduction of esters to ethers

2.1.6 Interception of Oxonium Ion Intermediate by Nucleophiles

Alternatively, oxonium ion **2.13** can be intercepted with other nucleophiles to form α -substituted ethers in isochroman acetals (Scheme 2.3). Jacobsen utilized thiourea organocatalysts to add vinyl nucleophiles enantioselectively in good to excellent yields.⁵⁰⁻

⁵¹ Schaus⁵²⁻⁵³ and Rueping⁵⁴⁻⁵⁵ both exploited the use of a catalytic Brønsted/Lewis acid system to add vinyl boronates and aldehydes, respectively. A copper-catalyzed addition of alkynes in the presence of TMSOTf was also presented by Watson in good to excellent yields.⁵⁶ Rychnovsky also intercepted the oxonium ion of acetals with nucleophiles including the addition allyl silanes, silyl enol ethers, and silyl ketene acetals.⁴⁹



Scheme 2.3 Synthesis of α -substituted ethers by adding nucleophiles to the oxonium ion.

2.2 Research Hypothesis

Through the use of different trapping reagents and monitoring by ReactIR, the time to form the acetal can be decreased, thereby shortening the overall reaction time. Through a one pot reaction with careful selection of reagents and timing, the reduction of aromatic esters can be achieved. Additionally, the oxonium ion formed by these reductive methods can be intercepted by a range of nucleophiles to form α -substituted ethers, a class of compounds that is not easy to synthesize by conventional methods such as the Williamson ether synthesis.

2.3 Research Design and Methods

2.3.1 Ester Substrate Scope

To develop a general and tunable method for the conversion of esters to ethers, a broad spectrum of esters must be synthesized in good yield using known methods.

Aromatic and non-aromatic esters with both electron donating and withdrawing groups will be synthesized (Figure 3). Other general types of esters will include cyclic esters, those with branching on either the carbonyl or alcohol side, or various substituents that are considered sensitive to the reaction conditions, such as a halide or amine group.

Ideally, the goal is to enable chemists to be able to match their substrates with the proposed ester scope and to have a predictable reductive method for the conversion of esters to either acetals or ethers.

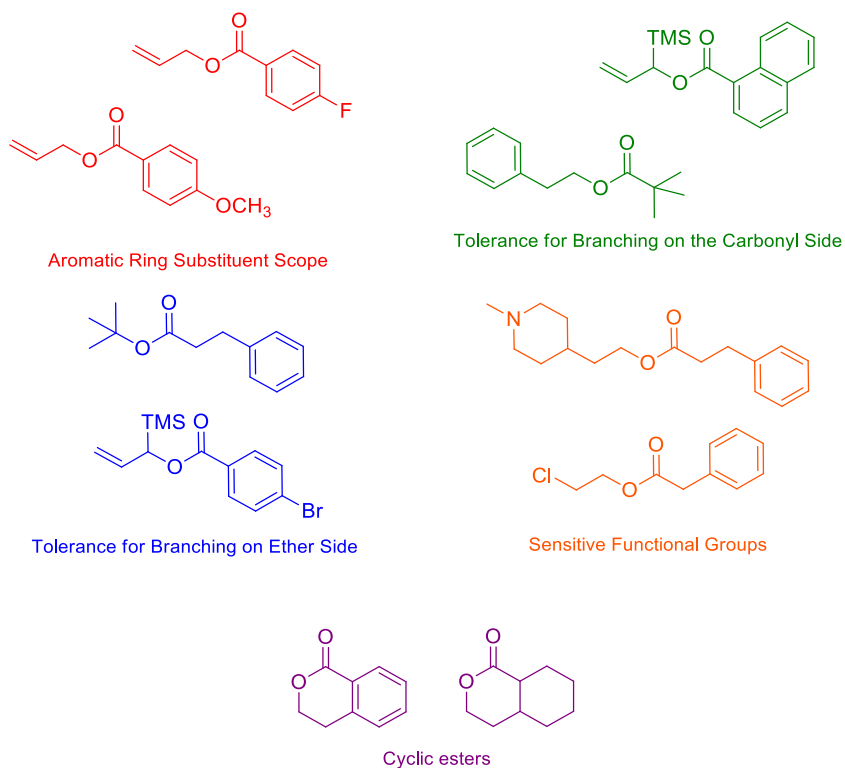


Figure 2.3 Substrate scope for the reduction of esters to ethers

2.3.2 In Situ Monitoring by ReactIR

React IR, *in situ* infrared spectroscopy, is ideal for monitoring the interconversion of functional groups during a reaction.⁵⁷ This technique was found to be better suited for cold temperature reactions compared to thin layer chromatography (TLC).⁵⁸ Reactive intermediates will likely be unstable in the TLC spotter and will break down on the TLC plate, whereas this will not occur with React IR. It is also capable of identifying any side products that are formed in the reaction as they will have their own distinct peaks.

Specifically, React IR is an essential tool for monitoring the conversion of an ester to acetal because it can monitor the loss of the carbonyl peak without the need for TLC. An IR spectrum is produced every minute and stacked to create a three-dimensional surface monitoring time, wavenumber, and absorbance units that accurately denotes the progress of a reaction. Due to this capability, React IR enables the determination of exact reaction times and the timing necessary for the addition of each reagent, therefore indicating the shortest possible reaction times. To do this, the carbonyl peak of the ester at $\sim 1720\text{ cm}^{-1}$ will be monitored and then trapping reagents will be added when full reduction of the ester is observed. Also, because React IR monitors the loss of the carbonyl peak, it can also aid in determining the precise molar equivalents of reducing agent necessary for each individual ester substrate. React IR can also monitor the formation of any possible side products formed, such as aldehyde (C-H stretch at 2700 cm^{-1}) or alcohol (O-H stretch at 3200 cm^{-1}).

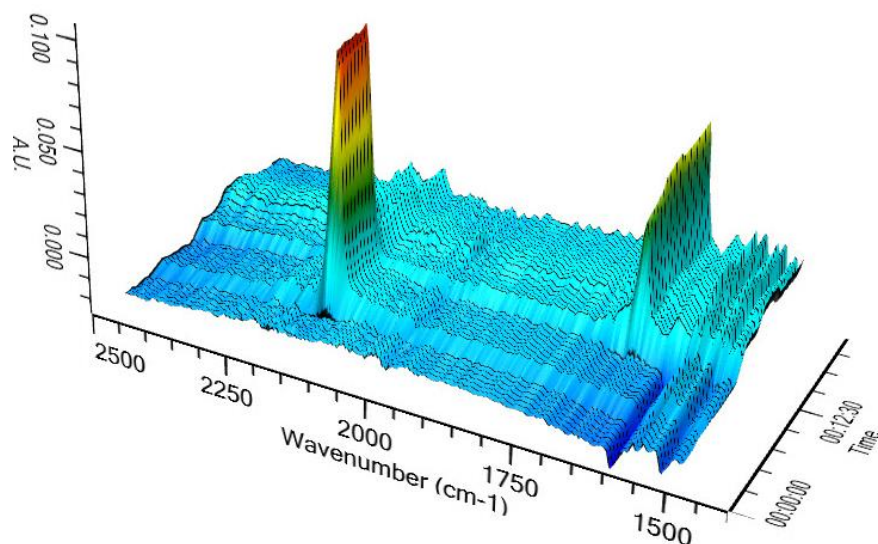
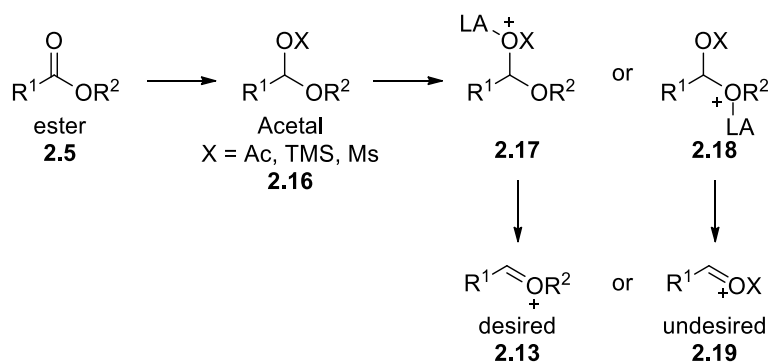


Figure 2.4 React IR 3D plot

2.3.3 Reduction of Non-Aromatic Esters to Ethers

The reduction of non-aromatic esters to ethers can be achieved through a two-step pathway. First, reduction of the ester will be screened using mild reducing agents such as DIBAL-H to form an aluminate acetal intermediate. This intermediate (**2.16**) can then be stabilized through the use of trapping agents such as silyl derivatives or sulfonylating reagents with the goal of reducing overall reaction times and potentially increasing reaction temperatures.⁵⁹



Scheme 2.4 Considerations for the reduction of esters to ethers

The reduction of the protected acetal to the ether can potentially have problems with the Lewis acid complexing at two different positions (Scheme 2.4). If the reaction proceeds as desired, the Lewis acid will complex with the acetal oxygen forming oxonium ion **2.13** which can be intercepted with a hydride to form the desired ether. Alternatively, if the Lewis acid complexes with the ether oxygen, it will form the undesired oxonium ion **2.19** resulting in the formation of byproducts. Ideally, the trapping reagent that is chosen will be electron donating so that the acetal oxygen is more susceptible to Lewis acid binding versus the ether oxygen.

2.3.4 Reduction of Aromatic Esters via One-Pot Reductive Method and Synthesis of α -Substituted Ethers

One of the goals of this project is to successfully reduce aromatic esters to ethers. This is more complex due to the conjugation of the aromatic ring with the carbonyl, making the aluminate acetal unstable and more prone to over-reduction. One instance where aromatic esters have been successfully converted to their ether counterparts using a hydride source is the work done by Batey and coworkers.⁶⁰ His group employed Rychnovsky's method (DIBAL then Ac₂O, DMAP, pyr) to produce the acetoxy-protected acetal using a picolinate ester. The nitrogen in the pyridine ring complexes to and stabilizes the aluminate-acetal intermediate, preventing it from breaking down and enabling the acetoxy-protected acetal to form (Figure 2.5). While the picolinate ester provides the desired stabilization, it also limits the ester substrate scope considerably. Alternatively, SDBBA or LDBBA have been used in this fashion. These reagents can form

a six-membered transition state after the initial reduction of the carbonyl group, resulting in the stabilized aluminate acetal **2.21** (Figure 2.5).

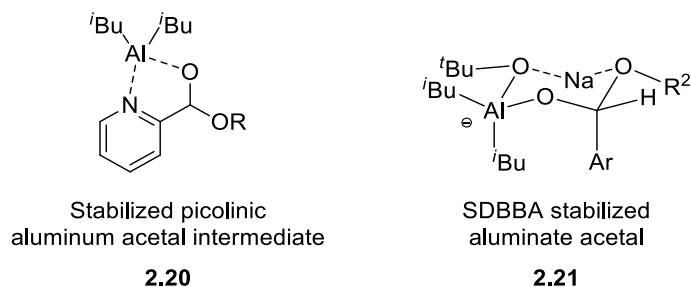


Figure 2.5 Comparison stabilized aromatic aluminate acetal intermediates

With the development of a one pot procedure, the synthesis of α -substituted ethers is an additional goal for this project by intercepting oxonium ion **2.13** with a carbon nucleophile. Although the synthesis of α -substituted ethers has been demonstrated in the literature by capturing the oxonium ion with nucleophiles, it has not been shown via a one-pot variant starting from an ester. While diastereoselective nucleophilic addition has been achieved using either a chiral auxiliary or substrate control via a cyclic oxonium, it has not been accomplished in an enantioselective manner with acyclic ethers.

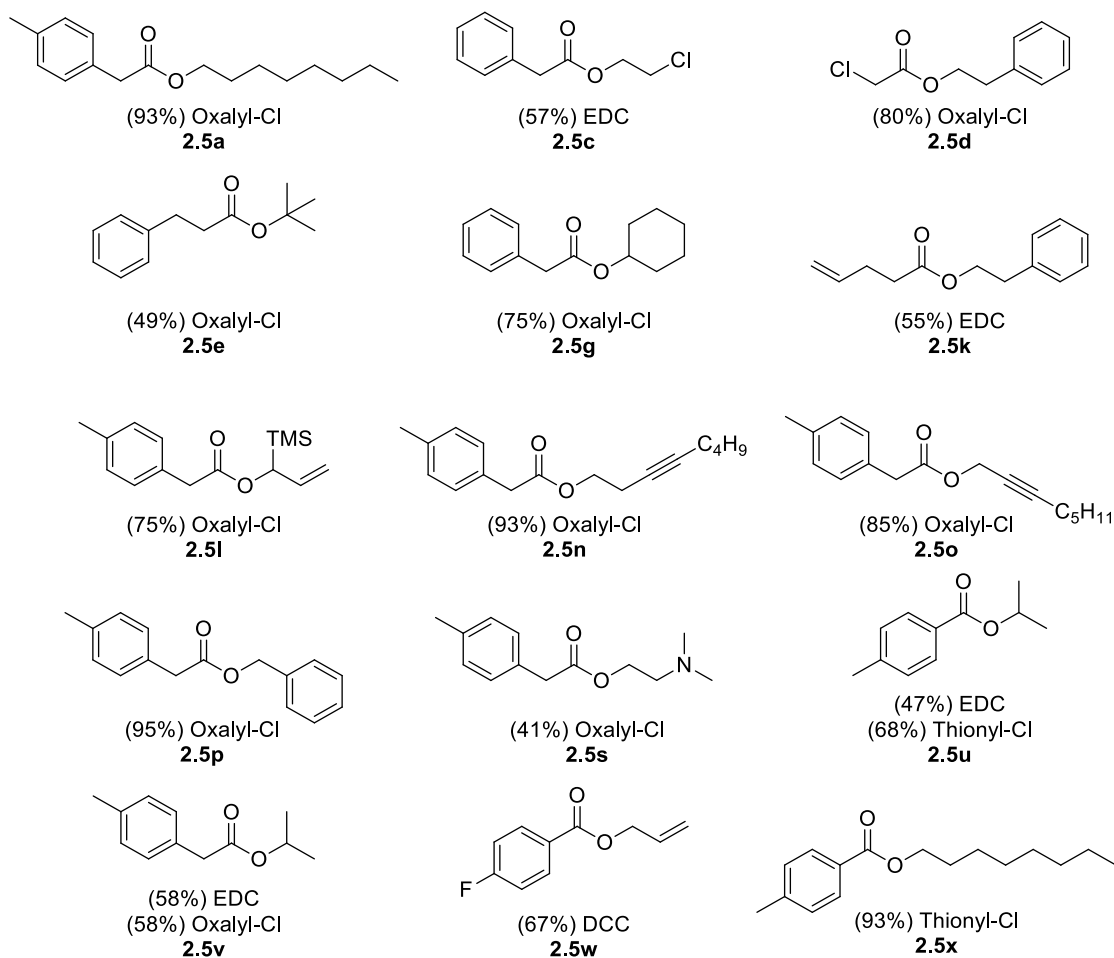
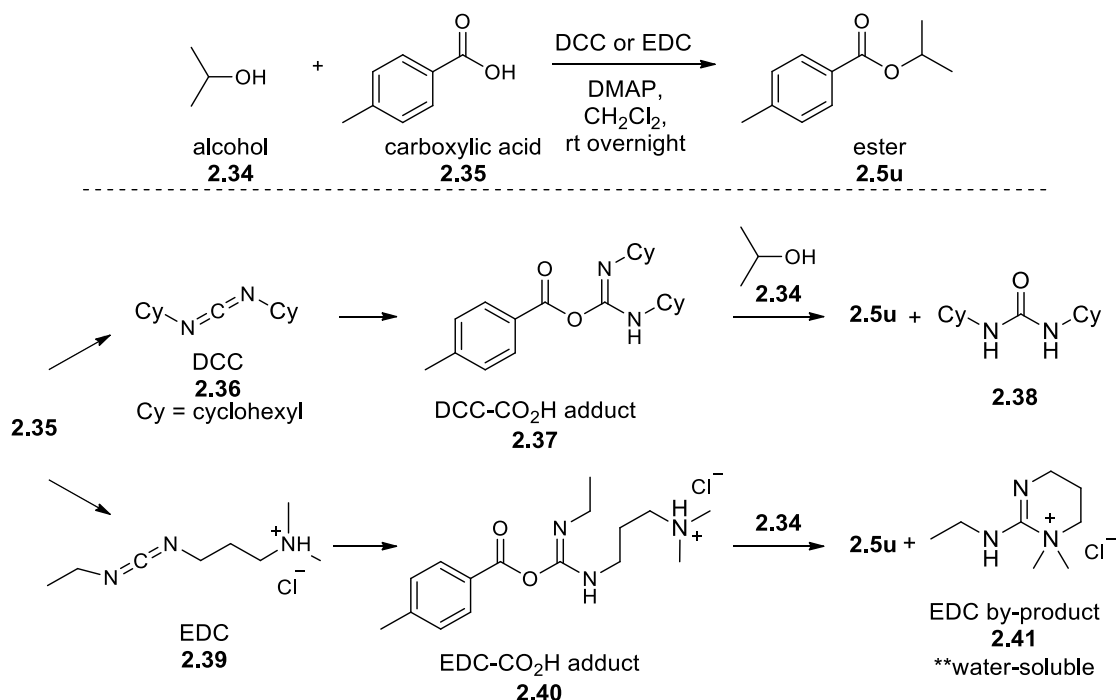


Figure 2.6 Substrate scope of esters synthesized by EDC/DCC or thionyl/oxalyl chloride

The low yields when using DCC (**2.36**) could be attributed to the production of the solid urea by-product which presented difficulties during filtration and purification. The benefit of EDC (**2.39**) is that the urea by-product is water soluble, however, this did not result in increased yields. Both methods rely on the formation of an adduct between the coupling reagent and the carboxylic acid (**2.37** and **2.40**, Scheme 6). This is known as the active ester intermediate and it is much more reactive than the initial carboxylic acid. This intermediate is then intercepted by the alcohol (**2.34**), which forms the urea by-product (**2.38** with DCC and **2.41** with EDC) and the desired ester product **2.5u**. Both

reactions are slow and generally require overnight stirring and can be low yielding. The EDC by-product **2.41** also dissolves into the water layer, which can be seen by TLC as it is UV active. Also, by removing an aliquot of the reaction before quenching, the DCC **2.37** and EDC **2.40** adducts can be observed by ^1H NMR. Because the adducts do not fully convert to product in reasonable times, this likely resulted in the low yields that were observed.



Scheme 2.6 Complications using DCC or EDC coupling procedures

Much higher yields were achieved on average using the acid chloride method, producing most esters in the mid 80% range. The acid chloride is produced by oxalyl chloride after stirring for 1 hour, followed by removal of volatiles and then the addition of the alcohol and amine base and stirring for an additional hour to generate the ester. Use of thionyl chloride generally required refluxing at 40 °C for 1-3 hours and was used to make the aromatic carboxylic acids. Esters **2.5u**, **2.5w**, and **2.5x** were the aromatic

substrates synthesized, and esters **2.5a-2.5s** and **2.5v** show an expanded substrate scope for non-aromatic esters. Esters **2.5e-g** contain bulky groups in either the carbonyl or ether side. Other esters including **2.5c-d** and **2.5s** contain sensitive functional group such as halogens or tertiary amines, which will help to establish the parameters for the substrate scope. All products have been fully characterized by ^1H and ^{13}C NMR, as well as IR.

2.4.2 Conversion of Esters to Acetals Using Non-Aromatic Esters

The first step in the reduction of esters to ethers is to form the protected acetal intermediate **2.7**. ReactIR was chosen to follow the loss of the carbonyl peak found at 1728 cm^{-1} as these reactions are run at very cold temperatures to prevent the over reduction to alcohol (Figure 2.7). One non-aromatic ester (**2.5a**) was chosen for screening the reaction progress which included the UV active tolyl-ring and a long carbon chain for increased weight preventing evaporation of acetal and ether products.

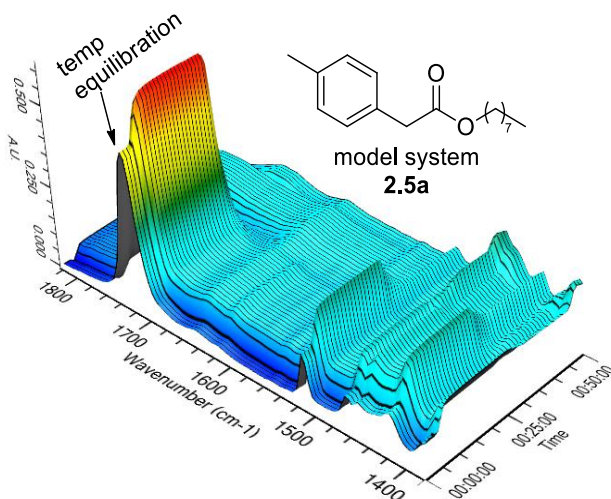


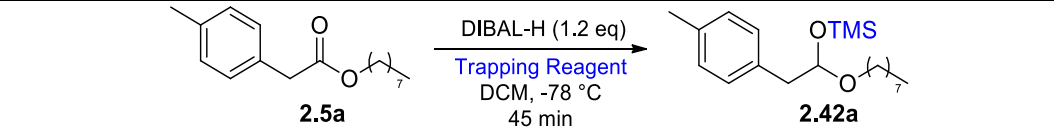
Figure 2.7 React IR surface of the reduction of non-aromatic ester **2.5a** depicting the loss of the carbonyl stretch at 1728 cm^{-1}

The intensity of the absorbance of the carbonyl peak, recorded in absorbance units (A.U.) decreased from 0.52 to 0.02 during the addition of DIBAL-H over a 10 minute period. DIBAL-H was added slowly at a rate of one drop every 5 seconds to prevent an increase in temperature of the reaction and subsequent over-reduction. This also ensured that the ReactIR would be able to gain clean spectra without error. It was found that complete reduction of ester **2.5a** to the corresponding aluminum acetal intermediate occurred within the 10 minutes that it took to add DIBAL-H dropwise. Previous work by the Rychnovsky group, whom did not use ReactIR monitoring, allowed the reductions to stir for at least 30-45 minutes.⁴⁶ ReactIR also allowed determination of the number of equivalents of DIBAL-H required to fully reduce the ester (for **2.5a** it was found to be 1.2 eq). This was verified by taking ¹H NMR of the crude reaction after quenching and extraction.

With the reduction determined, the next step was to screen several trimethylsilyl (TMS) reagents in which to capture the aluminate intermediate as the protected acetal **2.42a**. Table 2.1 shows a range of TMS-trapping reagents used in the screening process as well as any additives that might have aided in the trapping of the acetal intermediate.⁵⁹ TMSOTf was chosen due to the good triflate leaving group, however as shown in Table 2.1, no acetal was produced. TMSCl along with an amine base was chosen due to its cost efficiency and the highest yielding example was in the presence of N-methylimidazole (69%). The presence of the amine base was to prevent the formation of HCl. TMS-imidazole (TMS-imid) proved to be the ideal choice and additional base was not needed. Using three equivalents of TMS-imid at -78 °C provided protected acetal **2.42a** with 98% conversion. The acetal intermediate could be produced at lower equivalents of TMS-imid

(1.5, 2.0, and 2.5 of TMS-imid.), however, the crude NMR was not as clean and so required purification before moving onto the second step. A similar yield was achieved at a warmer temperature of -40 °C (94%) which proves promising for industrial applications.

Table 2.1 TMS trapping reagent screen where base additives used are indicated

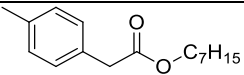
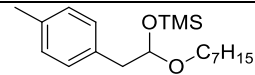
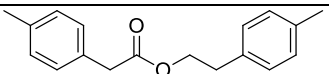
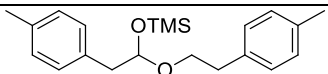
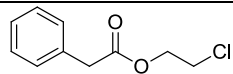
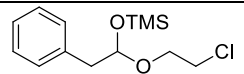
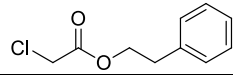
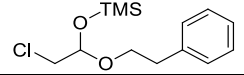
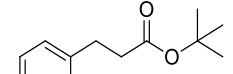
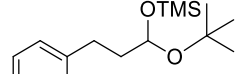
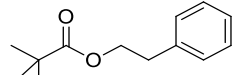
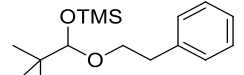
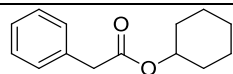
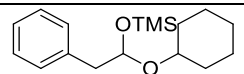
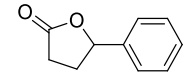
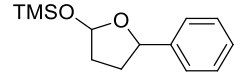
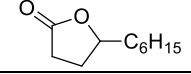
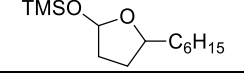
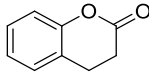
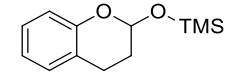
				
Entry	Trapping Reagent	Base	Temperature (°C)	Crude Yield (%)
1	TMSOTf	-----	-78	-----
2	TMSCl	pyridine	-78	20
3	TMSCl	N-Me-imid	-78	69
4	TMS-imid	-----	-78	98
5	TMS-imid	-----	-40	94
6	TMS-imid	-----	0	32

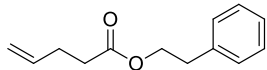
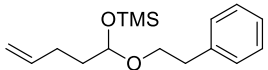
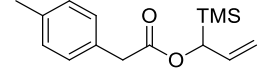
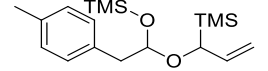
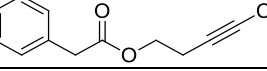
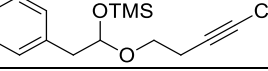
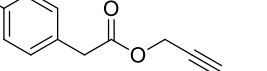
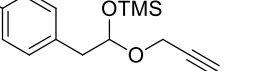
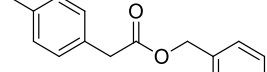
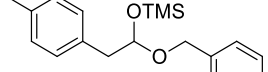
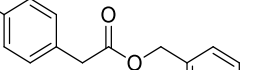
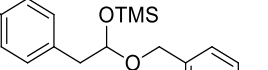
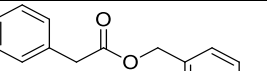
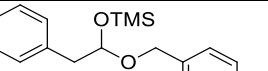
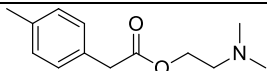
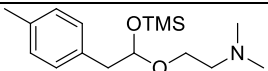
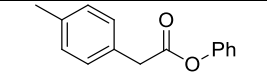
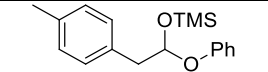
When compared to the Rychnovsky method, which uses acetic anhydride as the trapping reagent, TMS-imid significantly decreases the time required to form the protected acetal from 12-14 hours to 35 min. Shorter reaction times are very desirable since the reaction is carried out at -78 °C using dry ice and acetone and requires either more expensive chillers to maintain the temperature or refilling the dry ice bath every few hours. Additionally, while column chromatography could be performed on TMS-acetal **2.42a**, it was more advantageous to carry the material through to the desired ether product without further purification, highlighting an additional benefit of TMS-imid.

An extensive substrate scope was conducted by using ReactIR to monitor the reduction of the ester and to determine the number of equivalencies of DIBAL-H necessary to achieve reduction to the acetal (Table 2.2). The scope includes esters with

alkyl groups (**2.5a** and **2.5b**), halogens situated on either side of the ester (**2.5c** and **2.5d**), a variety of bulky groups (**2.5e-g**), lactones (**2.5h-j**), as well as esters containing alkenes, alkynes, and benzyl substitutions on the ether side (**2.5k-r**). General observations of the reduction were noted regarding the functional groups within the scope. Largely, esters containing halogens (entry 3), or bulky side groups on either side of the ester (entry 5 - 7), required a larger amount of the reducing agent. Additionally, the presence of a tertiary amine also required an additional excess of DIBAL-H while also decreasing the overall yield (entry 19). This is most likely due to the halogen (entry 3) and nitrogen (entry 19) interacting with DIBAL-H, requiring the increased equivalencies. Additionally, the bulkiness at the carbonyl group can obstruct hydride delivery and so additional DIBAL was necessary. Otherwise, all substrates converted to the TMS-acetal in excellent yields (81-99%) excluding entry 12 bearing the oxyallyl silane moiety (65%), entry 19 containing the nitrogen substituent (27%), and entry 20 containing a phenoxy group (no acetal observed).

Table 2.2 Substrate scope for the synthesis of TMS-protected non-aromatic acetals

$ \begin{array}{c} \text{DIBAL} \\ \text{TMS-imid 3 eq} \\ \text{DCM (1M)} \\ 45 \text{ min, } -78^\circ\text{C} \end{array} \begin{array}{c} \text{R}^1\text{CH}_2\text{C(=O)OR}^2 \\ \text{2.5} \end{array} \longrightarrow \begin{array}{c} \text{R}^1\text{CH}_2\text{C(OTMS)OR}^2 \\ \text{2.42} \end{array} $						
Entry	Substrate	Ester	DIBAL (eq)	Crude (%)	Product	Acetal
1	2.5a		1.2	98	2.42a	
2	2.5b		1.2	98	2.42b	
3	2.5c		1.6	81	2.42c	
4	2.5d		1.2	99	2.42d	
5	2.5e		1.7	97	2.42e	
6	2.5f		1.6	89	2.42f	
7	2.5g		1.5	91	2.42g	
8	2.5h		1.2	98	2.42h	
9	2.5i		1.2	98	2.42i	
10	2.5j		1.1	85	2.42j	

11	2.5k		1.2	95	2.42k	
12	2.5l		1.2	65	2.42l	
14	2.5m		1.2	92	2.42m	
15	2.5n		1.2	91	2.42n	
16	2.5o		1.2	93	2.42o	
17	2.5p		1.2	98	2.42p	
18	2.5q		1.2	95	2.42q	
19	2.5r		1.6	27	2.42r	
20	2.5s		1.2	0	2.42s	

2.4.3 Conversion of Esters to Acetals Using Aromatic Esters

A second goal is to apply this reductive conversion to aromatic esters which has not been demonstrated previously by the Rychnovsky group. Only two cases could be found that demonstrated success with aromatic esters. The first was by Nicolaou, who used the foul smelling Lawesson's reagent to convert the ester to a thioester in the first step.⁴⁰ The second was by Batey who utilized Rychnovsky's method with a stabilized picolinic ester.⁶¹

The conjugation with the aromatic ring weakens the π -bond in aromatic esters. While this allows for an easier reduction of aromatic esters to alcohols using nucleophilic hydride reagents such as DIBAL-H, it is also much more difficult to stop at the acetal intermediate. As with the non-aromatic ester model system, the aromatic ester **2.5u** reduction was first monitored by ReactIR and can be seen in Figure 2.8. The carbonyl peak is observed at 1708 cm^{-1} . The decrease in wavenumbers as compared to a non-aromatic ester (1728 cm^{-1}) can be attributed to the carbonyl group conjugation with the aromatic ring causing electrons to delocalize and decrease the double bond character.

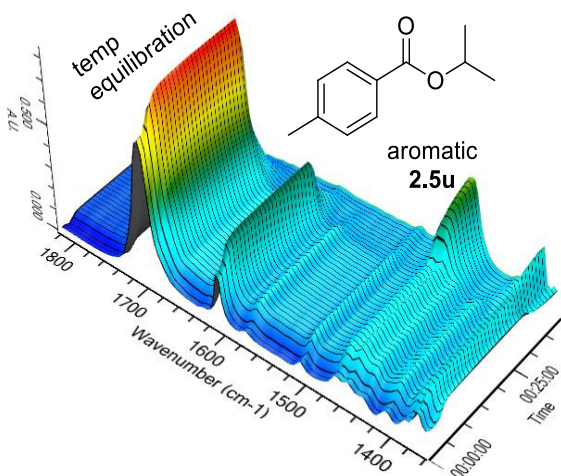
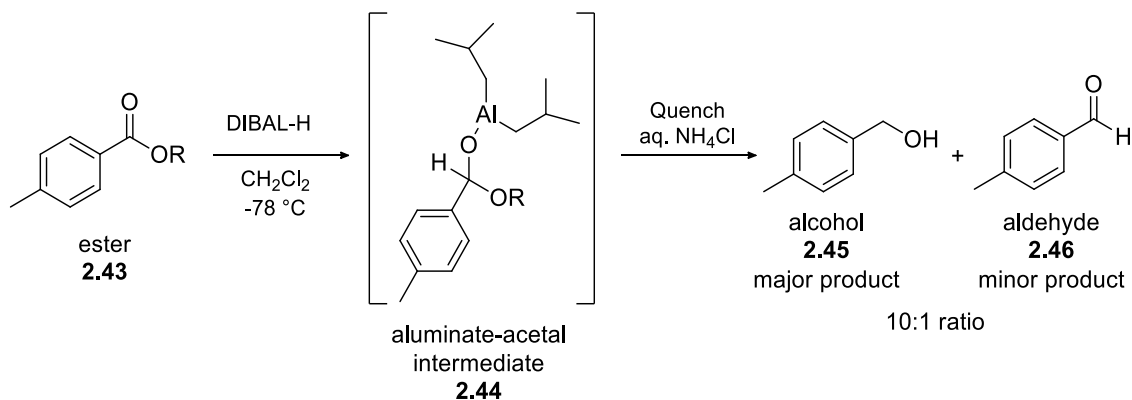


Figure 2.8 ReactIR surface depicting the reduction of aromatic ester **2.5u** by decrease of the carbonyl stretch at 1708 cm^{-1} .

It was determined by ReactIR that the aromatic ester could be reduced in just 10 minutes, same as with the non-aromatic ester. However, the aromatic ester required 2 equivalents of DIBAL-H while the non-aromatic ester required only 1.2 equivalents. When crude products were observed by ^1H NMR, only alcohol (over-reduction) and aldehyde (desired single reduction) were observed. The aromatic aluminate intermediate **2.44** is considerably less stable and more susceptible to over-reduce to alcohol **2.45**.



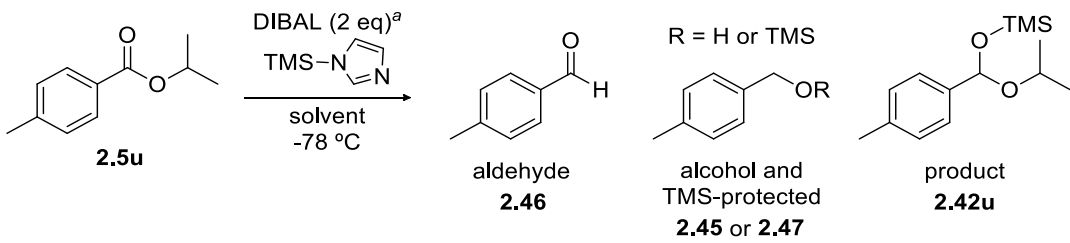
Scheme 2.7 DIBAL-H reduction of aromatic ester **2.43**.

To be able to capture the protected acetal, TMS-imid was again chosen using the same conditions as for the non-aromatic ester substrate. The standard method of DIBAL-H then TMS-imid did not provide any of the desired protected acetal product. Other iterations, such as having TMS-imid present before adding DIBAL, prevented complete reduction of the ester. It was found that to form the protected acetal product, a unique addition method was applied in which DIBAL-H and TMS-imid were added in alternating increments. First, 1.2 equivalents of DIBAL-H was added followed by 2.0 equivalents of TMS-imid, then the remaining 0.8 equivalents of DIBAL-H was added followed by the remaining 1.0 equivalents of TMS-imid. This addition process allowed

for the formation of a small amount of the protected aromatic acetal **2.42u** as identified by crude ^1H NMR (11-16%, Table 2.3).

The ratios of products were calculated from ^1H NMR based on integration of the starting ester **2.5u**, desired acetal product **2.42u**, and the following potential side products: alcohol **2.45**, aldehyde **2.46**, and TMS-protected alcohol **2.47**. To try to increase the yield, a solvent screen was performed (Table 2.3), which identified MTBE was the highest yielding solvent providing 19% of the desired acetal. Reaction times were increased from 30 minutes for the non-aromatic ester to 3-6 hours for the aromatic ester, which resulted in a slight increase in yield, but these were not always consistent. Unfortunately, a method could not be determined to make this a viable process.

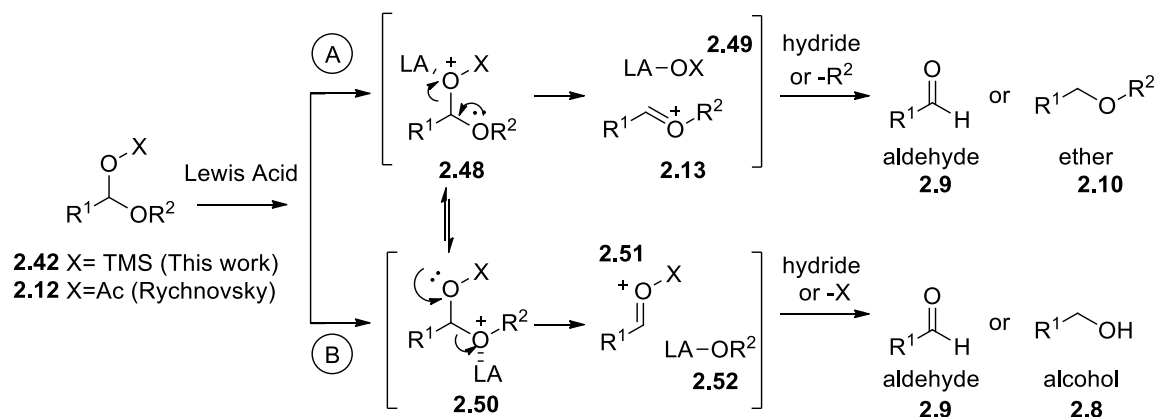
Table 2.3 Solvent screen for the reduction of aromatic ester **2.5u**

						
Entry	Solvent	Time	Starting Material ^b	Aldehyde	Alcohol and TMS-Prod ^c	Product
1	MTBE	3	21.0	1.8	60.6	16.4
2	MTBE	6	21.5	0.6	58.1	19.8
3	DCM	2	13.8	2.0	64.1	16.6
4	DCM	4.5	11.4	10.0	67.1	11.4
5	toluene	3	11.0	8.2	62.0	15.7
6	toluene	6	4.1	12.4	69.0	14.5
7	hexanes	2	10.4	0.8	80.0	8.8
8	ACN	4	70.5	2.2	27.3	--
9	THF	3	100	--	--	--
10	--	3	44.6	0.8	42.9	11.6

Note: a) Added in the order of 1.2. eq DIBAL, 2 eq TMS-imid, 0.8 eq DIBAL, 1 eq TMS-imid. b) All amounts above are NMR yields based on the relative integration of the CH_3 peaks. c) Ratio of the alcohol and the TMS protected acetal combined integrate together due to the overlapping of the peaks.

2.4.4 Reduction of the TMS-Protected Acetal to the Ether Product

The second step of the reduction process to form the ether starting from the acetal has been accomplished successfully for the non-aromatic acetal model system only.⁶² The conditions used by Rychnovsky were initially followed since this step was not predicted to be as difficult, however, there are differences between acetal **2.42** and Rychnovsky's acetal **2.12**.



Scheme 2.8 Two routes for Lewis acid complexation with the protected acetal

As shown in Scheme 2.9, two routes are possible for the Lewis acid to complex with the protected acetal. If the Lewis acid complexes with the protected oxygen (O-X), it follows route A, forming oxonium **2.13** retaining both R^1 and R^2 to produce the desired ether product **2.10** and with the potential to produce aldehyde by-product **2.9**. The production of aldehyde **2.9** is dependent on the reactivity of R^2 and its ability to leave as a stabilized group from oxonium **2.13**. The second route B occurs when the Lewis acid complexes with the ether oxygen bearing the R^2 group, resulting in the formation of oxonium ion **2.51**. This produces aldehyde **2.9** with the potential for over-reduction to alcohol **2.8**. If the protecting group X is an electron withdrawing acetate group, as in Rychnovsky's case, the more likely path is route B based on the electron density of the

oxygen binding, however an equilibrium with route A would still allow formation of ether **2.10**. In this work, the TMS group is electron donating and so more likely to start with route A and bind the Lewis acid, however it may not break down to the oxonium as readily (not as good of a leaving group) and equilibrate with the undesired route B. Because of this ability of the protecting group to affect the direction of the Lewis acid binding, the choice of Lewis acid is key for optimizing this step.

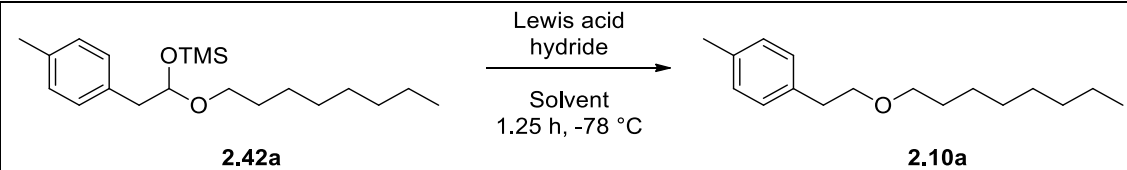
Initially the acetal was treated with Et_3SiH at $-78\text{ }^\circ\text{C}$ and then $\text{BF}_3\cdot\text{Et}_2\text{O}$ was added dropwise 10 minutes later as demonstrated by the Rychnovsky group. The reaction was monitored by TLC, which indicated complete conversion of the acetal in 1.25 hours. Using this method, the desired ether product was only isolated in 46% yield, with aldehyde accounting for the mass balance.

With these initial results in hand, a screen of common Lewis acids and hydride sources was performed (Table 4). The use of Bu_3SnH was chosen as a hydride source due to its increased reactivity compared to Et_3SiH . Despite the increased reactivity, Bu_3SnH was harder to remove by chromatography as both it and the ether are very non-polar, resulting in lower yields. TMSOTf was chosen as a Lewis acid due to the excellent triflate leaving group, increasing the reactivity. The optimal pairing was found using 2.5 equivalents of Et_3SiH and TMSOTf (entry 4) producing the desired ether product **2.10a** in an 84% yield. This represents an overall two step yield of 79% from ester **2.5a**.

To see if yields could be improved further, a brief solvent screen was completed, which identified DCM as the best solvent giving an overall yield of 84%, followed closely by toluene with an 80% yield (Table 4). Although these yields are promising, it

was determined that product loss of the ether still occurred during solvent removal, even with the increased molecular weight, and therefore careful protocols were followed.

Table 2.4 Lewis acid and hydride screen for the conversion of TMS-protected acetals to ethers.

					
<div style="display: flex; justify-content: space-between;"> 2.42a 2.10a </div>					
Entry	Solvent	Lewis acid	Hydride	Eq ^a	Yield (%)
1	DCM	BF ₃ ·OEt ₂	Bu ₃ SnH	2.5	59
2	DCM	TMSOTf	Bu ₃ SnH	2.5	47
3	DCM	BF ₃ ·OEt ₂	Et ₃ SiH	2.5	46
4	DCM	TMSOTf	Et ₃ SiH	2.5	84
5	DCM	TMSOTf	Et ₃ SiH	1.2	50
6	toluene	TMSOTf	Et ₃ SiH	2.5	80
7	hexanes	TMSOTf	Et ₃ SiH	2.5	57
8	THF	TMSOTf	Et ₃ SiH	1.2	0

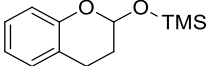
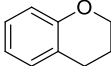
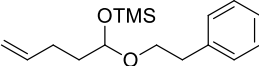
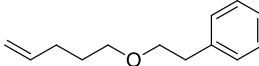
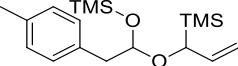
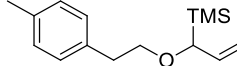
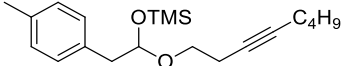
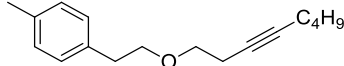
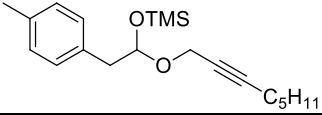
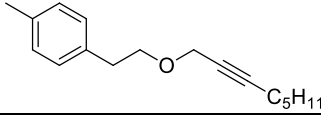
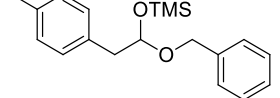
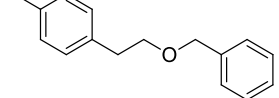
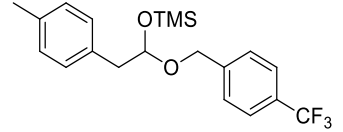
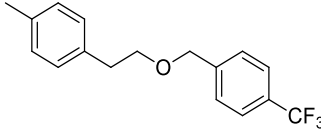
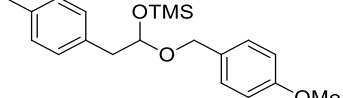
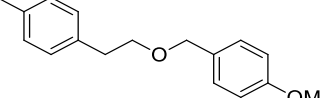
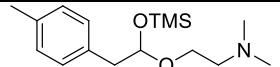
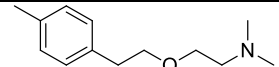
Note: a) Number of equivalencies added to the reaction for both the Lewis acid and hydride source.

After the development of the two-step reduction of esters to ethers for non-aromatic esters was defined, the substrate scope screen was completed (Table 2.2, step 1; Table 2.5, step 2). This method works for alkyl (entry 1, 2, 5, and 7), halo (entry 3), and cyclic ethers (entry 8-9), which tend to convert in good yields. A few exceptions are when the halogen is on the carbonyl side (entry 4) or the ether is phenolic (entry 10), both resulting in no ether product. Bulky alkyl groups are tolerated on the ether oxygen (entry 5), but not on the carbonyl side (entry 6). Terminal alkenes are tolerated with a decreased yield (entry 11-12) and alkynes to a lesser extent (entry 14-15). Benzyl groups on the ether side produced lower yields (entry 16). This is likely due to the loss of the benzyl group during oxonium ion formation. To further investigate this hypothesis, both electron

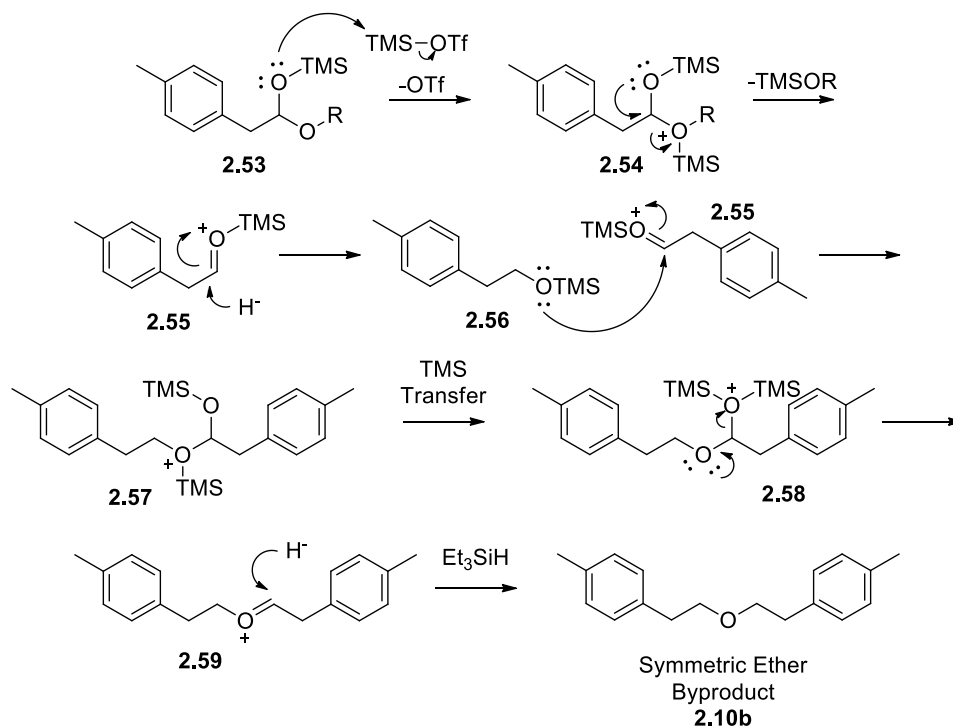
withdrawing and electron donating derivatives were utilized (entry 17 and 18 respectively). As predicted the electron withdrawing group gave a similar yield to the benzyl group, and the electron donating group further stabilized the loss of the benzyl group giving no ether product.

Table 2.5 Substrate scope for the reduction of TMS-protected acetals to ethers

$ \begin{array}{ccc} \text{OTMS} & \xrightarrow[\text{DCM}]{\text{TMSOTf, Et}_3\text{SiH}} & \\ & & \\ \text{R}^1-\text{C}-\text{OR}^2 & \xrightarrow[1.25 \text{ h, } -78^\circ\text{C}]{\text{1.25 h, } -78^\circ\text{C}} & \text{R}^1-\text{CH}_2-\text{OR}^2 \\ \text{2.20} & & \text{2.10} \end{array} $					
Entry	Substrate	Acetal	Yield (%)	Substrate	Ether
1	2.42a		84	2.10a	
2	2.42b		82	2.10b	
3	2.42c		94	2.10c	
4	2.42d		0	2.10d	
5	2.42e		73	2.10e	
6	2.42f		0	2.10f	
7	2.42g		59	2.10g	
8	2.42h		59	2.10h	
9	2.42i		80	2.10i	

10	2.42j		0	2.10j	
11	2.42k		56	2.10k	
12	2.42l		61	2.10l	
14	2.42m		39	2.10m	
15	2.42n		22	2.10n	
16	2.42o		36	2.10o	
17	2.42p		30	2.10p	
18	2.42q		0	2.10q	
19	2.42r		0	2.10r	

Due to inconsistent yields, additives such as 2,6-di-*tert*-butylpyridine (DTBP) were added to counteract the presence of triflic acid, however this did not improve yields.⁴⁹ Additionally on some of the lower yielding substrates (entry 14-18), it was determined that a symmetric ether was being produced. Symmetric ether **2.10b** is most likely synthesized through the formation of undesired oxonium **2.55** (Scheme 2.9), which can be reduced to the silyl protected alcohol **2.56**. Then **2.56** can couple with oxonium ion **2.55** to form di-silyl acetal **2.57**. Acetal **2.57** then undergoes a TMS transfer to produce **2.58**, which collapses to form oxonium ion **2.59**. After hydride delivery, symmetric ether **2.10b** is formed (Scheme 2.10). A similar synthetic route was published by Olah for the synthesis of symmetric and asymmetric ethers.⁶³ The identity of symmetric ether **2.10b** was confirmed by ¹H NMR using an authentic sample prepared by this reductive conversion method (Table 2.2 entry 2; Table 2.5 entry 2).

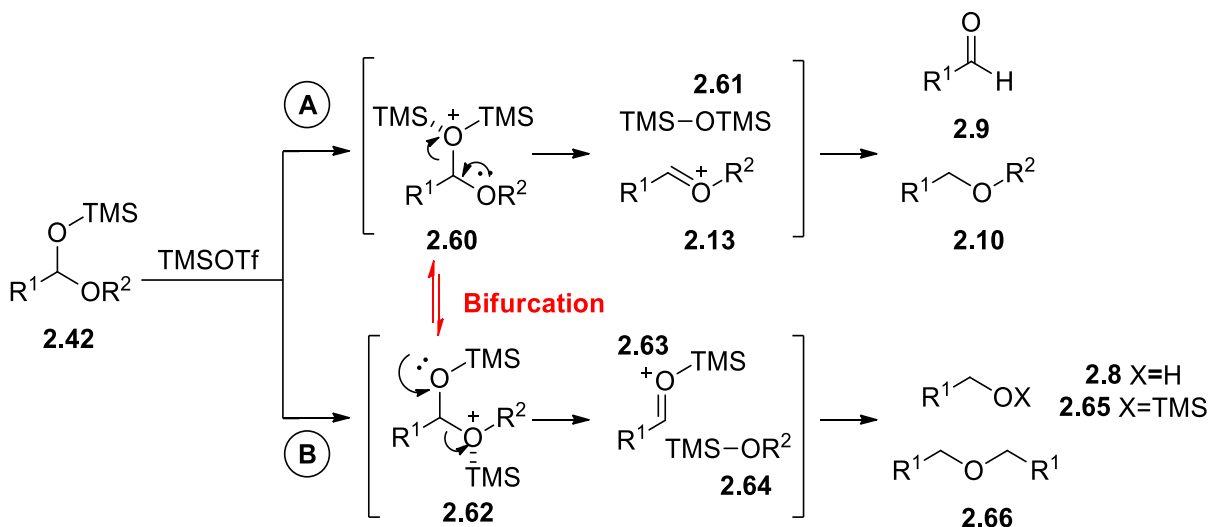


Scheme 2.9 Proposed mechanism for the formation of the symmetric ether byproduct

2.4.5 Bifurcation Determination of TMS-Acetal Conversion to Ethers

While the formation of a variety of by-products was unexpected for this conversion, a better understanding of the energetics of Lewis acid complexation was sought using computational analysis. Bifurcated transition states are a common occurrence in organic chemistry where undesired by-products from two or more competing pathways are produced and can be determined through computational analysis.⁶⁴

Upon reconsideration of the two reactive pathways as seen in Scheme 2.8, the Lewis acid was replaced with TMS. While the preferred route A would require the TMS group to complex with the acetal oxygen, there is a potential for it to complex with the ether oxygen. Additionally, the TMS group can equilibrate between **2.60** and **2.62**, creating a potential reaction bifurcation (Scheme 2.10). The bifurcation could lead to insight on why certain substrates were lower yielding.



Scheme 2.10 Post transition state bifurcation to desired A and undesired B products

Work was completed to determine if there is an energetically favorable substrate-based pathway for the conversion of TMS acetals to their ether counterparts. Structures were inputted using AMPAC software and transition states were calculated using Gaussian09 with the B3LYP/6-31G (d,p) level of theory. Initial computations have been calculated using the Mississippi Center for Supercomputing Research (MCSR), showing a bifurcation is present between **2.60** and **2.62**, but due to the number of atoms present, the calculations took long to acquire. To speed up initial calculations, an acetal with methyl group on either side was used. Calculations were completed in a three-step process starting with the optimization of TMS-acetal **2.42** with the Lewis acid TMS^+ . This was then followed by a constrained optimization where the structures were frozen and the bond between TMS^+ and either oxygen within TMS-acetal **2.42** were extended or shortened between 1.2 and 3.2 Å using a 0.1 Å step size. After the constrained optimizations were completed a 2-D scan was produced, plotting the step count versus the overall energy as shown in Figure 2.9 where the overall energy increases at step 10 before decreasing.

The structural geometry was then saved at the energy maximum and resubmitted to Gaussian09 to complete a transition state (TS) search. If the TS fell into a rotational TS, or local energy maximum, the distance between the TMS^+ was adjusted and the TS was resubmitted. It was determined that for acetal **2.42** where $\text{R}^1=\text{R}^2=\text{Me}$ there was a 0.36 kcal difference in energy from **2.13** and **2.63**, where **2.63** was lower in energy and thus more favorable. Work will continue in this endeavor with acetals **2.42a, c, e, h, l, n, o,** and **p** to help better understand the correlation substrate and yield.

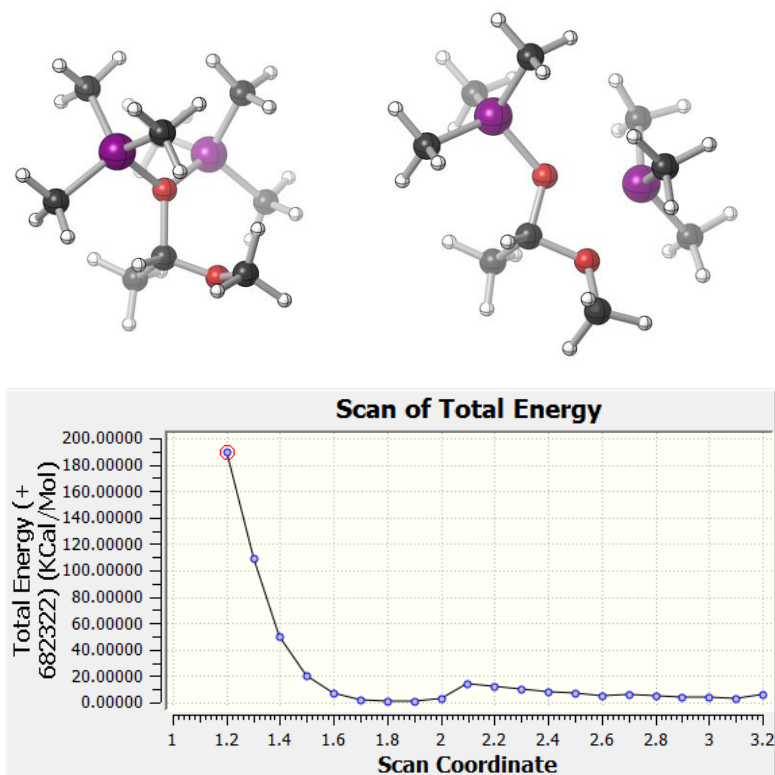


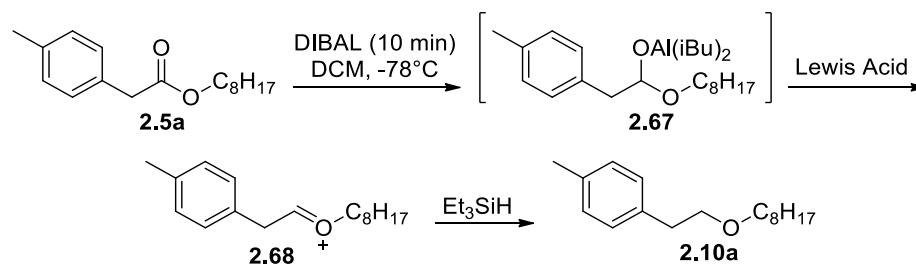
Figure 2.9: Geometry of starting TMS-acetal moving towards bifurcation

2.4.6 One-Pot Conversion and Addition of Nucleophiles to the Oxonium Ion

Intermediate

With the conversion of esters to ethers established,⁶² efforts were made towards developing a one-pot method to convert esters to ethers as well as synthesizing α -substituted ethers using carbon-based nucleophiles (Scheme 2.11). A one-pot reduction of esters to ethers has been completed before either starting with carboxylic acids,⁶⁵ or through the use of stronger Lewis acids.^{44, 66} The goal is to adjust the current method

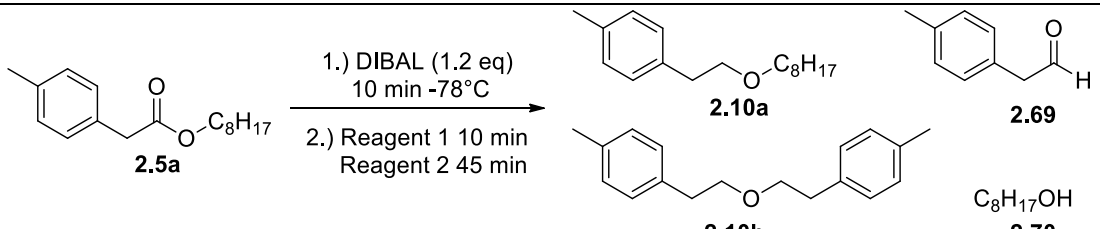
from a two-pot to a one-pot conversion of esters to ethers by directly binding to and reducing aluminate acetal **2.67** (Scheme 2.11).



Scheme 2.11 One-pot reduction with aluminate acetal intermediate

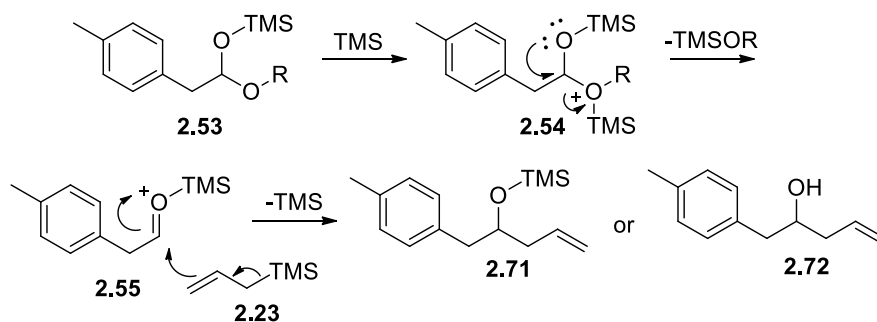
As seen in Table 2.6, a variety of Lewis acids, hydride sources, and solvents were screened as well as the order of addition. However, it was difficult to isolate the desired ether product, and the formation of byproducts such as aldehyde **2.69**, octanol **2.70**, and the symmetric ether **2.10b** became predominate as determined by ^1H NMR. A solvent screen was performed (entries 1-4) and DCM was again found to be ideal (entry 4, producing 82% ether and 10% of symmetric ether **2.10b**). For entries 1-4, the Lewis acid was added prior to the hydride source, using 2.5 equivalents of both. Changing the order of addition such that hydride was added first initially decreased the amount of ether (entry 5), but increasing reducing the hydride equivalents and increasing the Lewis acid worked well (81% ether, entry 6). Unfortunately, aldehyde **2.69** and ether **2.10b** became more prevalent with this order of addition. Other Lewis acids were tried but did not yield any desired product. While the ratio of ether to other byproducts could be optimized based on crude ^1H NMR to 82% (entry 4), the yield of isolated ether was low (44%). Disappointingly, a reliable one-pot method for the reduction of esters to ethers could not be realized.

Table 2.6 One-pot reduction of esters to ethers

<div style="text-align: center;">  </div>										
Entry	Reagent 1	Eq	Reagent 2	Eq	Solvent	2.10a^a	2.10a (Isolated)^b	2.70^a	2.69^a	2.10b^a
1	TMSOTf	2.5	Et ₃ SiH	2.5	Et ₂ O	44%	26%	--	54%	--
2	TMSOTf	2.5	Et ₃ SiH	2.5	DCE	57%	55%	--	--	26%
3	TMSOTf	2.5	Et ₃ SiH	2.5	heptane	71%	57%	--	12%	18%
4	TMSOTf	2.5	Et ₃ SiH	2.5	DCM	82%	44%	--	--	10%
5	Et ₃ SiH	1.1	TMSOTf	5	DCM	16%	--	55%	29%	--
6	Et ₃ SiH	1.1	TMSOTf	5	DCM	81%	--	--	3%	16%
7	Et ₃ SiH	2.5	TMSOTf	5	DCM	74%	--	16%	2%	9%
8	Et ₃ SiH	2.5	TiCl ₄	2.5	DCM	--	--	--	--	--
9	Et ₃ SiH	2.5	SnCl ₄	2.5	DCM	--	--	--	--	--

Note: a) Ratios were calculated through ¹H NMR integrations using the CH₃ peak unless otherwise noted. b) yield after column chromatography

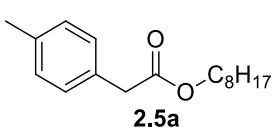
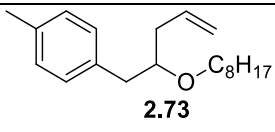
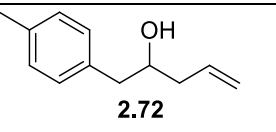
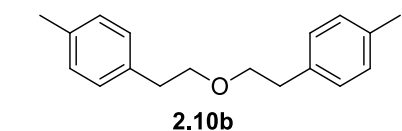
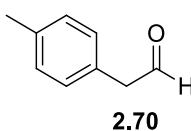
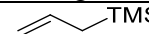
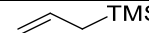
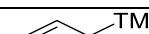
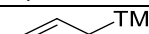
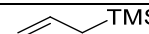
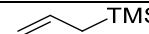
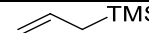
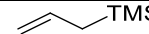
A variety of carbon nucleophiles such as allyl silane, silyl enol ethers, and dialkylzincs were screened with various Lewis acids in DCM in an attempt to isolate α -substituted ethers (Scheme 2.12). Rychnovsky was successful in addition of allyl silane **2.23** and a variety of vinyl enol ethers to acetoxy-protected acetals.⁴⁹ Again, formation of by-products was fairly predominant. It was found that addition of the nucleophile after the Lewis acid was critical towards preventing the production of octanol **2.69** and aldehyde **2.70** (entry 3-4). Of note, TiCl_4 and SnCl_4 as the Lewis acid increased yields to 82% and 86%, respectively, with the production of a separate by-product in each case (entries 5-6). Other chlorine-based Lewis acids were not able to produce the desired product or by-product (entries 7-8). This new by-product was determined to be alcohol **2.72**. It likely formed after the addition of allyl silane to oxonium ion **2.55**, producing the alcohol **2.72** and/or the TMS-protected variant **2.71** (Scheme 2.13). This also confirms a new product as a result of an undesired pathway of breakdown of acetal **2.42**.



Scheme 2.12 Proposed mechanism for the synthesis of secondary allyl alcohols.

At this point the one-pot method using either a hydride or carbon nucleophile do not prove to be viable, likely confirming why these have not been noted in the literature.

Table 2.7 One-pot nucleophile addition for the synthesis of α -substituted ethers

<div style="display: flex; align-items: center; justify-content: space-around;"> <div style="text-align: center;">  <p>2.5a</p> </div> <div style="text-align: center;"> <p>1.) DIBAL (10 min) DCM, -78 °C</p> <p>2.) Reagent 1 (10 min) Reagent 2 (45 min)</p> </div> <div style="display: flex; flex-wrap: wrap; justify-content: space-around;"> <div style="text-align: center;">  <p>2.73</p> </div> <div style="text-align: center;">  <p>2.72</p> </div> <div style="text-align: center;"> <p>C₈H₁₇OH</p> <p>2.69</p> </div> <div style="text-align: center;">  <p>2.10b</p> </div> <div style="text-align: center;">  <p>2.70</p> </div> </div> </div>									
Entry	Reagent 1	Eq	Reagent 2	Eq	2.73^a	2.70^a	2.69^a	2.72^a	2.10b^a
1		2.5	TMSOTf	5	50%	44%	-----	6%	-----
2		2.5	-----	-----	-----	-----	-----	-----	-----
3	TMSOTf	2.5		2.5	19%	58%	17%	6%	-----
4	TMSOTf	2.5		5	19%	56%	18%	7%	-----
5		2.5	TiCl ₄	2.5	82%	-----	-----	18%	-----
6		2.5	SnCl ₄	2.5	86%	-----	-----	-----	14%
7		2.5	AlCl ₃	2.5	-----	-----	-----	-----	-----
8		2.5	ZnCl ₂	2.5	-----	-----	-----	-----	-----

Note: a) Ratios calculated by ¹H NMR integration of the CH₃ peaks.

2.5 Summary and Conclusion

A successful method for the reduction of non-aromatic esters to ethers has been developed.⁶² Use of the React IR was paramount in decreasing reaction times of the ester to the acetal aluminate to only 10 minutes and was also crucial in determining the amount of reducing agent necessary for complete reduction. A screen of trapping reagents identified TMS-imidazole as the ideal reagent, which led to complete reaction times of 45 minutes, a significant decrease to current literature times by almost 90%. This drastic decrease in reaction times is crucial especially for industrial synthesis, along with the fact that the reduction worked at -40 °C. Formation and work up of the protected acetal intermediate produced clean ¹H NMR spectra and no additional purification was needed, allowing material to be carried through to the ether directly.

It was also determined that aromatic esters completely reduced within 10 minutes after the addition of reducing agent, however, a unique addition along with trapping reagent was needed and unfortunately only small amounts of product could be formed. As hydride reduction of aromatic esters to ethers has not been demonstrated within the literature as a general method, this result is promising, and yields can likely be increased through an understanding of acetal complexation to Lewis acids with computational analysis.

A simple screening of Lewis acids and hydride sources led to the discovery that TMSOTf and Et₃SiH optimized the production of the desired ether product, in moderate to excellent yields in a total reaction time of 1.25 hours. Esters that can be submitted to this reductive method include alkyl, halogenated, cyclic, and those that contain bulky substituents on the ether side. Alkene and alkyne groups can also be submitted to this

method at reduced yields. Substitution of the hydride with different nucleophiles has not been realized at this point with the current method but would provide a way to access challenging α -substituted ethers if it were successful. An ultimate goal would be the development of a one-pot reductive alkylation of esters.

2.6 Experimental

2.6.1 General Methods

2.6.1.1 Experimental Techniques

Unless otherwise noted, all reactions were carried out using flame-dried glassware and standard syringe, cannula, and septa techniques when necessary.⁶⁷ Tetrahydrofuran (THF), diethyl ether (Et₂O), hexanes, dichloromethane (DCM), and toluene were dried by passage through a column of activated alumina on an mBraun solvent purification system.⁶⁸ Triethylamine (TEA), N,N-dimethylformamide (DMF), and acetonitrile (ACN) were dried by passage through a column of activated alumina on an Innovative Technologies system. Trimethylsilyl chloride and Hunig's base were distilled from calcium hydride under argon. Pyridine was distilled from potassium hydroxide under nitrogen. Analytical thin layer chromatography was performed using Sorbent Technologies 250 μ m glass-backed UV254 silica gel plates. The plates were first visualized by fluorescence upon 254 nm irradiation then by iodine chamber. The plates were then dipped in one of the following stains followed by heating: p-anisaldehyde, phosphomolybdic acid, vanillin, ceric ammonium molybdate, potassium iodoplatinate, ninhydrin or bromocresol green. Flash column chromatography was performed using Sorbent Technologies 40-63 μ m, pore size 60 Å silica gel with solvent systems indicated.

Solvent removal was achieved using a Buchi R3 rotary evaporator with a V900 diaphragm pump (~10 mmHg). All yields refer to isolated material that is chromatographically (TLC or HPLC) and spectroscopically (^1H NMR) homogenous.

2.6.1.2 Characterization

All melting points were taken with a Thomas Hoover melting point apparatus and are uncorrected. Infrared spectra were recorded on a Nicolet Nexus 470 FTIR spectrometer as neat liquids, oils, solids or as thin films formed from evaporation of NMR solvent over the ATR plate. High-resolution mass spectra were recorded at the Old Dominion University College of Science Major Instrumentation Center (COSMIC) on a Bruker 12 Tesla APEX-Qe FTICR-MS with an Apollo II ion source.

2.6.1.3 NMR Parameters

Proton nuclear magnetic resonance spectra were recorded on a Bruker UltraShield Plus 400 MHz spectrometer and are reported in parts per million from internal chloroform (7.26 ppm), methanol (3.35, 4.78 ppm), benzene (7.26 ppm), or dimethylsulfoxide (2.49 ppm) on the δ scale and are reported as follows: chemical shift [multiplicity (s=singlet, d=doublet, t=triplet, q=quartet, qu=quintet, m=multiplet, or derivatives thereof), coupling constant(s) in hertz, integration, interpretation].⁶⁹ ^{13}C NMR data were recorded on a Bruker UltraShield Plus 100 MHz spectrometer and are reported as follows: chemical shift (multiplicity as determined from DEPT (CH , CH_3 up and CH_2 down and/or HSQC experiments).

2.6.2 Synthesis of Intermediates

General Method A for the Synthesis of Non-Aromatic Esters (2.5a-s, u)

Carboxylic acid (1.0 eq) was added to a 100 mL, flame dried, round bottom flask and purged under N₂ before anhydrous DCM (0.2 M) was added. Alcohol (1.1 eq) was added followed by either DCC or EDC (1.1 eq) and DMAP (0.5 eq). The reaction was then left to stir until complete conversion was observed by TLC.

- When using DCC as the coupling agent the reaction mixture was filtered through Celite® and then added to distilled water before being extracted three times with DCM.
- When using EDC as the coupling agent the reaction mixture was concentrated in vacuo and the remaining oil was taken up into distilled water and extracted three times with EtOAc.

The combined organic layers were dried over Na₂SO₄, filtered, and concentrated in vacuo. Column chromatography - SiO₂ using EtOAc/hexanes.

General Method B for the Synthesis of Non-Aromatic Esters (2.5a-s, u)

Carboxylic acid (1.0 eq) was placed in a 25 mL, flame dried, round bottom flask, and purged under N₂ before being dissolved in DCM (1.0 M). Two drops of DMF were added to the reaction before oxalyl chloride (1.1 eq) was added dropwise via syringe. The reaction stirred for 1 hour before the solvent and excess oxalyl chloride was removed in vacuo. The flask was then purged under N₂ again before alcohol (3.5 eq) was added followed by pyridine (4.8 eq) dropwise via syringe. The reaction stirred at RT until completion as monitored by TLC. The reaction was quenched with saturated aqueous

sodium bicarbonate and taken up in DCM. The aqueous layer was extracted three times with DCM. The organic layers were combined, dried over Na₂SO₄, filtered through Celite®, and concentrated in vacuo. Column chromatography – SiO₂ with EtOAc/hexanes.

General Method C for the Synthesis of Aromatic Esters (2.5t, u, v)

Carboxylic acid (1.0 eq) was added to a 25 mL flame dried, round bottom flask and purged under N₂ before being dissolved in DCM (1.0 M). Two drops of DMF were added to the reaction before thionyl chloride (1.1 eq) was added dropwise via syringe. The reaction stirred for 1 hour at 40 °C before the solvent and excess thionyl chloride was removed in vacuo. The flask was then purged under N₂ again before alcohol (3.5 eq) was added followed by pyridine (4.8 eq) dropwise via syringe. The reaction stirred at RT until completion as monitored by TLC. The reaction was quenched with saturated aqueous sodium bicarbonate and taken up in DCM. The aqueous layer was extracted three times with DCM. The organic layers were combined, dried over Na₂SO₄, filtered through Celite®, and concentrated in vacuo. Column chromatography – SiO₂ with EtOAc/hexanes.

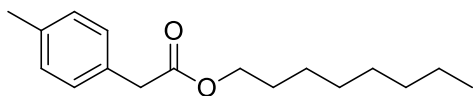
General Method D for the Synthesis of TMS-Protected Acetals (2.42a-2.42s)

Ester (1.0 eq) was added to a 10 mL, flame dried, round bottom flask and purged under N₂ before being dissolved in DCM (1.0 M). The ReactIR was prepared by cleaning the probe with MeOH and taking a background spectrum. A solvent reference for DCM and hexanes was also loaded into the experiment file. The flask was attached to the ReactIR

and spectra were set to collect every minute. The reaction was placed in a dewar and cooled to $-78\text{ }^{\circ}\text{C}$ with dry ice and acetone. After cooling for 15-30 minutes, DIBAL-H (1.2 eq.) was added dropwise over a period of 10 minutes. The reduction of the carbonyl peak was monitored by ReactIR, and the amount of DIBAL-H was increased by increments of 0.3 equivalents if complete reduction was not achieved within 10 minutes. TMS-imid (3 eq.) was added dropwise and the reaction stirred for 30 minutes before being quenched with saturated aqueous NH_4Cl . The quenched solution was warmed to room temperature and then DCM was added as well as Rochelle salts to assist with emulsions. The aqueous layer was extracted 3 times with DCM. The combined organic layers were collected and dried over Na_2SO_4 , filtered, and concentrated in vacuo using rotovap. The acetal product was carried on without further purification.

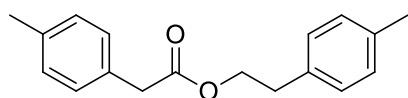
General Method E for the Synthesis of Ethers (2.10a-2.10q)

The acetal (from General Method D) was added to flame dried 10 mL round bottom flask that was purged with N_2 before being dissolved in DCM (1.0 M). The reaction was placed in a dewar before being cooled to $-78\text{ }^{\circ}\text{C}$ using a dry ice and acetone bath. After cooling for 15-30 minutes, Et_3SiH (2.5 eq) was added dropwise via syringe. The reaction stirred for 10 minutes before adding TMSOTf (2.5 eq) dropwise via syringe. The reaction stirred for 1.25 hours and was monitored by TLC. The reaction was quenched with saturated aqueous NaHCO_3 and allowed to warm to RT before being added to DCM. The aqueous layer was extracted three times with DCM and the combined organic layers were dried over Na_2SO_4 , filtered, and concentrated in vacuo. Column chromatography - SiO_2 with ether/hexanes.



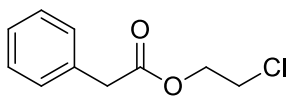
Octyl 2-(p-tolyl)acetate (2.5a): According to

general method B, p-tolyl acetic acid (3.00 g, 20.0 mmol) was converted to ester **2.5a**. The second step was complete in 1 hour as monitored by TLC. Column chromatography (SiO₂, 10 – 20% EtOAc/hex) yielded a pale-yellow oil; yield 4.9g, 93%; R_f = 0.36 (10% EtOAc/hex); IR (thin film) 2954, 2924, 1855, 1735, 1252, 1151 cm⁻¹. ¹H NMR (400 MHz, CDCl₃) δ 7.15 (m, 4H) δ 4.07 (t, J = 6.72 Hz, 2H), δ 3.57 (s, 2H), δ 2.33 (s, 3H), δ 1.60 (p, J = 7.08, 2H), δ 1.38 (m, 10H), δ 0.88 (t, J = 6.76, 3H); ¹³C NMR (100 MHz, CDCl₃) δ : 172.0 (s), 136.7 (s), 131.3 (s), 129.3 (d), 129.2 (d), 65.1 (q), 41.2 (t), 31.9 (t), 31.0 (t), 29.3 (t), 28.7 (t), 26.0 (t), 22.8 (t), 21.2 (q), 14.2 (q).



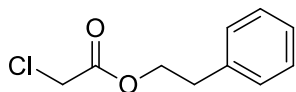
4-Methylphenethyl 2-(p-tolyl)acetate (2.5b):

According to general method B, p-tolyl acetic acid (0.50 g, 3.34 mmol) was converted to ester **2.5b**. The reaction was complete in 1.5 hours as monitored by TLC. Column chromatography (SiO₂, 5-10-20-40% EtOAc/hex) yielded a pale yellow oil; yield 0.78 g, 88%; R_f = 0.59 (20% EtOAc/hex); IR (thin film) 2952, 2917, 1730, 1136 cm⁻¹; ¹H NMR (CDCl₃, 400 MHz) δ : 7.06 (d, J = 8.0 Hz, 4H), 7.03 (d, J = 8.0 Hz, 4H), 4.25 (t, J = 7.0 Hz, 2H), 3.55 (s, 2H), 2.86 (t, J = 7.0 Hz, 2H), 2.33 (s, 3H), 2.32 (s, 3H); ¹³C NMR (CDCl₃, 100 MHz) δ : 171.7 (s), 136.6 (s), 136.0 (s), 134.7 (s), 131.0 (s), 129.3 (d), 129.2 (d, 2 peaks), 128.8 (d), 65.5 (t), 41.0 (t), 34.6 (t), 21.1 (q), 21.0 (q).



2-Chloroethyl 2-phenylacetate (2.5c). Using general method A, phenylacetic acid (1.00 g, 5.03 mmol) was converted to ester

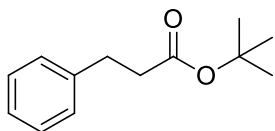
2.5c. Column chromatography (SiO₂ 5-10-20% EtOAc/hex) yielded a colorless liquid; yield 0.83 g, 57%. Characterization data can be found at the provided reference.⁷⁰



2-Chloroethyl 2-phenylacetate (2.5d). Using general method

A, phenylacetic acid (1.00 g, 5.03 mmol) was converted to ester

2.5d. Column chromatography (SiO₂ 5-10-20% EtOAc/hex) yielded a colorless liquid; yield 1.67 g, 79%. Characterization data can be found at the provided reference.⁷⁰

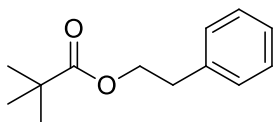


t-Butyl-3-phenylpropanoate (2.5e): According to general

method B, phenyl propanoic acid (1.00 g, 6.66 mmol) was

converted to ester **2.5e**. The second step was completed in 1 hour as monitored by TLC.

Column chromatography (SiO₂, 1-5-10-20% EtOAc/hex) yielded a pale yellow oil; yield 0.67 g, 49%. Characterization data found at the provided reference.



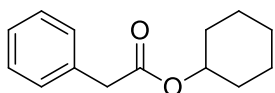
Phenethyl pivalate (2.5f)⁷¹: According to general method B,

pivalic acid (2.00 g, 19.6 mmol) was converted to ester **2.5f**. The

second step was completed in 1 hour as monitored by TLC. Column chromatography

(SiO₂, 1-5-10-20% EtOAc/hex) yielded a pale yellow oil; yield 1.55 g, 39%.

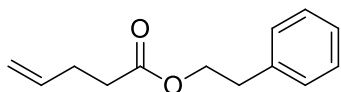
Characterization data can be found at the reference provided.⁷²



Cyclohexyl 2-phenylacetate (2.5g): Using general method A,

phenylacetic acid (2.00 g, 14.7 mmol) was converted to ester

2.5g. Column chromatography (SiO₂ 5-10-20% EtOAc/hex) yielded a pale yellow oil; yield 2.65 g, 83%. Characterization data can be found at the provided reference.⁷³

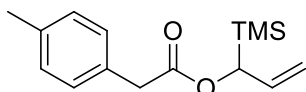


Phenyl pent-4-enoate (2.5k). Using general method A,

pent-4-enoic acid (1.0 ml, 8.09 mmol) was converted to ester

2.5k. Column chromatography (SiO₂ 5-10-20% EtOAc/hex) yielded a colorless liquid;

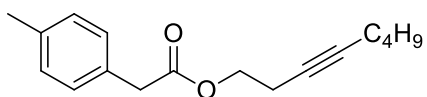
yield 0.82 g, 55%; R_f = 0.60 (20% EtOAc/hex); IR (thin film) 3100, 1732, 1243, 1165, 698 cm^{-1} ; ^1H NMR (400 MHz, CDCl_3) δ : 7.35-7.20 (m, 5H), 5.79 (ddt, J = 16.7, 10.3, 6.2 Hz, 1H), 5.07-4.98 (m, 2H), 4.31 (t, J = 7.2 Hz, 2H), 2.95 (t, J = 6.8 Hz, 2H), 2.43-2.34 (m, 4H); ^{13}C NMR (100 MHz, CDCl_3) δ : 172.9 (s), 137.8 (s), 136.7 (d), 128.9 (d), 128.4 (d), 126.5 (d), 115.4 (t), 64.8 (t), 35.1 (t), 33.5 (t), 28.8 (t); HRMS (ESI): Exact mass calculated for $\text{C}_{13}\text{H}_{16}\text{O}_2\text{Na}$ $[\text{M} + \text{Na}]^+$ 227.104251, found 227.104387.



1-(Trimethylsilyl)allyl 2-(p-tolyl)acetate (2.5l): According to general method B, p-tolyl acetic acid (1.00 g, 6.66 mmol) was

converted to ester **2.5l**. The reaction was complete in 3 hours as monitored by TLC.

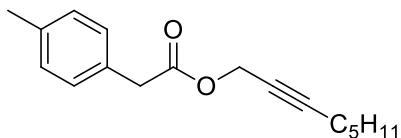
Column chromatography (SiO_2 , 5-10-20-40% EtOAc/hex) yielded a colorless oil; yield 2.65 g, 75%; R_f = 0.43 (10% EtOAc/hex); IR (thin film) 2957, 1731, 1633 cm^{-1} ; ^1H NMR (CDCl_3 , 400 MHz) δ : 7.19 (d, J = 8.0 Hz, 2H), 7.13 (d, J = 8.0 Hz, 2H), 5.84 (ddd, J = 16.8, 10.9, 5.7 Hz, 1H), 5.20 (dt, J = 5.7, 1.9 Hz, 1H), 4.94 (dt, J = 11.0, 1.6 Hz, 1H), 4.90 (dt, J = 16.8, 1.6 Hz, 1H), 3.63 (s, 2H), 2.34 (s, 3H), 0.00 (s, 9H); ^{13}C NMR (CDCl_3 , 100 MHz) δ : 171.3 (s), 136.6 (s), 134.8 (d), 131.2 (s), 129.4 (d), 129.2 (d), 111.3 (t), 70.9 (d), 41.3 (t), 21.1 (q), -4.08 (q).



Oct-3-yn-1-yl 2-(p-tolyl)acetate (2.5m): According to general method B, p-tolyl acetic acid (2.00 g, 13.3

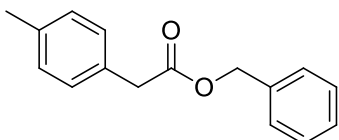
mmol) was converted to ester **2.5m**. The reaction stirred overnight and was monitored by TLC. Column chromatography (SiO_2 , 5-10-20-40% EtOAc/hex) yielded a yellow oil; yield 3.22 g, 93%; R_f = 0.50 (10% EtOAc/hex); IR (thin film) 2930, 2957, 1737, 1137 cm^{-1} ; ^1H NMR (CDCl_3 , 400 MHz) δ : 7.20 (d, J = 8.0 Hz, 2H), 7.14 (d, J = 8.0 Hz, 2H), 4.18 (t, J = 6.2 Hz, 2H), 3.61 (s, 2H), 2.50 (tt, J = 7.0, 2.3 Hz, 2H), 2.36 (s, 3H), 2.16 (tt,

6.7, 2.3 Hz, 2H), 1.46 (m, 4H), 0.95 (t, 3H). ^{13}C NMR (CDCl_3 , 100 MHz) δ : 171.5 (s), 136.6 (s), 130.9 (s), 129.2 (d), 129.1 (d), 82.0 (s), 75.4 (s), 6.32 (t), 40.8 (t), 31.0 (t), 21.9 (t), 21.0 (q), 19.2 (t), 18.4 (t), 13.6 (q).



Oct-2-yn-1-yl 2-(p-tolyl)acetate (2.5n): According to general method B p-tolyl acetic acid (2.0 g, 13.3 mmol)

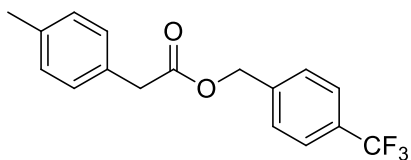
was converted to ester **2.5n**. The reaction was complete in 18 hours as monitored by TLC. Column chromatography (SiO_2 , 5-10-20-40% EtOAc/hex) yielded a colorless oil; yield 2.91 g, 85% R_f = 0.50 (10% EtOAc/hex); IR (thin film) 2930, 2860, 2236, 1740 cm^{-1} ; ^1H NMR (CDCl_3 , 400 MHz) δ : 7.23 (d, J = 8.1 Hz, 2H), 7.17 (d, J = 8.1 Hz, 2H), 4.73 (t, J = 2.2 Hz, 2H), 3.66 (s, 2H), 2.38 (s, 3H), 2.26 (tt, J = 7.1, 2.2 Hz, 2H), 1.56 (p, J = 7.1 Hz, 2H), 1.38 (m, 4H), 0.97 (t, J = 7.0 Hz, 3H); ^{13}C NMR (CDCl_3 , 100 MHz) δ : 171.1 (s), 136.7 (s), 130.7 (s), 129.3 (d), 129.2 (d), 87.8 (s), 74.0 (s), 53.2 (t), 40.65 (t), 31.05 (t), 28.2 (t), 22.2 (t), 21.1 (q), 18.7 (t), 14.0 (q)



Benzyl 2-(p-tolyl)acetate (2.5o): According to general method B, p-tolyl acetic acid (2.0 g, 13.3 mmol) was

converted to ester **2.5o**. The second step stirred overnight as monitored by TLC. Column chromatography (SiO_2 3-6% EtOAc/hex) yielded a yellow oil; yield 2.28 g, 71%.

Characterization data can be found at the provided reference.⁷⁴

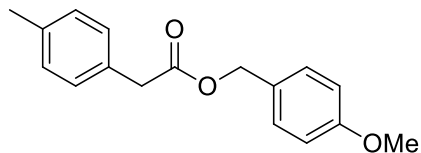


4-(Trifluoromethyl)benzyl 2-(p-tolyl)acetate (2.5p):

According to general method B p-tolyl acetic acid (2.0 g, 13.3 mmol) was converted to ester **2.5p**. The

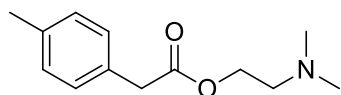
reaction ran over night as was monitored by TLC. Column chromatography (SiO_2 , 5-10-20-40% EtOAc/hex) yielded a pale yellow solid; yield 3.74 g, 91%; mp 45-47 °C; R_f =

0.43 (10% EtOAc/hex); IR (thin film) 1726 cm^{-1} ; ^1H NMR (CDCl_3 , 400 MHz) δ : 7.59 (d, $J = 8.1$ Hz, 2H), 7.39 (d, $J = 8.1$ Hz, 2H), 7.17 (d, $J = 8.2$ Hz, 2H), 7.13 (d, $J = 8.2$ Hz, 2H), 5.17 (s, 2H), 3.65 (s, 2H), 2.34 (s, 3H); ^{13}C NMR (CDCl_3 , 100 MHz) δ : 171.4 (s), 139.9 (s), 139.8 (s), 136.9 (s), 136.6 (s), 130.6 (s), 129.3 (d), 129.1 (d), 128.0 (d), 125.5 (q, $J = 3.8$ Hz)*, 65.5 (t), 40.9 (t), 21.1 (q). *Due to C-F splitting



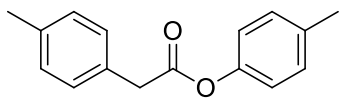
4-Methoxybenzyl 2-(p-tolyl)acetate (2.5q):

According to general method B, p-tolyl acetic acid (2.00 g, 1.3 mmol) was converted to ester **2.5q**. The reaction was complete in 2 hours as monitored by TLC. It was purified on a Combiflash using a linear gradient of EtOAc/hex (0 to 100%) to yield a yellow oil; yield 3.02 g, 84%; $R_f = 0.33$ (10% EtOAc/hex); IR (thin film) 1732 cm^{-1} ; ^1H NMR (CDCl_3 , 400 MHz) δ : 7.26 (m, 2H), 7.15 (d, $J = 8.2$ Hz, 2H), 7.13 (d, $J = 8.2$ Hz, 2H), 6.87 (m, 2H), 5.05 (s, 2H), 3.80 (s, 3H), 3.60 (s, 2H), 2.33 (s, 3H). ^{13}C NMR (CDCl_3 , 100 MHz) δ : 171.7 (s), 159.6 (s), 136.7 (s), 130.9 (s), 130.0 (d), 129.3 (d), 129.2 (d), 128.1 (s), 113.9 (d), 66.4 (t), 55.3 (q), 40.9 (t), 21.1 (q).



2-(Dimethylamino)ethyl 2-(p-tolyl)acetate (2.5r):

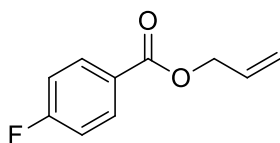
According to general method B, p-tolyl acetic acid (2.00 g, 13.3 mmol) was converted to ester **2.5r**. The reaction stirred overnight for 18 hrs. It was purified on a Combiflash using a linear gradient of EtOAc/hex (0 to 100%) to furnish a yellow oil; Yield 1.32 g, 45%; $R_f = 0.16$ (50% EtOAc/hex); IR (thin film) 1732 cm^{-1} ; ^1H NMR (CDCl_3 , 400 MHz) δ : 7.14 (m, 4H), 4.18 (t, $J = 5.8$ Hz, 2H), 3.60 (s, 2H), 2.26 (s, 6H), 2.55 (t, $J = 5.8$ Hz, 2H), 2.32 (s, 3H); ^{13}C NMR (CDCl_3 , 100 MHz) δ : 171.9 (s), 136.6 (s), 130.9 (s), 129.2 (d), 129.1 (d), 62.6 (t), 57.7 (t), 45.7 (q), 40.8 (t), 21.1 (q).



p-Tolyl 2-(p-tolyl)acetate (2.5s): According to general method B, p-tolyl acetic acid (1.05 g, 4.37 mmol) was

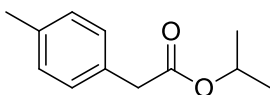
converted to ester **2.5s**. The reaction stirred overnight and was monitored by TLC.

Column chromatography (SiO₂, 8% EtOAc/hex) yielded a white solid; yield 41%; mp 38-43 °C R_f = 0.29 (10% EtOAc/hex); IR (thin film) 3026, 2918, 1758, 1119 cm⁻¹; ¹H NMR (CDCl₃, 400 MHz) δ : 7.27 (d, J = 8.0 Hz, 2H), 7.17 (d, J = 8.0 Hz, 2H), 7.14 (d, J = 8.4 Hz, 2H), 6.93 (d, J = 8.4 Hz, 2H), 3.81 (s, 2H), 2.36 (s, 3H), 2.33 (s, 3H); ¹³C NMR (CDCl₃, 100 MHz) δ : 170.4 (s), 148.5 (s), 136.9 (s), 135.4 (s), 130.5 (s), 129.9 (s), 129.4 (s), 129.2 (s), 121.1 (s), 41.0 (t), 21.1 (q), 20.9 (q).



Allyl 4-fluorobenzoate (2.5t). Using general method A, 4-fluorobenzoic acid (1.03 g, 7.35 mmol) was converted to ester

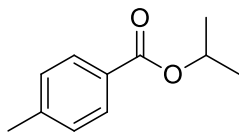
2.5t. Column chromatography (SiO₂ 5-10-20% EtOAc/hex) yielded a pale-yellow oil; yield 0.89 g, 67%; R_f = 0.59 (20% EtOAc/hexanes); IR (thin film) 1719, 1601, 1263, 765 cm⁻¹; ¹H NMR (400 MHz, CDCl₃) δ : 8.07 (dddd, J = 2.8 Hz, 2H), 7.14-7.07 (m, 2H), 6.03 (ddt, J = 17.2, 10.8, 5.6 Hz, 1H), 5.4 (dq, J = 17.2, 1.6 Hz, 1H), 5.29 (dq, J = 10.4, 1.2 Hz, 1H), 4.81 (dt, J = 5.6, 1.6 Hz, 2H); ¹³C NMR (100 MHz, CDCl₃) δ : 166.3 (d, J = 255 Hz)*, 164.5 (s), 132.2 (d, J = 9.4 Hz)*, 132.10 (d), 126.4 (d, J = 2.9 Hz)*, 118.4 (t), 115.5 (d, J = 22.4 Hz)*, 65.6 (t). *Due to C-F splitting



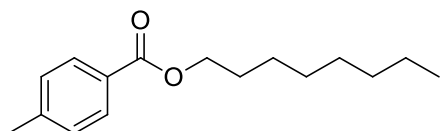
Isopropyl 2-(p-tolyl)acetate (2.5u) According to general method B, p-tolylacetic acid (3.93 g, 26.2 mmol) was converted to ester

2.5u. The second step was completed in 45 minutes as monitored by TLC. Column chromatography (SiO₂, 1-2.5-5-10% EtOAc/hex) yielded a pale yellow oil; yield 4.23 g, 83%; R_f = 0.57 (20% EtOAc/hex); IR (thin film) 2979, 2934, 1727, 1144, 1105 cm⁻¹. ¹H

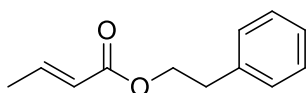
NMR (400 MHz, CDCl₃) δ : 7.15 (m, 4H), 5.00 (m, J = 6.2 Hz, 1H), 3.53 (s, 2H), 2.32 (s, 3H), 1.22 (d, J = 6.24 Hz, 6H). ¹³C NMR (100 MHz, CDCl₃) δ : 171.5 (s), 136.7 (s), 131.4 (s), 129.3 (d), 129.2 (d), 68.2 (d), 41.5 (t), 21.9 (q), 21.2 (q).



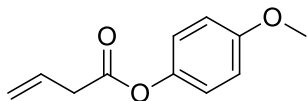
Isopropyl 4-methylbenzoate (2.5v): Using general method A, 4-methylbenzoic acid (1.70 g, 12.5 mmol) was converted to ester **2.5v**. Column chromatography (SiO₂ 5-10-20% EtOAc/hex) yielded a colorless oil; yield 1.00 g, 58%. Characterization data can be found at the provided reference.⁷⁵



Octyl 4-methylbenzoate (2.5w) According to general method C, p-toluic acid (2.00 g, 14.7 mmol) in DCM (9.8 mL) was converted to ester **2.5w**. The second step stirred overnight for 20 hours as monitored by TLC. Column chromatography (SiO₂, 5–10% EtOAc/hex) yielded a pale yellow oil; yield 3.39 g, 93%; R_f = 0.69 (EtOAc/hex); IR cm⁻¹ (thin film): 2963, 1730 cm⁻¹; ¹H NMR (400 MHz, CDCl₃) δ : 7.93 (dt, J = 8.4, 1.9 Hz, 2H), δ 7.23 (m, 2H), δ 4.29 (t, J = 6.7 Hz, 2H), δ 2.41 (s, 3H), δ 1.76 (p, J = 6.8, 2H) δ 1.32 (m, 10H), δ 0.88 (t, J = 6.8 Hz, 3H) ¹³C NMR (100 MHz, CDCl₃) δ : 166.7 (s), 143.34 (s), 129.54 (s), 128.99 (d), 127.79 (d), 64.91 (t), 31.79 (t), 29.71 (t), 28.74 (t), 26.05 (t), 22.64 (t), 21.59 (q), 14.07 (q); MS: m/z (%) = 248 (6.1) [M⁺].

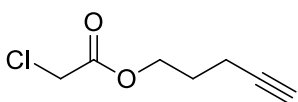


(E)-Phenethyl but-2-enoate (2.5x): (E)-but-2-enoic acid (1.00 g, 11.6 mmol) was converted to ester **2.5x**. The second step of the reaction was complete in 1 hour as monitored by TLC. Column chromatography (SiO₂ 5-10-20% EtOAc/hex) provided a pale yellow liquid; yield 1.90 g, 86%. Characterization data can be found at the provided reference.⁷⁶



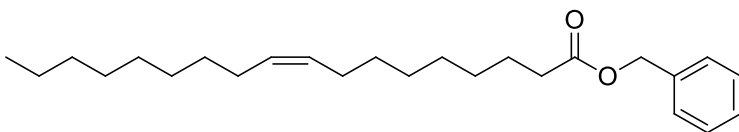
4-Methoxyphenyl-3-butenolate (2.5aa) According to general

method B, vinyl acetic acid (1.0 g, 11.6 mmol) was converted to ester **2.5aa**. The reaction was completed in 16 hours as monitored by TLC. Column chromatography (SiO₂, 1–2.5–5–10% EtOAc/hex) yielded a pale yellow oil; yield 0.79 g, 35%; *R_f* = 0.46 (20% EtOAc/hex). IR (thin film) 2935, 2837, 1753, 1504, 1245, 1191, 1135 cm⁻¹. ¹H NMR (400 MHz, CDCl₃) δ: 7.01 (td, *J* = 5.9, 3.6 Hz, 2H), δ 6.88 (td, *J* = 5.8, 3.5 Hz, 2H), δ 6.03 (ddt, *J* = 17.1, 10.2, 7.0 Hz, 1H), δ 5.28 (dd, *J* = 13.4, 1.4 Hz, 1H), δ 5.25 (dd, *J* = 6.3, 1.2 Hz, 1H), δ 3.80 (s, 3H), δ 3.32 (dt, *J* = 6.9, 1.4 Hz, 2H). ¹³C NMR (100 MHz, CDCl₃) δ: 170.5 (s), 157.4 (s), 144.3 (s), 129.9 (d), 122.4 (d), 119.3 (d), 114.6 (t), 55.7 (q), 39.2 (t).



Pent-4-yn-1-yl 2-chloroacetate (2.5ab) According to general

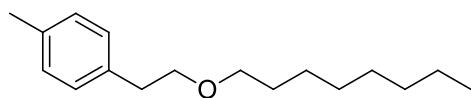
method B, 2-chloroacetic acid (0.50 g, 5.3 mmol) was converted to ester **2.5ab**. The reaction stirred for 19 hrs as monitored by TLC. Column chromatography (SiO₂, 5-10-20-40% EtOAc/hex) yielded a colorless oil; yield 0.30 g, 35.8%; *R_f* = 0.42 (20% EtOAc/hex); IR (thin film) 3294, 2961, 1738, 1171, 1026, 640 cm⁻¹. ¹H NMR (400 MHz, CDCl₃) δ: 4.31 (t, *J* = 6.3 Hz, 2H), δ 4.06 (s, 2H), δ 2.31 (td, *J* = 7.0, 2.6 Hz, 2H), δ 1.92 (t, *J* = 2.7 Hz, 1H), δ 1.90 (p, *J* = 6.4 Hz, 2H). ¹³C NMR (100 MHz, CDCl₃) δ: 197.4 (s), 82.8 (s), 69.4 (d), 64.8 (t), 41.0 (t), 27.5 (t), 15.2 (t).



Benzyl oleate (2.5ac)

According to general method B oleoyl chloride (549 μL, 1.66 mmol) was converted to ester **2.5ac** by adding alcohol and pyridine only. The reaction was complete in 4.5 hours as monitored by TLC. Column chromatography (SiO₂, 5-10-20-40% EtOAc/hex) yielded a pale yellow oil;

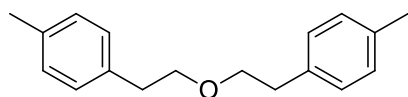
yield 0.52 g, 84%; R_f = 0.70 (20% EtOAc/hex); IR (thin film) 2922, 2852, 1737, 1455, 1212, 1161, 732, 695 cm^{-1} . ^1H NMR (400 MHz, CDCl_3) δ 7.35 ppm, (m, 5H); δ 5.34 ppm, (m, 2H); δ 5.11 ppm, (s, 1H); δ 2.35 ppm, (t, J = 7.48 Hz, 2H); δ 2.00 ppm, (m, 4H); δ 1.64 ppm, (m, 2H); δ 1.28 ppm, (m, 14H); δ 0.88 ppm, (m, 5H). ^{13}C NMR (100 MHz, CDCl_3) δ : 173.8 (s), 136.3 (d), 130.2 (s), 129.9 (d), 128.7 (d), 128.3 (d), 66.2 (t), 34.5 (t), 32.1 (t), 30.0 (t), 29.9 (t), 29.7 (t), 29.5 (t), 29.3 (t), 29.2 (t), 27.4 (t), 27.3 (t), 25.1 (t), 22.9 (t), 14.3 (q).



1-Methyl-4-(2-(octyloxy)ethyl)benzene (2.10a)

According to general methods D/E, ester **2.5a** (100 mg, 4.03 mmol) was converted to ether **2.10a** using 1.2 equivalents of DIBAL-H.

Column chromatography (SiO_2 , 1-5-10 Et_2O /hex) yielded a colorless oil; yield 62.1 mg, 84%; R_f = 0.31 (10% Et_2O /hex). ^1H NMR (400 MHz, CDCl_3) δ 7.11 (m, 4H); δ 3.60 (t, J = 7.4 Hz, 2H); δ 3.42 (t, J = 6.7 Hz, 2H); δ 2.85 (t, J = 7.4 Hz, 2H); δ 2.32 (s, 3H); δ 1.56 (m, 2H); δ 1.28 (m, 10H); δ 0.88 (t, J = 6.7 Hz, 3H). ^{13}C NMR (100 MHz, CDCl_3) ppm: 136.1 (s), 135.7 (s), 129.2 (d), 128.0 (d), 72.2 (t), 71.3 (t), 36.1 (t), 32.0 (t), 29.9 (t), 29.6 (t), 29.4 (t), 26.4 (t), 22.9 (t), 21.2 (q), 14.3 (q).

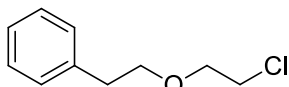


4,4'-(Oxybis(ethane-2,1-diyl))bis(methylbenzene)

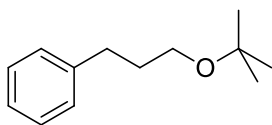
(2.10b): According to general methods D/E ester **2.5b**

(335 mg, 13.2 mmol) was converted to ether **2.10b** using 1.2 equivalents of DIBAL.

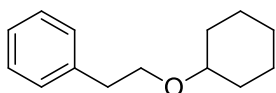
Column chromatography (SiO_2 , 1-5-10 Et_2O /hex) yielded a pale yellow oil; yield 0.20 g, 82%; R_f = 0.51 (10% EtOAc/hex); ^1H NMR (CDCl_3 , 400 MHz) δ : 7.09 (s, 8H), 3.62 (t, J = 7.3 Hz, 4H), 2.84 (t, J = 7.3 Hz, 4H), 2.32 (s, 6H).



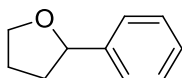
2-(2-Chloroethoxy)ethylbenzene (2.10c): According to general methods D/E ester **2.5c** (410 mg, 1.50 mmol) was converted to ether **2.10c** using 1.2 equivalents of DIBAL. Column chromatography (SiO₂, 1-5-10 Et₂O/hex) yielded a colorless oil; yield 0.26 g, 94%; R_f = 0.42 (10% EtOAc/hex); ¹H NMR (CDCl₃, 400 MHz) δ : 7.20 (m, 5H), 3.63 (t, J = 7.2 Hz, 4H), 2.88 (t, J = 7.2 Hz, 4H). ¹³C NMR (100 MHz, CDCl₃) δ : 139.0 (s), 128.9 (d), 128.3 (d), 126.2 (d), 71.9 (t), 36.3 (t).



(3-(tert-Butoxy)propyl)benzene (2.10e): According to general methods D/E ester **2.5e** (470 mg, 2.44 mmol) was converted to ether **2.10e** using 1.7 equivalents of DIBAL. Column chromatography (SiO₂, 1-5-10 Et₂O/hex) yielded a colorless oil; Yield 0.344 g, 73%; R_f = 0.52 (10% EtOAc/hex); IR (thin film) 2972, 1197, 1081 cm⁻¹; ¹H NMR (CDCl₃, 400 MHz) δ : 7.15 (m, 5H), 3.29 (t, J = 6.5 Hz, 2H), 2.61 (t, J = 7.4 Hz, 2H), 1.81 (t, J = 6.5 Hz, 1H), 1.77 (t, J = 7.4 Hz, 1H), 1.11 (s, 9H); ¹³C NMR (CDCl₃, 100 MHz) δ : 142.3 (s), 128.5 (d), 128.3 (d), 125.7 (d), 72.6 (s), 60.8 (t), 32.5 (t), 32.1 (t), 27.6 (q).

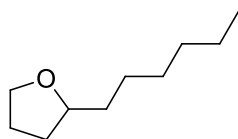


(2-(Cyclohexyloxy)ethyl)benzene (2.10g): According to general methods D/E ester **2.5g** (505 mg, 1.73 mmol) was converted to ether **2.10g** using 1.5 equivalents of DIBAL. Column chromatography (SiO₂, 1-5-10 Et₂O/hex) yielded a colorless oil; yield 0.24 g, 64%. Characterization data can be found at the provided reference.⁷⁷

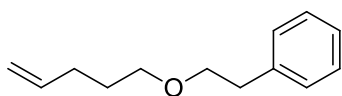


2-Phenyltetrahydrofuran (2.10h): According to general methods D/E ester **2.5h** (298 mg, 1.26 mmol) was converted to ether **2.10h** using 1.2 equivalents of DIBAL. Column chromatography (SiO₂, 1-5-10 Et₂O/hex) yielded a

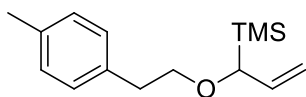
colorless oil; yield 0.11 g, 59%. Characterization data can be found at the provided reference.⁷⁸



2-Hexyltetrahydrofuran (2.10i): According to general methods D/E ester **2.5i** (293 mg, 1.20 mmol) was converted to ether **2.10i** using 1.2 equivalents of DIBAL. Column chromatography (SiO₂, 1-5-10 Et₂O/hex) yielded a colorless oil; yield 0.15 g, 80%. Characterization data can be found at the provided reference.⁷⁹

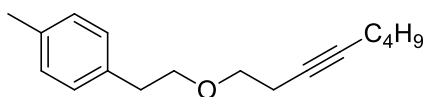


(2-(Pent-4-en-1-yloxy)ethyl)benzene (2.10k): According to general methods D/E ester **2.5k** (133 mg, 4.77 mmol) was converted to ether **2.10k** using 1.2 equivalents of DIBAL. Column chromatography (SiO₂, 1-5-10 Et₂O/hex) yielded a pale yellow oil; yield 0.052 g, 56%; R_f = 0.52 (10% EtOAc/hex); IR (thin film) 2936, 1640, 1109 cm⁻¹; ¹H NMR (CDCl₃, 100 MHz) δ : 7.24 (m, 5H), 5.80 (ddt, J = 17.0, 10.2, 6.7 Hz, 1H), 4.96 (m, 2H), 3.62 (t, J = 7.2 Hz, 2H), 3.45 (t, J = 6.6 Hz, 2H), 2.89 (t, J = 7.2 Hz, 2H), 2.10 (m, 2H), 1.66 (m, 2H). ¹³C NMR (CDCl₃, 100 MHz) δ : 139.1 (s), 138.3 (d), 128.9 (d), 128.3 (d), 126.2 (d), 114.7 (t), 71.8 (t), 70.3 (t), 36.4 (t), 30.3 (t), 28.9 (t).



Trimethyl(1-(4-methylphenethoxy)allyl)silane (2.10l): According to general methods D/E ester **2.5l** (644 mg, 1.91 mmol) was converted to ether **2.10l** using 1.2 equivalents of DIBAL. Column chromatography (SiO₂, 1-5-10 Et₂O/hex) yielded a colorless oil; yield 0.29 g, 61%; R_f = 0.64 (10% EtOAc/hex); IR (thin film) 2954, 1628, 1104 cm⁻¹; ¹H NMR (CDCl₃, 400 MHz) δ : 7.09 (m, 4H), 5.77 (ddd, J = 17.4, 10.5, 7.9 Hz, 1H), 4.98 (m, 2H), 3.82 (m, 1H), 3.54 (d, J = 6.9 Hz, 1H), 3.38 (m, 1H), 2.31 (s, 3H), 0.00 (s, 9H); ¹³C NMR (CDCl₃, 100

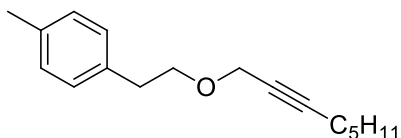
MHz) δ : 137.7 (d), 136.4 (s), 135.4 (s), 128.9 (d), 128.8 (d), 111.9 (t), 77.3 (d), 72.1 (t), 36.2 (t), 21.0 (q), -3.99 (q).



1-Methyl-4-(2-(oct-3-yn-1-yloxy)ethyl)benzene

(2.10m): According to general methods D/E ester

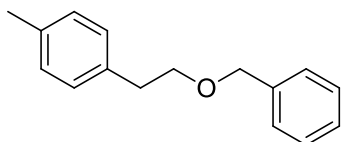
2.5m (553 mg, 1.66 mmol) was converted to ether **2.10m** using 1.2 equivalents of DIBAL. Column chromatography (SiO₂, 1-5-10 Et₂O/hex) yielded a colorless oil; yield 0.16 g, 39%; R_f = 0.46 (10% EtOAc/hex); IR (thin film) 2929, 1109 cm⁻¹; ¹H NMR (CDCl₃, 100 MHz) δ : 6.97 (m, 4H), 3.51 (t, J = 7.3 Hz, 2H), 3.40 (t, J = 7.2 Hz, 2H), 2.72 (t, J = 7.3 Hz, 2H), 2.29 (tt, J = 7.2, 2.4 Hz, 2H), 2.19 (s, 3H), 2.02 (tt, J = 7.0, 2.4 Hz, 2H), 1.30 (m, 4H), 0.77 (t, J = 7.2 Hz, 1H). ¹³C NMR (CDCl₃, 100 MHz) δ : 135.8 (s), 135.7 (s), 129.1 (d), 128.8 (d), 81.4 (s), 76.6 (s), 72.1 (t), 69.7 (t), 35.8 (t), 31.1 (t), 22.0 (t), 21.0 (q), 20.1 (t), 18.5 (t), 13.6 (q).



1-Methyl-4-(2-(oct-2-yn-1-yloxy)ethyl)benzene

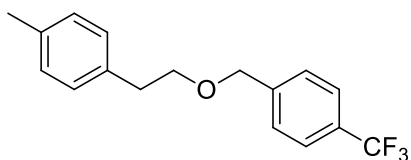
(2.10n): According to general methods D/E ester **2.5n**

(675 mg, 2.03 mmol) was converted to ether **2.10n** using 1.2 equivalents of DIBAL. Column chromatography (SiO₂, 1-5-10 Et₂O/hex) yielded a colorless oil; yield 0.11 g, 22%; R_f = 0.34 (10% EtOAc/hex); IR (thin film) 2931, 1081 cm⁻¹; ¹H NMR (CDCl₃, 100 MHz) δ : 7.11 (m, 4H), 4.14 (t, J = 2.2 Hz, 2H), 3.70 (t, J = 7.3 Hz, 2H), 2.88 (t, J = 7.3 Hz, 2H), 2.32 (s, 3H), 2.21 (tt, J = 7.1, 2.2 Hz, 2H), 1.52 (p, J = 7.1 Hz, 2H), 1.34 (m, 4H), 0.90 (t, J = 7.0 Hz, 3H). ¹³C NMR (CDCl₃, 100 MHz) δ : 135.7 (s), 135.6 (s), 129.1 (d), 128.7 (d), 70.8 (t), 58.7 (t), 35.7 (t), 31.0 (t), 29.7 (t), 28.3 (t), 22.2 (t), 21.0 (q), 18.6 (t), 14.0 (q).



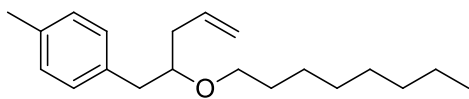
1-(2-(Benzyloxy)ethyl)-4-methylbenzene (2.10p):

According to general methods D/E ester **2.5p** (189 mg, 6.00 mmol) was converted to ether **2.10p** using 1.2 equivalents of DIBAL. Column chromatography (SiO₂, 1-5-10 Et₂O/hex) yielded a colorless oil; yield 0.053 g, 39%; R_f = 0.57 (10% EtOAc/hex); IR (thin film) 3025, 2919, 2856, 1099 cm⁻¹; ¹H NMR (CDCl₃, 100 MHz) δ : 7.0 (m, 5H), 7.10 (m, 4H), 4.59 (s, 2H), 3.66 (t, J = 7.2 Hz, 2H), 2.89 (t, J = 7.2 Hz, 2H), 2.31 (s, 3H); ¹³C NMR (CDCl₃, 100 MHz) δ : 138.5 (s), 135.8 (s), 135.7 (s), 129.1 (d), 128.8 (d), 128.4 (d), 127.7 (d), 127.6 (d), 73.0 (t), 71.5 (t), 36.0 (t), 21.9 (q).



1-Methyl-4-(2-((4-(trifluoromethyl)benzyl)oxy)ethyl)benzene (2.10q):

According to general methods D/E ester **2.5q** (531 mg, 1.39 mmol) was converted to ether **2.10q** using 1.2 equivalents of DIBAL. Column chromatography (SiO₂, 1-5-10 Et₂O/hex) yielded a colorless oil; yield 0.16 g, 36%; R_f = 0.42 (10% EtOAc/hex); IR (thin film) 2924, 1112, 1064 cm⁻¹; ¹H NMR (CDCl₃, 100 MHz) δ : 7.57 (d, J = 8.0 Hz, 2H), 7.40 (d, J = 8.0 Hz, 2H), 7.11 (m, 4H), 4.56 (s, 2H), 3.69 (t, J = 7.1 Hz, 2H), 2.90 (t, J = 7.1 Hz, 2H). ¹³C NMR (CDCl₃, 100 MHz) δ : 142.6 (s), 135.8 (s), 135.6 (s), 129.8 (s), 129.1 (d), 129.0 (d), 128.8 (d), 127.4 (d), 125.3 (q, J = 3.7 Hz)*, 72.1 (t), 71.8 (t), 35.9 (t), 21.0 (q). *Due to C-F splitting.



1-Methyl-4-(2-(octyloxy)pent-4-en-1-yl)benzene

(2.73): Ester **2.5a** (80 mg, 3.05 mmol) was added

to flame dried 10 mL round bottom flask that was purged with N₂ before being dissolved in DCM (1.0 M). The reaction was placed in a dewar before being cooled to -78⁰C using a dry ice and acetone bath. After cooling for 10 minutes 1.2 eq DIBAL was added

dropwise via syringe. The reaction stirred an additional 10 minutes before allyl silane (2.5 eq.) was added dropwise via syringe. The reaction stirred for 10 minutes before adding TMSOTf (2.5 eq.) dropwise via syringe. The reaction stirred for 1.25 hours and was monitored by TLC. The reaction was quenched with saturated aqueous NaHCO_3 and allowed to warm to RT before being added to DCM. The water was extracted three times with DCM, and the combined organic layers were dried over Na_2SO_4 , filtered, and concentrated in vacuo. Column chromatography (SiO_2 , 1-5-10 Et_2O /hex) yielded a colorless oil; yield 0.048 g, 55%; $R_f = 0.52$ (10% EtOAc /hex); IR (thin film): 2923, 2854, 1640, 1096 cm^{-1} ; ^1H NMR (CDCl_3 , 400 MHz) δ : 7.09 (m, 4H), 5.86 (ddt, $J = 18.0$, 9.5, 7.0 Hz, 1H), 5.07 (m, 2H), 3.47 (q, $J = 6.0$ Hz, 1H), 3.43 (dt, $J = 8.8$, 6.5 Hz, 1H), 3.33 (dt, $J = 8.8$, 6.5 Hz, 1H), 2.77 (dd, $J = 13.7$, 6.6 Hz, 1H), 2.69 (dd, 13.7, 6.0 Hz, 1H), 2.32 (s, 3H), 2.23 (m, 2H), 1.49 (p, $J = 6.8$ Hz, 2H), 1.24 (m, 10H), 0.88 (t, $J = 6.7$ Hz, 3H); ^{13}C NMR (CDCl_3 , 100 MHz) δ : 136.0 (s), 135.4 (s), 135.2 (d), 129.4 (d), 128.9 (d), 116.9 (d), 80.5 (d), 69.6 (t), 40.1 (t), 38.2 (t), 31.7 (t), 30.1 (t), 29.4 (t), 29.3 (t), 26.2 (t), 22.7 (t), 21.0 (q), 14.1 (q)

CHAPTER III - SYNTHESIS AND DERIVITIZATION OF QUINOLINE SCAFFOLDS FOR THE USE AS SMALL MOLECULE HIV-1 INTEGRASE INHIBITORS

3.1 Introduction

3.1.1 The Global Impact of HIV/AIDS – An Introduction to HIV-1

The initial diagnosis of the Human Immunodeficiency Virus (HIV), formerly known as Lymphadenopathy Associated Virus (LAV), was the beginning of one of the largest calls for research in present day history. Its discovery in 1981, followed by isolation in 1983 and protein sequencing in 1985, led to the foundation of research for one of the largest biological puzzles. Although HIV-1 is rarely the cause of death, it severely weakens the immune system allowing for other infections, such as pneumonia, to become lethal. The secondary infections of those infected with HIV have been the cause of death of approximately 35 million people, and 1.8 million new individuals are infected every year.⁸⁰

The origin of HIV-1 and HIV-2 can be traced back to the common chimpanzee and the sooty mangabey, respectively.⁸² It is thought that the first transfer of HIV-1 to humans was through the consumption of the flesh of these primates as they are commonly hunted in west equatorial Africa. Now, HIV-1 can be transmitted through the transfer of bodily fluids, such as blood transfusions, sexual intercourse, needle sharing, and mother to fetus transmission.⁸³ Roughly 25% of those infected with HIV-1 are unaware that they have contracted the virus and so continue to spread it. The highest concentration of HIV-1 is in Africa, which has some of the highest poverty levels and drug usage,⁸⁴ as well as restricted access to health care and contraceptives.⁸⁵

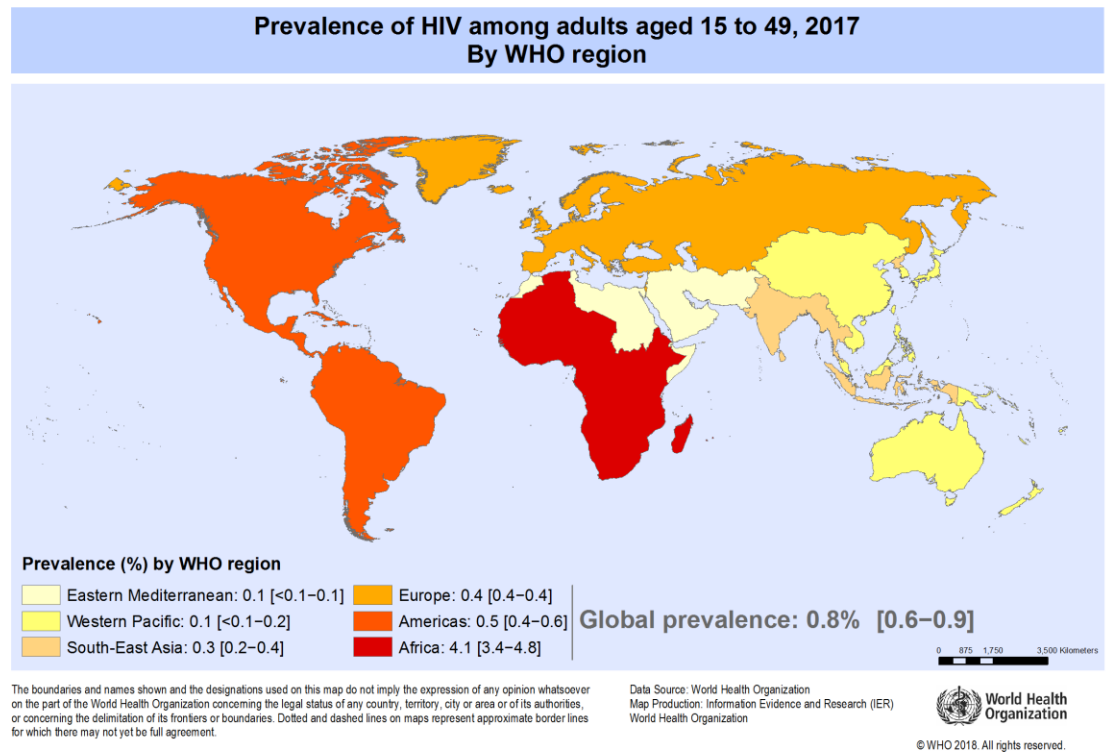


Figure 3.1 Map of HIV prevalence in adults⁸¹

3.1.2 Current Modes of Treatment for HIV-1

Currently, 59% of individuals with HIV are on some form of antiretroviral treatment. The most common type of treatment for HIV-1 is Highly Active Antiretroviral Therapy (HAART). HAART was first developed in 1996 and has led to a drastic decline of HIV-1 advancing to AIDS and related deaths, increasing the lifespan of an individual infected with HIV to approximately 46 years.⁸⁶ By using a combination of treatments, HAART has been able to effectively slow the replication of HIV-1, however, it cannot completely halt the virus. The first approved HIV drug, AZT, a nucleotide reverse transcriptase inhibitor (NRTI), is one of many types of HIV treatments that play a role

in HAART therapy. Other types of compounds used in HAART therapy include non-nucleotide reverse transcriptase inhibitors (nNRTI), and integrase strand transfer inhibitors (INSTI). Additionally, pharmacokinetic enhancers can be added to increase the effectiveness of the other components by manipulating the liver enzymes responsible for breaking them down.

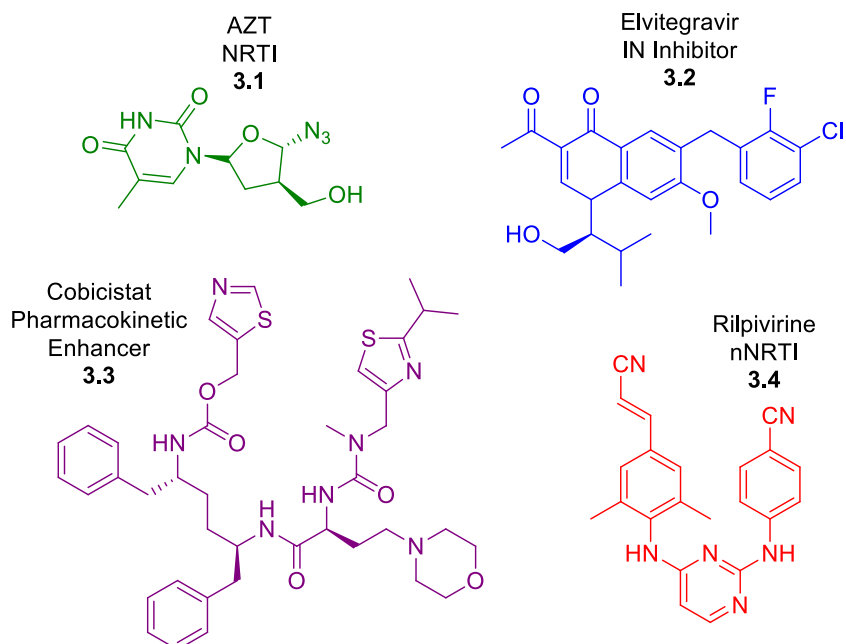


Figure 3.2 Common components in HAART HIV-1 treatments

The reason for the cocktail of drug treatment regimen is due to HIV's ability to mutate during its replication cycle. Because of this, researchers have had to develop multiple synthetic drug analogs that can inhibit the HIV-1 virus at various steps in the replication process. As shown in Table 3.1, there are several HAART variants on the market. Most HIV-1 patients will take several HAART treatments over their lifetime as HIV-1 continues to mutate and develop drug resistance.

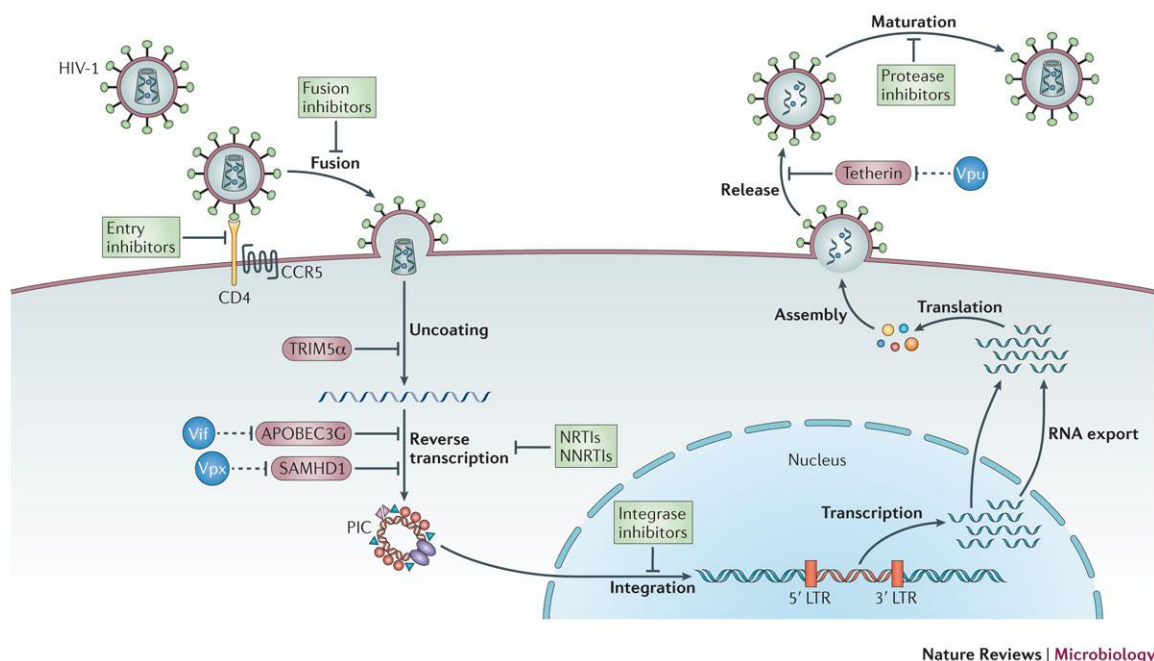
Table 3.1 List of common HAART HIV-1 treatments

Name	NRTI	nNRTI	INSTI	Pharmacokinetic enhancer
Triumeq	abacavir	lamivudine	dolutegravir	--
Juluca	--	rilpivirine	dolutegravir	--
Stribild	tenofovir disoproxil fumarate/emtricitabine	--	elvitegravir	cobicistat
Genvoya	tenofovir alafenamide/emtricitabine	--	elvitegravir	cobicistat
Atripla	tenofovir disoproxil fumarate/emtricitabine	efavirenz	--	--
Complera	tenofovir disoproxil fumarate/emtricitabine	rilpivirine	--	--
Odefsey	tenofovir alafenamide/emtricitabine	rilpivirine	--	--
Biktarvy	tenofovir alafenamide/emtricitabine	--	bictegravir	--

3.1.3 HIV-1 Lifecycle and Mechanism of Attack

Within the lifecycle of HIV-1, there are many steps in which researchers are actively studying to better understand the virus. The four main steps in HIV-1 replication are: fusion into the host cell wall, reverse transcription of the viral RNA, integration and transcription of the viral RNA to DNA, and then finally release and maturation of the new HIV-1 virus.⁸⁷

There are multiple pharmaceutical drugs that have been used as fusion, entry, NRTIs, inhibition/transcription, and maturation inhibitors. However, there are only three known FDA-approved IN inhibitors: dolutegravir (DVG), elvitegravir (EVG), and raltegravir (RAL). Due to HIV-1's ability to rapidly mutate, drug resistant strands against RAL and EVG have already appeared.⁸⁸ Fortunately, there have been no reports of resistance to DVG, however, it is only likely only a matter of time.



Nature Reviews | Microbiology

Figure 3.3 HIV lifecycle⁸⁷

3.1.4 HIV-1 Inhibition of the Catalytic Core Domain

IN is the enzyme responsible for inserting viral DNA (vDNA) into the host cell DNA and has two catalytic activities: 3' processing and DNA strand transfer,⁸⁹ both of which are catalyzed by either Mg^{2+} or Mn^{2+} .⁹⁰ The vDNA molecule exists in the form of a pre-integration complex (PIC). Once the PIC gains access to the nuclear compartments of the host's cell, the vDNA ends are inserted into the cellular chromosome, which is initiated by IN and completed by the host cell DNA.⁹¹ IN consists of three structural domains: the N-terminal domain (NTD), the catalytic core domain (CCD), and the C-terminal domain (CTD).⁹² The NTD folds into a compact three-helical bundle stabilized by coordination of a Zn^{2+} ion by histidine and cystine residues.⁹³ During integration, the NTD and the CTD make important interactions with DNA substrates, while the CCD harbors the active site for integration of the vDNA.⁹¹

The active site of HIV IN is key for viral mutations to occur, which is why it is essential to explore other inhibition sites on the enzyme.⁹⁴ HIV IN operates in a tetrameric form, where two dimers are separately formed at the CCD interface for vDNA interactions.⁹⁵ Lens epithelium-derived growth factor (LEDGF) and endogenous transcriptional coactivator (p75) promote the interaction between dimers within an allosteric binding pocket. This interaction has been shown to be a vital factor in HIV vDNA integration via the C-terminal integrase binding domain (IBD).⁹⁶⁻⁹⁸ This allosteric site has been of interest as a new inhibition site to potentially prevent this LEDGF/p75 binding interaction and ultimately inhibit vDNA integration.⁹⁹ Recent studies have shown that the use of small molecule inhibitors to interact with the IN dimer interface at the IBD binding site enable an immediate multimerization of the enzyme, rendering it unable to participate in vDNA integration.¹⁰⁰⁻¹⁰¹

3.1.5 Quinoline Scaffolds as HIV-1 Inhibitors

Recently, two candidates for IN inhibition have been shown to target the LEDGF/p75 binding interactions in the CCD, quinoline scaffolds **3.7**¹⁰² and **3.8**¹⁰³ (Figure 3.4).

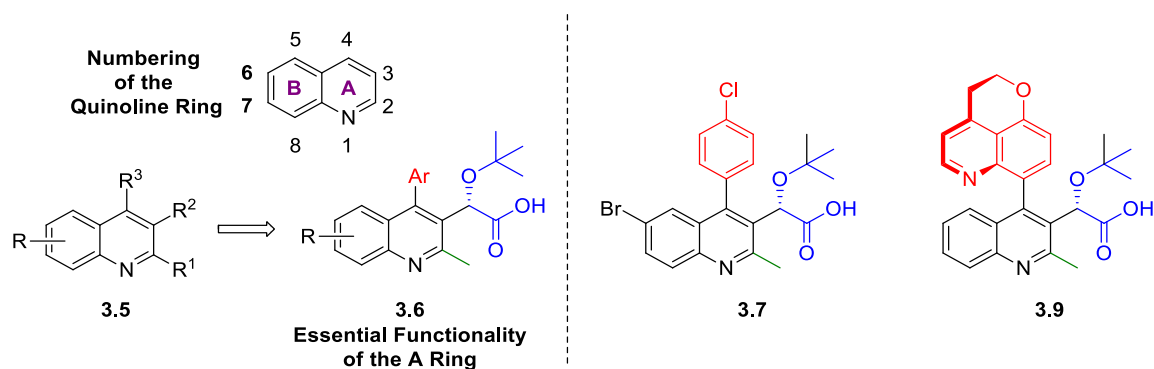


Figure 3.4 Trisubstituted biaryl quinoline scaffolds with quinoline structure notation

Figure 3.5, part A depicts the ribbon representation of the crystal structure for **3.7** within the integrase (IN) CCD binding pocket. In part B, the amino acids Trp 132 and Leu 102 are seen to interact with the aromatic ring in the northern region of the binding pocket and the acetic acid residue in the eastern region of the binding pocket of **3.7**. An understanding of the relevant noncovalent and steric interactions within this binding pocket can be assessed through manipulation of the aromatic substitution at the 4-position of the quinoline scaffold. To accomplish this, a library of 4-biaryl quinolines will be synthesized and a structure activity relationship (SAR) study will be carried out.

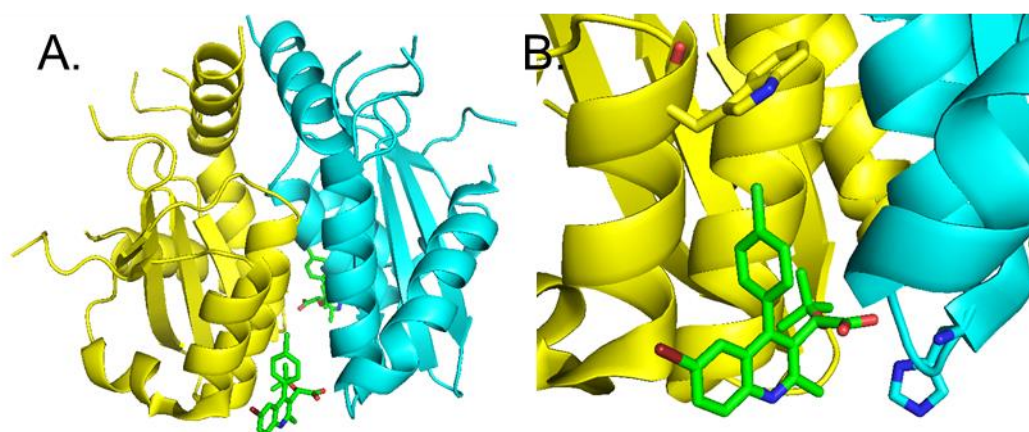
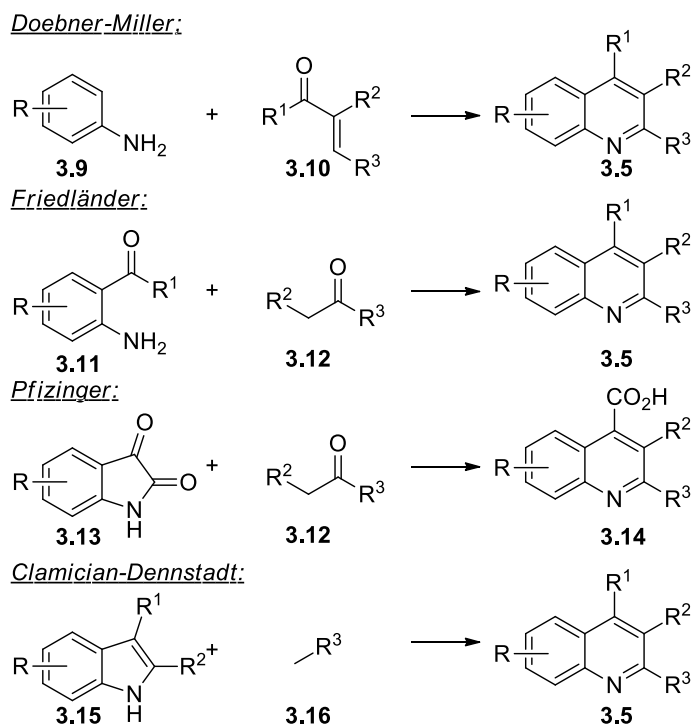


Figure 3.5 Ribbon representation of the IN CCD dimer with quinoline **3.7**

3.1.6 Synthesis of the Quinoline Scaffold

Approximately 60% of all FDA approved drugs contain a nitrogen heterocycle. The quinoline scaffold is the 4th most common six-membered aromatic nitrogen heterocycle and is found in 2% of FDA approved prescription drugs.¹⁰⁴ There are several synthetic strategies for synthesizing unsubstituted,¹⁰⁵ mono-substituted,¹⁰⁶ di-substituted,¹⁰⁷⁻¹⁰⁹ and tri-substituted quinolines,¹¹⁰⁻¹¹² that have been prepared from aniline, anthranilic, indole, and isatin derivatives, respectively (Scheme 3.1). Variations

of these methods include, but are not limited to: electrophilic,¹¹³⁻¹¹⁴ oxidative,¹¹⁵ iodine-catalyzed,¹¹⁶ and aza-Wittig cascade reactions.¹¹⁷



Scheme 3.1 A variety of synthetic strategies for the synthesis of quinolines

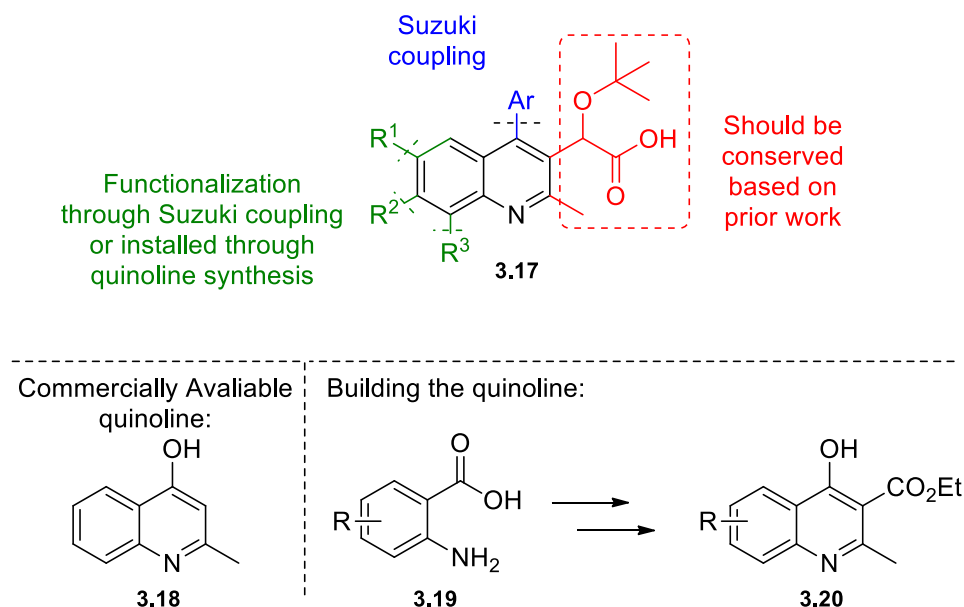
3.2 Research Hypothesis

Manipulation of the 4-position in the quinoline scaffold will enhance the noncovalent interaction of the allosteric IN site leading to the inhibition of IN. This will be accomplished through the development of a route to access a quinoline scaffold that can be derivatized at a later stage. The synthesized trisubstituted biaryl quinolines will be submitted to a IN multimerization assay to prove the potency of the compounds.

3.3 Research Design and Methods

3.3.1 Precursors for the Quinoline Scaffold

Biaryl quinolines such as **3.7** and **3.8** have been demonstrated inhibitory activity against HIV IN.¹⁰³ SAR studies revealed that the methyl and acetic acid residue at the 2- and 3-positions of the quinoline ring proved essential to inhibition, whereas the remaining substitutions at the 4-, 6-, 7-, and 8-positions enhance the potency. The two planned precursors to access the quinolines is shown in Scheme 3.2. Commercially available quinoline **3.18** will allow for derivatization specifically at the 4-position via a Suzuki coupling reaction. Various aryl groups will be installed, which will allow for exploration of the noncovalent interactions in the nonpolar pocket that are deemed essential for IN inhibition. To be able to study functionalization at the 6-, 7-, and 8-positions and probe noncovalent interactions in those regions, quinoline scaffold **3.20** will be synthesized starting from anthranilic acid derivatives (such as **3.19**), which can be converted via an isatoic anhydride intermediate.¹¹⁸ The approach to install the acetic acid residue also differs in both routes. Starting from quinoline **3.18** requires a Grignard reaction to add the two carbons of the side chain as an electrophile whereas the anthranilic acid route will intercept quinoline **3.20** and add the side chain via a one-carbon nucleophile.



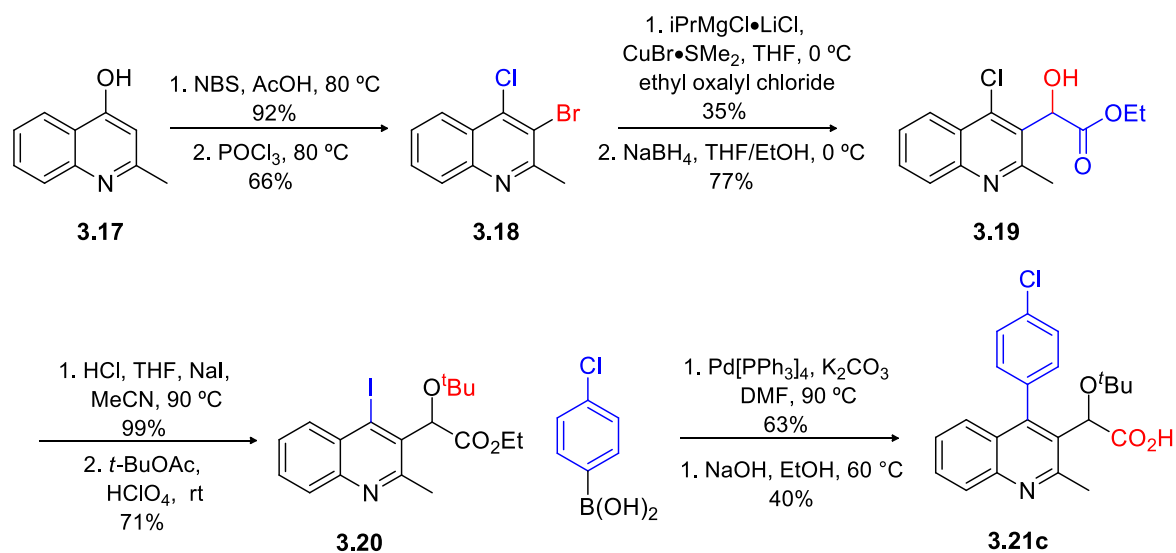
Scheme 3.2 Synthetic analysis of quinoline scaffold **3.17**

3.4 Results and Discussion

3.4.1 Forward Synthesis of the 4-Substituted Quinolines

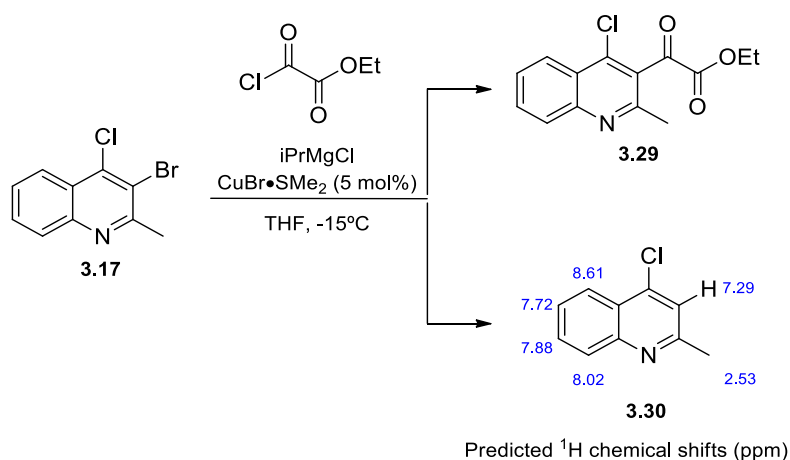
The 4-aryl quinoline derivatives were the initial targets as the route was previously developed by the Boehringer Ingelheim process group.¹¹⁹ The route begins with commercially available 4-hydroxyquinoline **3.18** and utilizes a late stage intermediate **3.20** that can be derivatized using a Suzuki coupling reaction.

At the beginning of this reaction sequence, bromination of 4-hydroxy-2-methyl quinoline **3.17** at the 3-position of the quinoline was successful and selective utilizing NBS in the presence of acetic acid at 80 °C (92% yield). This was followed by chlorination of the alcohol using neat POCl₃ to produce **3.18** in 66% yield. With the bromine and chlorine installed, the next step was to secure the necessary ethyl oxalate chloride at position 3 via a selective halogen-metal exchange.



Scheme 3.3 Synthesis of trisubstituted biaryl quinolines

A Grignard of **3.18** was formed in the presence of isopropyl magnesium chloride and a copper (I) bromide dimethylsulfide complex. Although complete conversion of **3.18** was observed, it was determined that a dehalogenated byproduct **3.30** was also forming (Scheme 3.4). Attempts to scale the reaction resulted in an increase in the formation of **3.30**. Reactions were therefore kept below 1 g to prevent the formation of **3.30**. Due to difficulties in purification, only low yields were obtained (35%).

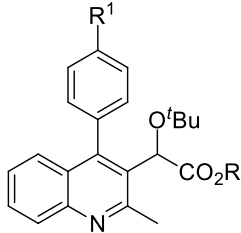
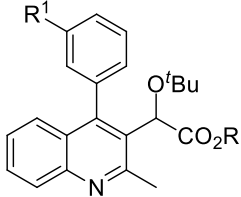
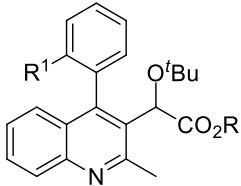


Scheme 3.4 Grignard addition with byproduct formation

Sodium borohydride reduction of the ketone produced α -hydroxy ester **3.19** in 77% yield and was followed by a Finkelstein trans-halogenation converting the 4-chloro to 4-iodo in 63% yield. The use of HCl is to form the protonated quinoline, thereby making it a better electrophile for displacement of the chlorine by iodine. Subsequent etherification via perchloric acid and *t*-butylacetate produced **3.20** in 71% yield and provided a bench stable intermediate prior to the derivatization step.

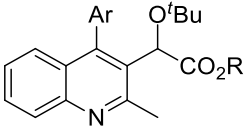
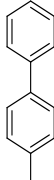
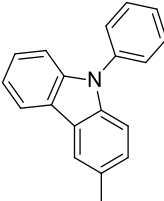
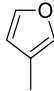
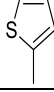
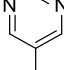
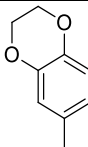
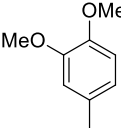
The final two steps involved a Suzuki coupling of commercially available aryl boronic acids at the 4-position of **3.20** followed by saponification of the ester to produce the acetic acid side chain. Table 3.2 shows a summary of the synthesized biaryl quinolines with ortho-, meta-, and para-substitutions. A variety of heterocyclic compounds is shown in Table 3.3. Yields for the Suzuki coupling and saponification ranged from 38-99% and 11-99%, respectively. No clear trend in yields could be determined regarding substrate or the positioning of the group on the ring.

Table 3.2 Summary of phenyl-substituted biaryl quinolines yields

<div style="display: flex; justify-content: space-around; align-items: center;"> <div style="text-align: center;">  <p>Para R=Et: 3.25a-j, l R=H: 3.21a-j, l</p> </div> <div style="text-align: center;">  <p>Meta R=Et: 3.26b-j R=H: 3.22b-j</p> </div> <div style="text-align: center;">  <p>Ortho R=Et: 3.27b-d, f-i, k R=H: 3.23b-d, f-i, k</p> </div> </div>								
Entry	R ¹		Para ^b		Meta ^b		Ortho ^b	
			3.25	3.21	3.26	3.22	3.27	3.23
1	a	H	55%	40%	--	--	--	--
2	b	F	67%	76%	83%	35%	85%	54%
3	c	Cl	63%	40%	92%	92%	84%	96%
4	d	CH ₃	49%	51%	91%	11%	98%	93%
5	e	CF ₃	51%	99%	68%	51%	--	--
6	f	OCH ₃	63%	57%	75%	54%	97%	14%
7	g	SCH ₃	97%	75%	78%	53%	56%	12%
8	H^a	OCF ₃ ^b	94%	57%	87%	86%	73%	13% 11%
9	i	CN	80%	34%	73%	49%	38%	56%
10	j	COCH ₃	63%	57%	50%	13%	--	--
11	k	CHO	--	--	--	--	70%	10%
12	l	NHCOCH ₃	67%	9%	--	--	--	--

Note: a) **3.23h** had two diastereomer that were separated and analyzed individually. b) all yields are of the purified compounds

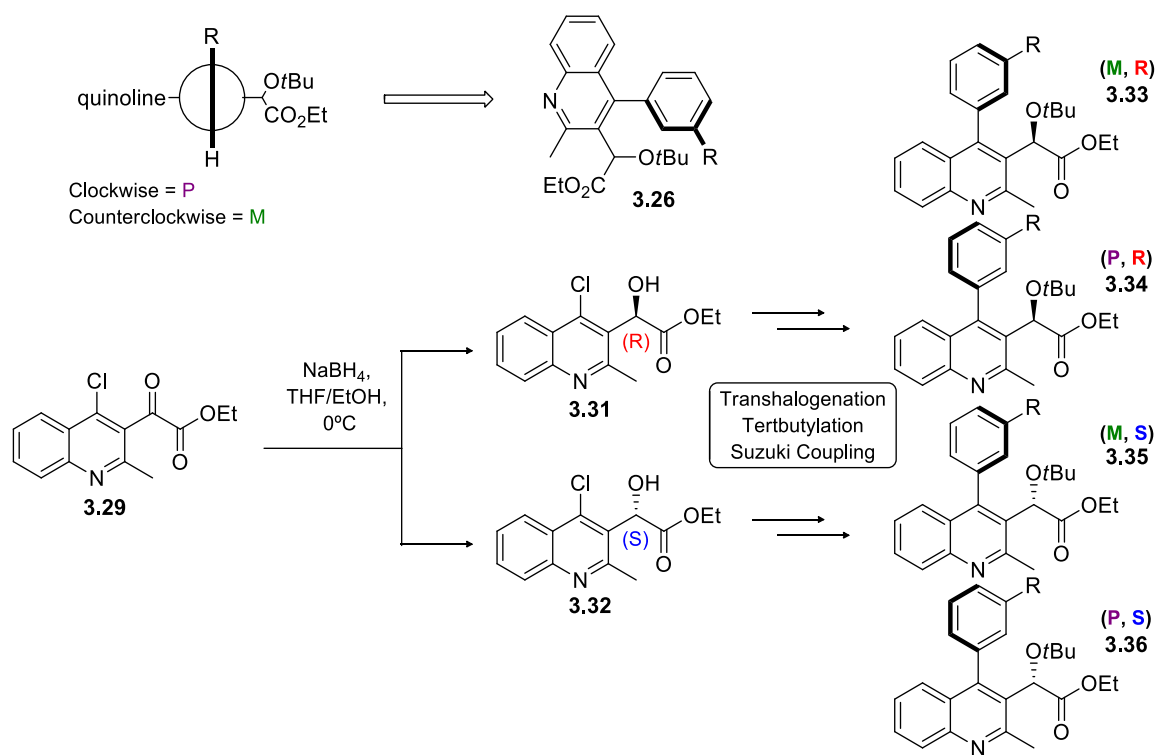
Table 3.3 Summary of heterocyclic and bicyclic biaryl quinoline yields

<div style="text-align: center;">  <p>Heterocyclic R=Et: 3.28a-g R=H: 3.24a-g</p> </div>				
Entry	Quinoline	R ¹	% Yield ^a 3.28	% Yield ^a 3.24
1	3.24a		59%	77%
2	3.24b		38%	86%
3	3.24c		99%	99%
4	3.24d		59%	59%
5	3.24e		72%	78%
6	3.24f		80%	78%
7	3.24g		52%	84%

Note: a) all yields are of the purified compounds

Substrates were analyzed as racemic mixtures, with the chiral center at the apex of the acetic acid residue. In addition, ortho- and meta-substituted compounds also formed two atropisomers. Atropisomers are stereoisomers with hindered rotation about a sigma

bond, where the energy differences due to steric strain or other contributors create a barrier of rotation making it possible for the isolation of the individual conformers.¹²⁰ Although enantiomers are indistinguishable by NMR, the addition of a rotational barrier creates an axis of chirality resulting in diastereomers that can be distinguished by NMR. All stereoisomers would be expected to interact differently in the protein binding pocket. Atropisomers were observed for the 2-trifluoromethoxy **3.23h-1** and **3.23h-2** derivatives which were analyzed separately where **3.23h-1** had an inhibition of 2.69 μ M, and **3.23h-2** showed no activity (Table 3.4).



Scheme 3.5 Synthesis of quinoline atropisomers, and their naming convention

3.4.2 Structural Elucidation of Biaryl Quinoline Scaffolds

Due to the complexity of the biaryl quinolines, all structures were characterized by 2D NMR in addition to ^1H , ^{13}C , DEPT, and IR. The structural elucidation of para derivative **3.21c** will be discussed first, as it was used to help understand the more complicated ortho and meta derivatives. In the case of the para substituent **3.21c**, the ^{13}C NMR and DEPT data revealed the presence of 22 unique carbons, including three methyls, one methylene (alkyl), nine methines (one alkyl, eight aryl), and nine quaternary carbons (one alkyl, eight aryl). COSY confirmed H_{12} to H_{14} connectivity on the aromatic ring and for the ethyl group. The eastern side of the quinoline scaffold was confirmed by HMBC with H_{21} correlating to carbons 2 and 9 while H_{18} correlated to carbons 1, 2, 4, and 9. Other key correlations included H_{10} to carbons 3, 14, 15, and H_{12} to 14, 15, providing the western side of the quinoline scaffold. The northern aromatic ring was slightly more complicated as COSY crosspeaks could not be identified due to overlapping of the ^1H aromatic signals. The key correlation showing connectivity of the northern region to the quinoline was observed between H_7 and carbon 4.

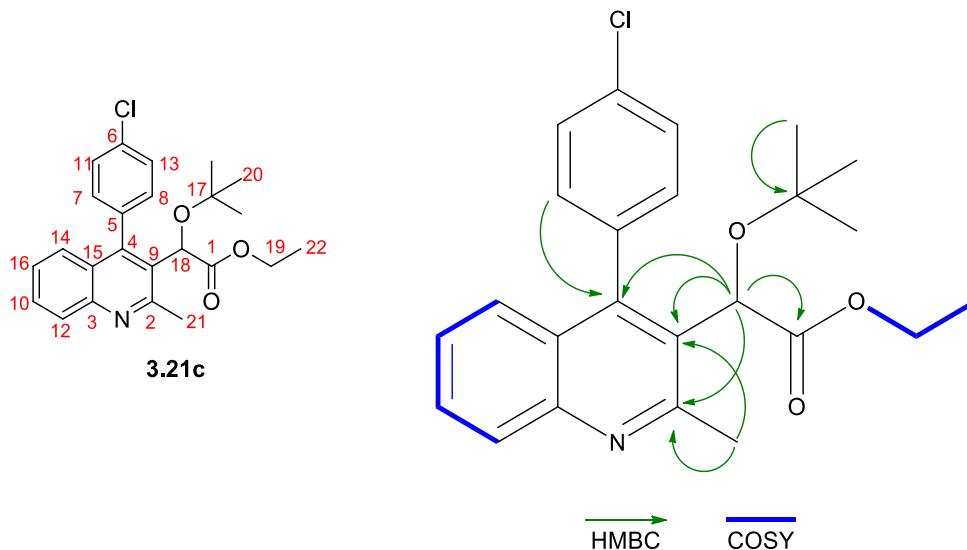


Figure 3.6 ^1H and ^{13}C assignments with HMBC and COSY correlations for **3.21c**

Elucidation became much more difficult when dealing with the formation of atropisomers. Most carbon peaks essentially double, which made identifying single carbon signals that belong to each isomer much more difficult. It also caused a lot of overlapping peaks in the ^1H and ^{13}C spectra (atropisomers **3.23c-1** and **3.23c-2** are used for example as in Figure 3.7). Therefore, DEPT NMR became essential with the ability to distinguish quaternary carbons. When DEPT-135 was used to analyze the spectra, the quaternary carbons disappeared. If DEPTq was used, then the quaternary carbons would have a 180° phase separation and appear upside down. Also, with the para-derivatives already elucidated, ^{13}C NMR chemical shifts similarities were able to be used as a guide for both the ortho- and meta-derivatives. An additional resource *Structural Determination of Organic Compounds* by Ernő Pretsch,¹²¹ was also heavily consulted to estimate where carbon shifts would occur.

For atropisomers **3.23c-1** and **3.23c-2**, COSY was used to identify 3 isolated spin systems: the protons of the quinoline scaffold, as well as the ethyl chain, and H_9 and H_{13}

on the northern ring (H₇ and H₈ were overlapping). Hydrogens H₁₈ and H₂₁ were again key in determining the eastern side of the quinoline scaffold by HMBC with H₁₈ → carbons 1, 2, 4, and 11 and H₂₁ → carbons 2 and 11. For the northern aromatic ring, H₉ correlated with carbon 6. The Pretsch book was utilized to determine the location of carbons 3, 5, and 6, which were the final assignments necessary to solve the elucidation.

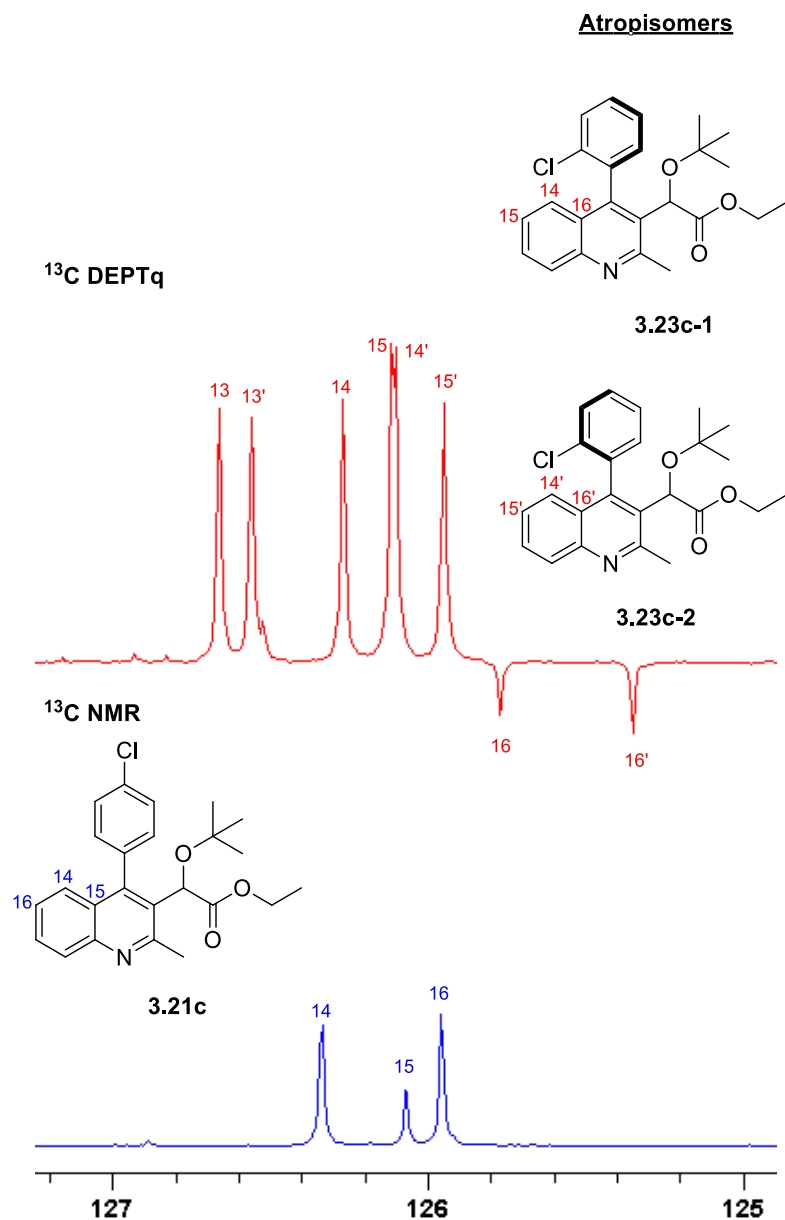


Figure 3.7 Comparison of **3.21c** and **3.23c-1** and **3.23c-2** ¹³C NMR spectral regions

Table 3.4 contains the structural assignments for **3.21c** and **3.23c-1** and **3.23c-2**, including ^1H coupling constants.

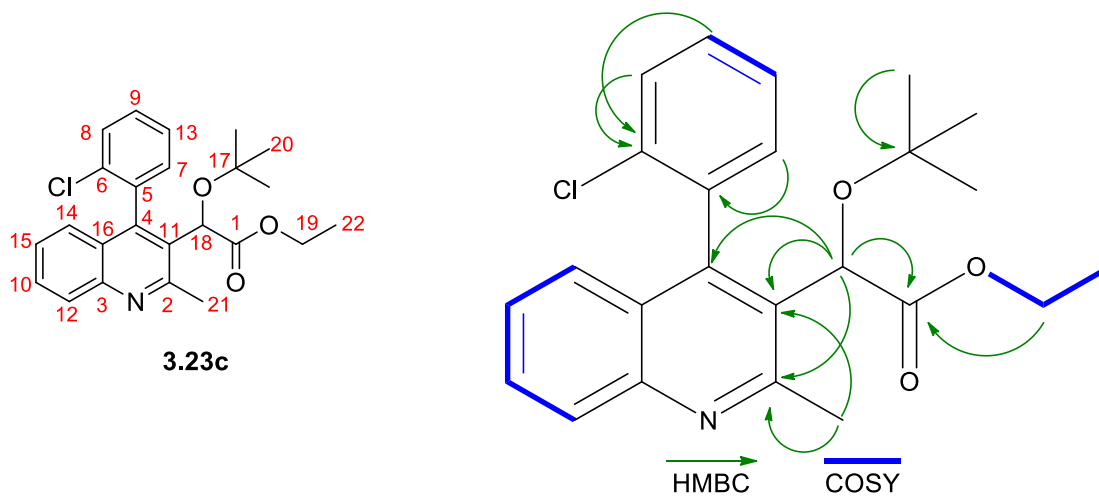


Figure 3.8 ^1H and ^{13}C assignments with HMBC and COSY correlations for **3.23c**

Table 3.4 ^1H and ^{13}C NMR Data of **3.21c** and **3.23c**

Entry	3.21c						3.23c-1 and 3.23c-2^a					
	δ_{c} (ppm)	m	δ_{H} (ppm)	m	J (Hz)	#H	δ_{c} (ppm)	m	δ_{H} (ppm)	m	J (Hz)	#H
1	172.4	s	-----	--	-----	--	172.50, 171.82	s	-----	--	-----	
2	159.4	s	-----	--	-----	--	159.61, 159.55	s	-----	--	-----	
3	146.8	s	-----	--	-----	--	146.67, 146.58	s	-----	--	-----	
4	145.2	s	-----	--	-----	--	144.36, 144.92	s	-----	--	-----	
5	134.7	s	-----	--	-----	--	137.25, 137.14	s	-----	--	-----	
6	134.6	s	-----	--	-----	--	134.99, 134.96	s	-----	--	-----	
7	132.3	d	7.47	dd	8.8, 2.4	1	133.84, 133.64	d	7.53-7.24	m	-----	1
8	131.2	d	7.28	m	-----	1	130.18, 129.94	d	7.53-7.24	m	-----	1
9	129.6	s	-----	--	-----	--	129.88, 129.86	d	7.56	m	-----	1
10	129.3	d	7.66	ddd	8.3, 6.8, 1.4	1	129.46, 129.37	d	7.64	ddd	8.3, 6.8, 1.4	1
11	128.8	d	7.53	m	-----	1	129.43, 129.34	s	-----	--	-----	
12	128.7	d	8.04	d	8.1	1	128.61, 128.53	d	8.05	d	8.4	1
13	128.3	d	7.53	m	-----	1	126.66, 126.56	d	7.53-7.24	m	-----	1
14	126.3	d	7.28	m	-----	1	126.28, 125.95	d	7.17	m	-----	1
15	126.1	s	-----	--	-----	--	126.11, 126.10	d	7.53-7.24	m	-----	1
16	125.9	d	7.37	ddd	8.3, 6.8, 1.2	1	125.77, 125.35	s	-----	--	-----	
17	76.1	s	-----	--	-----	--	76.27, 75.84	s	-----	--	-----	
18	70.8	d	5.10	s	-----	1	71.26, 70.84	d	5.11, 5.08	s		1
19	61.4	t	4.19	dq	10.8, 7.2	2	61.34, 61.84	t	4.10	m		2
20	28.1	q	1.00	s	-----	9	28.16, 27.95	q	1.11, 1.05	s	-----	9
21	24.9	q	2.85	s	-----	3	25.32, 24.97	q	3.00, 2.90	s	-----	3
22	14.2	q	1.23	t	7.2	3	14.13, 13.99	q	1.22, 1.15	t	7.1	

Note: a) **3.23c** was isolated as a 1:0.97 mixture of atropisomers

Analysis of the atropisomers proved to be quite difficult in some cases where other NMR phenomena interfered such as ^{13}C - ^{19}F couplings. Coupling of a single carbon signal would split two-fold due to the ^{13}C - ^{19}F coupling as well as the presence of the atropisomer giving a total of 4 peaks per carbon for the ring system with the associated fluorine. Therefore, ^{13}C - ^{19}F coupling constants became a key tool to determine carbon assignments, which can be seen in Figure 3.9.

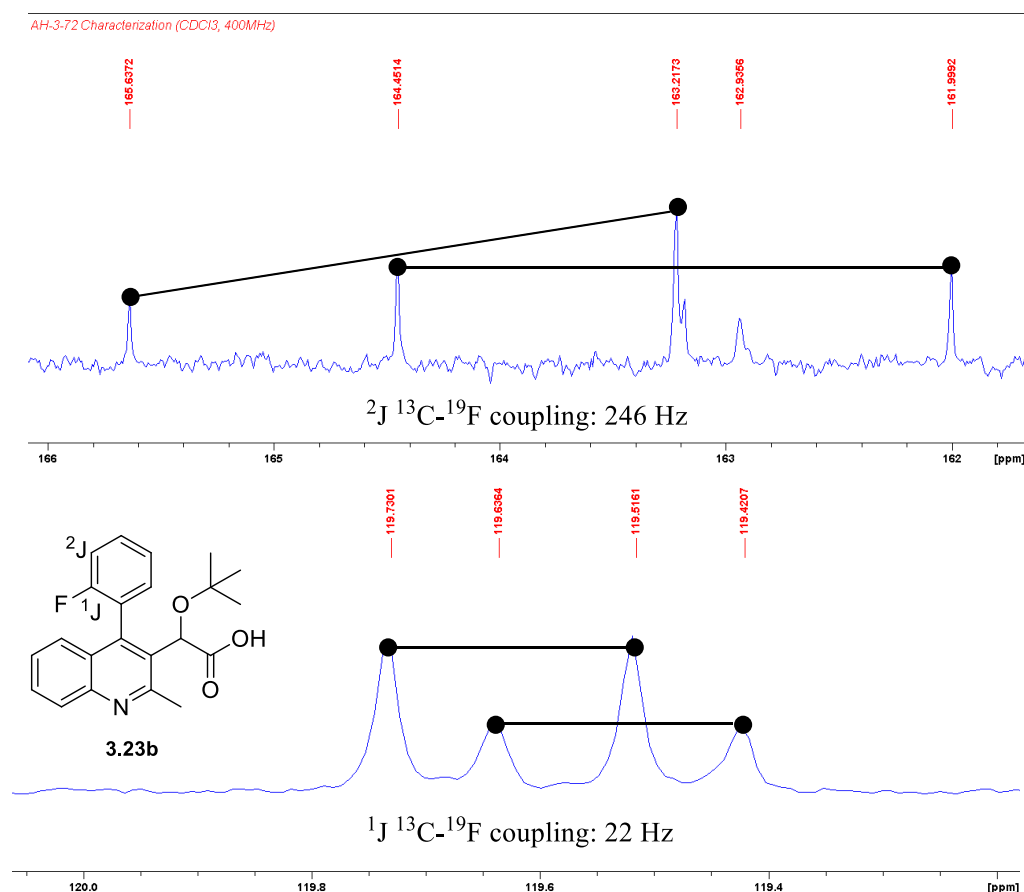


Figure 3.9 Carbon-fluorine couplings

3.4.3 Multimerization Assay

Due to the nature of these compounds to interact with IN at the dimer interface in the LEDGF/p75 binding pocket, they cause inhibition of the IN-LEDGF/p75 binding and

therefore aberrant IN multimerization.¹²² Quinolines **3.21** – **3.24** were submitted to a homogeneous time-resolved fluorescence (HTRF) based assay, which allows for the determination of EC₅₀ values for inhibitor-induced formation of higher order HIV-1 IN multimers. The assay involves the use of two recombinant IN enzymes containing either a hexahistidine (6xHis) tag or the FLAG epitope at the protein's N-terminus. Antibodies (anti-6xHis-XL665 and anti-FLAG-EuCryptate) that recognize and bind to the respective 6xHis and FLAG tags are added to measure the time-resolved fluorescence resonance energy transfer between the XL665 and EuCryptate fluorophores upon IN multimerization. Compounds that induce IN multimerization have an increased corresponding Förster resonance energy transfer (FRET) signal. Moreover, titration of a test compound into the assay will yield the EC₅₀ value for IN multimerization.¹²³ The data from this assay is presented in the following section. Compounds that have lower concentration values have greater multimerization and inhibition capabilities.

3.4.4 Structure Activity Relationships of Quinoline Substrates

The 4-phenylquinoline (**3.21a**, R¹ = H, entry 1) was used as a standard for the relative comparison of the ortho-, meta-, and para-substituted substituents. Looking at the para series, substitution of a methyl group at the 4-position (**3.21d**, R¹ = CH₃, entry 4) caused a 6-fold decrease in EC₅₀ value, indicating significant ability to inhibit IN. Alternatively, by substituting the methyl hydrogens for fluorine (**3.21e**, R¹ = CF₃, entry 5) also lessened the inhibitory capacity of the quinoline 3-fold. Additionally, 4-methoxy **3.21f** and 4-fluoromethoxy **3.21h** continued this trend yet to a lesser extent. Insertion of a halogen substituent as in **3.21b** and **3.21c** showed a significant increase in inhibition with

the 4-chloro (**3.21c**) derivative having the best inhibition of the series with an EC₅₀ value of 100 nM.

Table 3.5 SAR for substituted aromatic biaryl quinolines

<div style="display: flex; justify-content: space-around; align-items: center;"> <div style="text-align: center;"> <p>Para 3.21a-j, l</p> </div> <div style="text-align: center;"> <p>Meta 3.22b-j</p> </div> <div style="text-align: center;"> <p>Ortho 3.23b-d, f-i, k</p> </div> </div>							
Entry	R ¹	Para		Meta		Ortho	
1	H	3.21a	1.32 ± 0.53	--		--	
2	F	3.21b	0.49 ± 0.04	3.22b	2.11 ± 0.59	3.23b	0.58 ± 0.07
3	Cl	3.21c	0.10 ± 0.02	3.22c	3.79 ± 0.59	3.23c	0.26 ± 0.04
4	CH ₃	3.21d	0.24 ± 0.11	3.22d	0.95 ± 0.29	3.23d	0.51 ± 0.05
5	CF ₃	3.21e	0.72 ± 0.06	3.22e	7.33 ± 0.97	--	
6	OCH ₃	3.21f	0.23 ± 0.04	3.22f	1.38 ± 0.37	3.23f	8.39 ± 0.92
7	SCH ₃	3.21g	0.49 ± 0.01	3.22g	1.00 ± 0.14	3.23g	4.51 ± 0.71
8	OCF ₃	3.21h	0.35 ± 0.09	3.22h	3.34 ± 0.19	3.23h-1 2.23h-2	2.69 ± 0.85 No Activity
9	CN	3.21i	2.97 ± 0.81	3.22i	No Activity	3.23i	11.14 ± 0.85
10	COCH ₃	3.21j	1.39 ± 0.48	3.22j	3.21 ± 0.76	--	
11	CHO	--		--		3.23k	2.12 ± 0.67
12	NHCOCH ₃	3.21l	8.41 ± 0.73	--		--	

Note: *Ortho OCF₃ was isolated as separate diastereomers and submitted for SAR analysis individually

Initially it was thought that electron density at the aromatic ring was a significant factor; however, the presence of the chlorine substituent interfered with this trend. This led to the consideration of other factors such as size restrictions, steric interactions, and substrate- π interactions that may contribute to protein binding affinities and could explain this anomaly. Examining the trends again showed that electron density at the aromatic ring has a minimal, yet observable, effect on inhibition as compared to the size and steric factors. An example where this is apparent is the 4-cyano substituent (**3.21j**, entry 9)

which had a two-fold increase in EC₅₀, which was attributed to the ridged linear geometry of the substrate potentially resulting in restricting access to the binding pocket of the protein.

Unfortunately, steric interactions still could not completely explain the increase in enhanced potency of 4-chloro (**3.21c**, entry 3). Further understanding of this anomaly from the trend can be explained through stabilization via a chlorine- π interaction. A DFT study illustrates the importance of this interaction within the π -system of specific amino acid residues such as phenylalanine, histidine, and tryptophan.¹²⁴ A stabilization factor of -2.01 kcal/mol can be attributed to a chlorine- π interaction with Tyr-132 as the chlorine resides within 4 Å of the aromatic ring (Figure 3.7). The large dashed red line denotes the chlorine- π interaction and the small dashed blue lines denote hydrogen bonding between His-171 and Thr-174 with the acetic acid side.

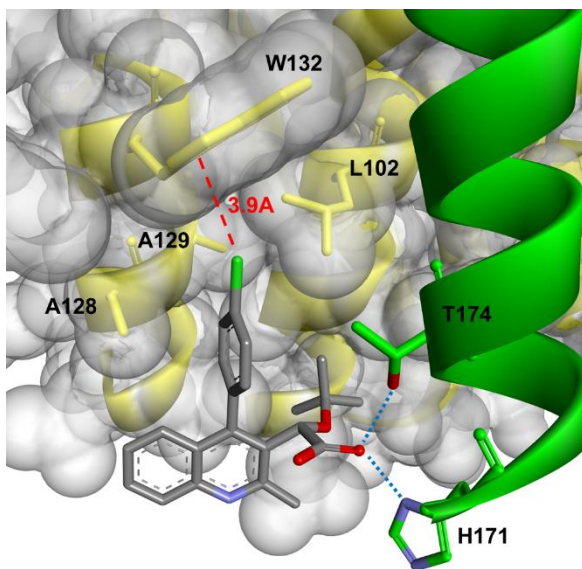
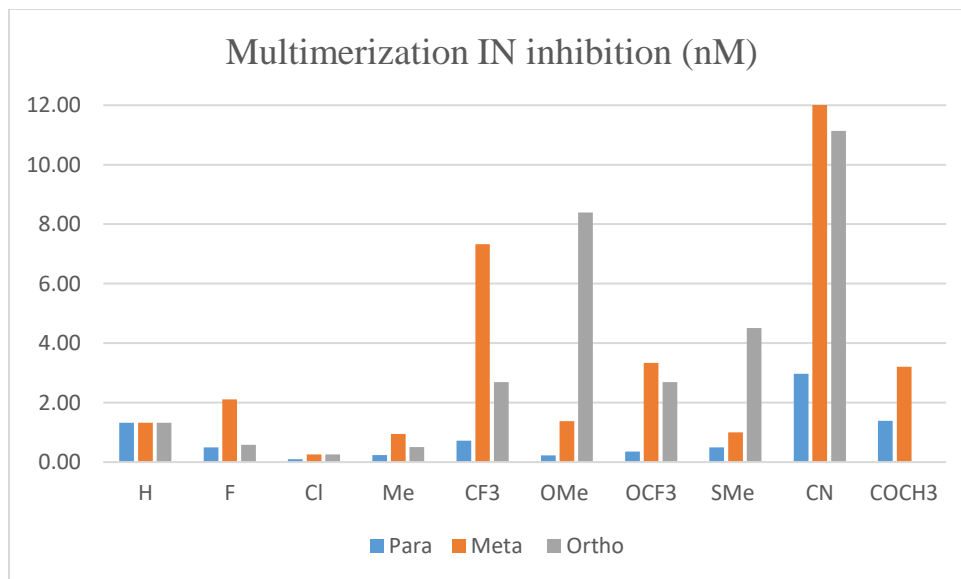


Figure 3.10 Ribbon representation of **3.21c** with the target IN binding pocket.

After analysis of the para-substituents, the ortho- and meta-substituted phenyl rings were examined, and a comparison was made with all three groups of substituted

biaryl quinolines (Table 3.5). Immediately it was evident that the para-substituents are superior when compared to both the ortho and meta derivatives in terms of the lowest values for inhibition data. The trend is para<ortho<meta with the exception of the 3-methoxy and 3-thiomethoxy, which can be attributed to unfavorable steric interactions within the protein binding pocket.

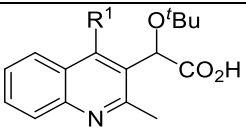
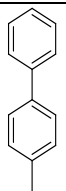
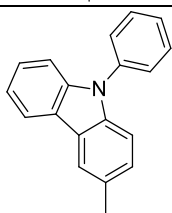

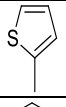
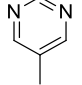
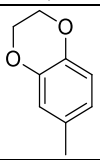
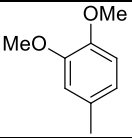


Note: meta-CN showed no activity. Ortho-COCH₃ was not synthesized.

Figure 3.11 SAR trends of the phenyl substitutions

The heterocyclic and bicyclic systems were also tested for their ability to inhibit IN (Table 3.6). Biphenyl **3.24a** and carbazole **3.24b** showed no activity, which supports the hypothesis that larger substrates will exceed the allowable space within the protein binding pocket. Additionally, thiofuran **3.24d** and pyrimidine **3.24e** also showed no activity, indicating the necessity of having noncovalent interactions in the para-position of the aryl ring as **3.21c**. The 2,3-benzo[b][1,4]dioxane derivative **3.24c** was the most promising with an EC₅₀ value of 80 nM, which naturally aligns with the need for a noncovalent interaction at the para-position.

Table 3.6 SAR data of heterocyclic biaryl quinoline substrates

 Heterocyclic 3.24a-g			
Entry	Quinoline	R ¹	EC ₅₀ Multimerization (μM)
1	3.24a		No Activity
2	3.24b		No Activity
3	3.24c		2.21 ± 0.56
5	3.24d		No Activity
6	3.24e		No Activity
6	3.24f		0.08 ± 0.01
7	3.24g		3.70 ± 0.90

3.5 Summary and Conclusion

Although HIV has been extensively studied for the past 40 years, the virus's innate mutative capabilities have been able to produce resistant strands to current available treatments. Despite the current advances, HIV has been shown to affect the

lives of millions worldwide each year. This chapter presents an eight-step synthesis of 4-substituted biaryl quinolines that have shown potency against HIV IN. Most steps can be completed at large scales (25 g), except for the Grignard addition of ethyl oxalyl chloride, which had to be kept below a reaction scale of 1 g to prevent the formation of a debrominated side product. Another key aspect is that many steps can be carried through without purification. Of the 38 biaryl quinolines synthesized, 4-chlorophenyl **3.21c** and 4-benzodioxane **3.24f** had the highest inhibition with EC₅₀ values of 0.10 μ M and 0.08 μ M, respectively, via a multimerization assay. Advancements have been made towards a synthetic route to achieve functionalization at the 6-, 7-, or 8-positions of the quinoline scaffold and is a focus of continued research in the Pigza research group.

3.6 Experimental

3.6.1 General Methods

3.6.1.1 Experimental Techniques

Unless otherwise noted, all reactions were carried out using flame-dried glassware and standard syringe, cannula, and septa techniques, when necessary.⁶⁷ Tetrahydrofuran (THF), diethyl ether (Et₂O), hexanes, dichloromethane (CH₂Cl₂), and toluene (PhCH₃) were dried by passage through a column of activated alumina on an mBraun SPS.⁶⁸ Triethylamine (TEA), N,N-dimethylformamide (DMF), and acetonitrile (ACN) were dried by passage through a column of activated alumina on an Innovative Technologies system. Trimethylsilyl chloride and Hunig's base were distilled from calcium hydride under argon. Pyridine was distilled from potassium hydroxide under nitrogen. 2-methyl-4-hydroxyquinoline was purchased from Combi-Blocks in San Diego, CA. All boronic

acids were purchased from either Combi-Blocks or Oakwood Chemicals in Georgia. Analytical thin layer chromatography was performed using Sorbent Technologies 250 μ m glass-backed UV254 silica gel plates. The plates were first visualized by fluorescence upon 254 nm irradiation then by iodine chamber. The plates were then dipped in one of the following stains followed by heating: p-anisaldehyde, phosphomolybdic acid, vanillin, ceric ammonium molybdate, potassium iodoplatinate, ninhydrin, or bromocresol green. Flash column chromatography was performed using Sorbent Technologies 40-63 μ m, pore size 60 Å silica gel with solvent systems indicated. Solvent removal was completed using a Buchi R3 rotary evaporator with a V900 diaphragm pump (~10 mmHg). All yields refer to isolated material that is chromatographically (TLC or HPLC) and spectroscopically (^1H NMR) homogenous.

3.6.1.2 Characterization

All melting points were taken with a Thomas Hoover melting point apparatus and are uncorrected. Infrared spectra were recorded on a Nicolet Nexus 470 FTIR spectrometer as neat liquids, oils, solids or as thin films formed from evaporation of NMR solvent over the ATR plate. HPLC were recorded on an Agilent 1260 Infinity using a Poroshell 120 EC-C18 (3.0 x 50 mm, 2.7 micron) column with a binary gradient of 0.1% TFA in H_2O (**A**) and 0.1% TFA in CH_3CN (**B**): [0 min: **A** (95%), **B** (5%); 7 min: **A** (5%), **B** (95%); 8 min: **A** (5%), **B** (95%)] monitoring 214, 254, and 280 nm. All final compounds were demonstrated to have $\geq 90\%$ purity by HPLC. Low-resolution mass spectra were recorded on a ThermoFinnigan LXQ ESI-LCMS by use of chemical ionization (CI). High-resolution mass spectra were recorded at the Old Dominion

University College of Science Major Instrumentation Center (COSMIC) on a Bruker 12 Tesla APEX-Qe FTICR-MS with an Apollo II ion source Combustion analysis was performed at Atlantic Microlabs on samples taken from the bulk of the material.

3.6.1.3 NMR Parameters

Proton nuclear magnetic resonance spectra were recorded on a Bruker UltraShield Plus 400 MHz spectrometer and are recorded in parts per million from internal chloroform (7.26 ppm), methanol, benzene, or dimethylsulfoxide on the δ scale and are reported as follows: chemical shift [multiplicity (s=singlet, d=doublet, t=triplet, q=quartet, qu=quintet, m=multiplet, or derivative thereof), coupling constant(s) in hertz, integration, interpretation].⁶⁹ ^{13}C NMR data were recorded on a Bruker UltraShield Plus 100 MHz spectrometer and are reported as follows: chemical shift (multiplicity as determined from DEPT (CH , CH_3 up and CH_2 down) and/or HSQC experiments).

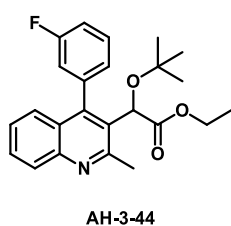
3.6.2 Synthesis of Intermediates

Supporting information for substrates **3.21a-l**, **3.24a,b,e-g**, **3.25a-l**, and **3.28a,b,e-g** can be found at the provided references.¹²⁵⁻¹²⁶

3.6.2.1 General Procedure for the Preparation of 4-Aryl Quinolines (3.25-3.28):

To a 0.5-2.0 mL microwave vial was added ethyl 2-(tert-butoxy)-2-(4-iodo-2-methylquinolin-3-yl)acetate (100 mg, 0.250 mmol), boronic acid (0.50 mmol), potassium carbonate (0.70 mmol), and tetrakis(triphenylphosphine)palladium(0) (0.05 mmol). The vial was immediately sealed then evacuated and charged with nitrogen three times.

Dimethylformamide (800 μ L) and water (80 μ L) were then added via syringe. The reaction was heated to 90 $^{\circ}$ C for a total of 3-16 hours and were monitored via HPLC and TLC. The reaction was cooled to ambient temperature then diluted with water (1 mL) and ethyl acetate (2 mL). The aqueous phase was removed, and the organic phase was filtered through a Celite $^{\circ}$ plug. The filtrate was washed with water (five 1 mL portions), dried over magnesium sulfate, gravity filtered, and concentrated to afford a crude oil. The residue was chromatographed over 12 g of silica gel eluted with hexanes-acetone (9:1 \rightarrow 4:1 \rightarrow 2:1). Product rich fractions were pooled and evaporated to isolate the 4-aryl quinoline products.

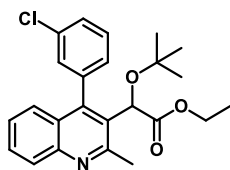


Ethyl 2-(tert-butoxy)-2-(4-(3-fluorophenyl)-2-methylquinolin-3-

yl)acetate (3.26b): The product was isolated as a 1:0.78 mixture of atropisomers using the peaks at 2.86 and 2.85 ppm. Orange-red oil,

yield = 76.8 mg, 83%. IR (thin film) 1751 cm^{-1} ; ^1H NMR (CDCl_3 ,

400 MHz) δ : 8.05 (d, J = 8.4 Hz, 1H), 7.67 (m, 1H), 7.49 (m, 1H), 7.32 (m, 1H), 7.32 (m, 1H), 7.32 (m, 1H), 7.32 (m, 1H), 7.09 (m, 1H), 5.12 (minor), 5.10 (major) (s, 1H), 4.19 (m, 2H), 2.86 (major), 2.85 (minor) (s, 3H), 1.23 (q, J = 6.4 Hz, 3H), 1.00 (s, 9H); ^{13}C NMR (CDCl_3 , 100 MHz) δ : [172.40, 172.17] (s), [163.86, 161.40] (d, J = 248.0 Hz)*, [159.44, 159.43] (s), 146.70 (s), [145.16, 145.10] (s), [138.46, 138.38] (d, J = 7.7 Hz)*, [133.83, 133.64] (d), [132.15, 132.02] (d, J = 14.0 Hz)*, [130.27, 130.13] (d, J = 8.4 Hz)*, [129.51, 129.49] (s), [128.60, 128.47] (d, J = 12.5 Hz), [126.68, 125.61,] (d, J = 108.1), [126.38, 126.06] (d, J = 31.5 Hz), [125.61, 125.58] (s), [115.63, 115.42] (d, J = 4.5 Hz), [117.13, 116.92] (d), [76.15, 76.11] (s), [70.77, 70.76] (d), [61.51, 61.43] (t), 28.06 (q), [24.82, 24.80] (q), [14.13, 14.10] (q). *Due to C-F coupling



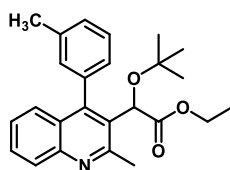
AH-3-39

Ethyl 2-(tert-butoxy)-2-(4-(3-chlorophenyl)-2-methylquinolin-3-yl)acetate (3.26c):

The product was isolated as a 1:0.80 mixture of atropisomers using the peaks at 2.86 and 2.84 ppm. Orange-red oil,

yield = 85.1 mg, 92%. IR (thin film) 1640 cm^{-1} ; ^1H NMR (CDCl_3 ,

400 MHz) δ : 8.04 (d, $J = 7.2\text{ Hz}$, 1H), 7.67 (m, 1H), 7.52 (m, 1H), 7.49 (m, 1H), 7.44 (m, 1H), 7.38 (m, 1H), 7.38 (m, 1H), 7.30 (m, 1H), 5.07 (minor), 5.06 (major) (s, 1H), 4.19 (m, 2H), 2.86 (major), 2.85 (minor) (s, 3H), 1.23 (dt, $J = 16.7, 7.2\text{ Hz}$, 3H), 1.01 (minor), 1.00 (major) (s, 9H); ^{13}C NMR (CDCl_3 , 100 MHz) δ : [172.39, 172.06] (s), 159.51 (s), 146.75 (s), 145.01 (s), 138.10 (s), [134.58, 134.11] (s), 131.07 (d), [129.85, 129.79] (d), [129.55, 129.48] (s), [129.42, 129.28] (d), 129.03 (d), [128.65, 128.62] (d), 127.85 (d), 126.34 (d), [126.07, 126.01] (d), [125.97, 125.88] (s), 76.13 (s), 70.76 (d), [61.52, 61.42] (t), [28.07, 28.03] (q), [24.90, 24.83] (q).



AH-3-59

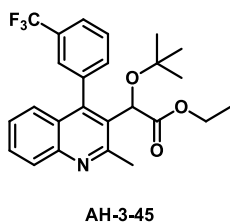
Ethyl 4,6-dihydroxy-2-methylquinoline-3-carboxylate (3.26d):

The product was isolated as a 1:0.91 mixture of atropisomers using the peaks at 5.16 and 5.15 ppm. Yellow Oil, yield = 83.4 mg, 91%;

IR (thin film) 1749 cm^{-1} ; ^1H NMR (CDCl_3 , 400 MHz) δ : 8.04 (d, $J =$

8.4 Hz, 1H), 7.64 (m, 1H), 7.48-7.26 (m, 4H), 7.15-7.04 (m, 2H), 5.16 major, 5.15 minor (s, 1H), 4.15 (m, 2H), 2.86 major, 2.85 minor (s, 3H), 2.43 major, 2.42 minor (s, 3H), 1.24 major, 1.21 minor (t, $J = 7.1\text{ Hz}$, 3H), 0.99 major, 0.98 minor (s, 9H); ^{13}C NMR (CDCl_3 , 100 MHz) δ : [172.64, 172.51] (s), [159.47, 159.44] (s), [146.93, 146.65] (s), 138.04 (s), 137.58 (s), [136.09, 136.06] (s), 131.38 (d), 130.47 (d), 129.70 (s), [129.28, 129.23] (d), [129.19, 129.09] (d), [128.34, 128.32] (d), [127.85, 127.75] (d), [126.86,

126.82] (d), [126.41, 126.35] (s), 125.72 (d), 76.03 (s), [70.87, 70.82] (d), [61.37, 61.20] (t), [28.10, 28.01] (q), [24.75, 24.69] (q), [21.53, 21.42] (q), [14.23, 14.13] (q).



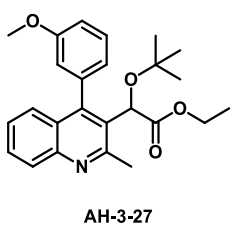
Ethyl 2-(tert-butoxy)-2-(2-methyl-4-(3-

(trifluoromethyl)phenyl)quinolin-3-yl)acetate (3.26e): The product

was isolated as an 1:0.75 mixture of atropisomers using the peaks at

2.89 and 2.88 ppm. Red-orange oil, yield = 70.9 mg, 68%. IR (thin

film) 1752 cm^{-1} ; ^1H NMR (CDCl_3 , 400 MHz) δ : 8.07 (d, $J = 8.4$ Hz, 1H), 7.83 (m, 1H), 7.77-7.60 (m, 3H), 7.55 (m, 1H), 7.38 (m, 1H), 7.25 (m, 1H), 5.02 (major), 5.01 (minor), (s, 1H), 4.18 (m, 2H), 2.89 (major), 2.88 (minor) (s, 3H), 1.22 (td, $J = 7.1, 4.4$ Hz, 3H), 0.99 (s, 9H); ^{13}C NMR (CDCl_3 , 100 MHz) δ : [172.26, 171.92] (s), [159.47, 159.39] (s), [146.65, 146.63] (s), [145.06, 145.01] (s), [137.19, 137.12] (s), [134.24, 134.09] (d), [132.24, 132.04] (d), [131.0, 130.6] (q, $J = 33.2$ Hz)*, [129.79, 128.85] (q, $J = 37.2$ Hz)*, 129.75 (s), [128.57, 128.54] (d), [127.87, 126.59] (q, $J = 131.5$ Hz)*, 125.93 (s), [125.37, 125.24] (q, $J = 9.6$ Hz)*, [76.74, 76.14] (s), [70.71, 70.63] (d), [61.60, 61.47] (t), [27.98, 27.95] (q), [24.74, 24.70] (q) [14.11, 13.91] (q). *Due to C-F coupling.



Ethyl 2-(tert-butoxy)-2-(4-(3-methoxyphenyl)-2-methylquinolin-

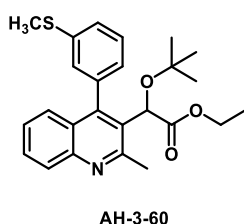
3-yl)acetate (3.26f): The product was isolated as an 1:0.72 mixture

of atropisomers using the peaks at 0.98 and 0.96 ppm. Orange Oil,

yield = 71.5 mg, 75%; IR (thin film) 1749 cm^{-1} ; ^1H NMR (CDCl_3 ,

400 MHz) δ : 8.45 (d, $J = 8.4$ Hz, 1H), 7.65 (m, 1H), 7.45 (m, 4H), 7.37 (m, 1H), 7.06 (m, 1H), 5.20 (major), 5.19 (minor) (s, 1H), 4.19 (q, $J = 7.2$ Hz, 2H), 3.84 (major) 3.82 (minor) (s, 3H), 2.85 (s, 3H), 1.22 (dt, $J = 7.2, 5.4$ Hz, 3H), 1.01 (minor), 1.00 (major) (s, 9H); ^{13}C NMR (CDCl_3 , 100 MHz) δ : [172.62, 172.57] (s), [159.57, 159.45, 159.43,

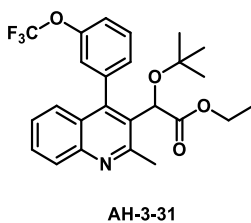
159.06] (s), [146.64, 146.63, 146.58, 146.50] (s), [137.45, 137.44] (s), [132.15, 132.06] (s), 129.93 (s), [129.61, 129.53, 129.50] (d), [129.28, 129.06] (d), [128.60, 128.48, 128.35, 128.33] (d), [126.78, 126.75, 125.83, 125.80] (d), [126.78, 126.75] (d), 126.20 (s), [125.83, 125.80] (d), [123.15, 122.22] (d), [116.31, 115.36] (d), [114.28, 114.13] (d), 76.07 (s), [70.89, 70.83] (d), [61.42, 61.35] (t), [55.35, 55.28] (q), [28.12, 28.10] (q), [24.72, 24.71] (q), [14.18, 14.13] (q).



Ethyl 2-(tert-butoxy)-2-(2-methyl-4-(3-

(methylthio)phenyl)quinolin-3-yl)acetate (3.26g): The product was isolated as a 1:0.76 mixture of atropisomers using the peaks at 5.16 and 5.14 ppm. Yellow Oil, yield = 77.3 mg, 78%; IR (thin

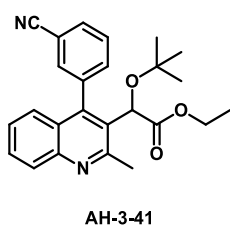
film) 1748 cm^{-1} ; ^1H NMR (CDCl_3 , 400 MHz) δ : 8.04 (d, $J = 8.5$ Hz, 1H), 7.65 (m, 1H), 7.49-7.22 (m, 5H), 7.20-7.05 (m, 1H), [5.16, 5.14] (s, 1H), 4.15 (m, 2H), [2.85, 2.84] (s, 3H), [2.50, 2.47] (s, 3H), 1.23 (m, 3H), [1.00, 0.99] (s, 9H); ^{13}C NMR (CDCl_3 , 100 MHz) δ : [172.50, 172.49] (s), 159.43 (s), [146.85, 146.72] (s), [139.30, 138.64] (s), [136.92, 136.80] (s), [131.39, 130.48] (d), [129.54, 129.50] (s), [129.30, 129.17] (d), [129.09, 129.06] (d), [128.48, 128.40] (d), [128.31, 128.20] (d), [126.84, 126.66] (d), [126.36, 126.27] (d), [126.40, 126.14] (s), [125.84, 125.68] (d), [76.11, 76.08] (s), [70.87, 70.84] (d), [61.47, 61.36] (t), [28.10, 28.01] (q), [24.83, 24.78] (q), [21.53, 21.42] (q), [14.22, 14.13] (q).



Ethyl-2-(tert-butoxy)-2-(2-methyl-4-(3-

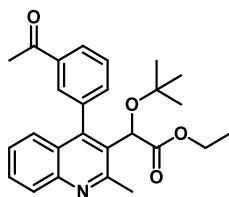
(trifluoromethoxy)phenyl)quinolin-3-yl)acetate (3.26h): The product was isolated as an 1:0.72 of atropisomers using the peaks at 0.98 and 0.96 ppm. Orange oil, yield = 78.1, 87%. IR (thin film)

1753, 1723 cm^{-1} . ^1H NMR (CDCl_3 , 400 MHz) δ : 8.06 (d, $J = 8.4$ Hz, 1H), 7.68 (m, 1H), 7.59 (m, 1H), 7.48 (m, 1H), 7.39 (m, 2H), 7.28 (m, 2H), 5.08 (major), 5.07 (minor) (s, 1H), 4.19 (m, 2H), 2.85 (s, 3H), 1.22 (dt, $J = 7.1, 5.7$ Hz), 0.98 (minor), 0.96 (major) (s, 9H); ^{13}C NMR (CDCl_3 , 100 MHz) δ : [172.34, 172.16] (s), [159.47, 159.42] (s), [149.29, 148.81] (q, $J = 2.2$ Hz)*, [146.76, 146.74] (s), 144.69 (s), [138.27, 138.25] (s), [132.15, 132.06, 131.97, 191.95] (s), 130.09 (d), [129.52, 129.44] (d), [128.62, 128.47] (d), [126.22, 126.12] (d), [125.80, 125.75] (d), 123.63 (d), 122.63 (d), 121.79 (s), [121.19, 121.03] (d), [76.16, 76.11] (s), [70.73, 70.58] (d), [61.58, 61.47] (t), [27.95, 27.92] (q), [24.81, 24.79] (q), [14.14, 13.97] (q). *Due to C-F coupling



Ethyl 2-(tert-butoxy)-2-(4-(3-cyanophenyl)-2-methylquinolin-3-yl)acetate (3.26i): The product was isolated as an 1:0.79 mixture of atropisomers using the peaks at 4.99 and 4.97 ppm. Orange-red oil.

Yield = 68.8 mg, 73%. ^1H NMR (CDCl_3 , 400 MHz) δ : 8.07 (d, $J = 8.3$ Hz, 1H), 7.84 (m, 1H), 7.84 (m, 1H), 7.68 (dt, $J = 7.7, 1.4$ Hz, 1H), 7.66 (m, 1H), 7.61 (m, 1H), 7.40 (m, 1H), 7.17 (m, 1H), 4.99 (minor), 4.97 (major) (s, 1H), 4.17 (m, 2H), 2.88 (major), 2.27 (minor) (s, 3H), 1.25 (dt, $J = 14.4, 7.2$ Hz, 3H), 1.00 (s, 9H); ^{13}C NMR (CDCl_3 , 100 MHz) δ : [172.14, 171.48] (s), [159.34, 159.26] (s), [146.73, 146.71] (s), [144.04, 143.98] (s), [137.80, 137.77] (s), [135.40, 133.98] (d), 134.52 (d), 133.12 (s), 129.68 (s), 129.43 (d), [128.94, 128.75] (d), [126.42, 126.36] (d), [125.88, 125.85] (d), [118.28, 118.19] (s), [112.91, 112.44] (s), [76.26, 76.22] (s), [70.70, 70.66] (d), [61.68, 61.57] (t), [28.03, 28.01] (d), [24.85, 24.81] (q), [14.15, 14.14] (q).



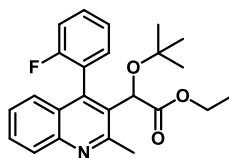
AH-3-29

Ethyl 2-(4-(3-acetylphenyl)-2-methylquinolin-3-yl)-2-(tert-butoxy)acetate (3.26j): The product was isolated as an 1:0.81

mixture of atropisomers using the peaks at 2.64 and 2.61 ppm.

Orange-red oil. Yield = 49.1 mg, 50%. IR (thin film) 1749, 1684 cm^{-1}

^1H NMR (CDCl_3 , 400 MHz) δ : 8.15 (m, 1H), 8.06 (d, $J = 8.3$, 1H), 7.91 (m, 1H), 7.66 (m, 1H), 7.66 (m, 1H), 7.55 (m, 1H), 7.37 (m, 1H), 7.23 (m, 1H), 5.05 (major), 5.01 (minor) (s, 1H), 4.17 (m, 2H), 2.87 (major), 2.86 (minor) (s, 3H), 2.64 (major), 2.61 (minor) (s, 3H), 1.24 (dt, $J = 12.5$, 7.2 Hz, 3H), 0.98 (minor), 0.97 (major) (s, 9H); ^{13}C NMR (CDCl_3 , 100 MHz) δ : [197.60, 197.43] (s), [172.32, 172.30] (s), [159.45, 159.38] (s), 146.64 (s), 145.60 (s), 138.66 (s), 137.20 (s), [136.81, 136.78] (s), [135.40, 135.24] (d), [132.16, 132.06] (d), [129.76, 129.71] (s), [129.56, 129.52] (d), [128.90, 128.63] (d), [128.52, 128.40] (d), [128.36, 128.28] (d), [126.33, 126.11] (d), 115.01 (d), [76.18, 76.13] (s), 70.77 (d), [61.68, 61.48] (t), [28.06, 28.01] (q), 26.72 (q), 24.33 (q), 14.14 (q).



AH-3-70

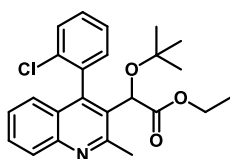
Ethyl 2-(tert-butoxy)-2-(4-(2-fluorophenyl)-2-methylquinolin-3-yl)acetate (3.27b): The product was isolated as an 1:0.66 mixture of

atropisomers using the peaks at 2.95 and 2.86 ppm. Orange Oil, yield

= 74.0 mg, 80%. IR (thin film) 1749 cm^{-1} ; ^1H NMR (CDCl_3 , 400

MHz) δ : 8.05 (d, $J = 8.4$ Hz, 1H), 7.66 (ddt, $J = 8.4$, 6.7, 1.6 Hz, 1H), 7.58-7.43 (m, 2H), 7.42-7.16 (m, 4H), 5.14 major, 5.13 minor (s, 1H), 4.13 (m, 2H), 2.95 minor, 2.86 major (s, 3H), 1.23 major, 1.13 minor (t, $J = 7.1$ Hz, 3H), 1.08 minor, 1.01 major (s, 9H); ^{13}C NMR (CDCl_3 , 100 MHz) δ : [172.40, 171.78] (s), [161.19, 158.72] (d, $J = 125.2$ Hz)*, [159.71, 159.38] (s), [146.71, 146.48] (s), [141.11, 140.92] (s), [132.86, 132.83] (d), [131.04, 130.31] (d), [130.94, 130.71] (d, $J = 8.1$ Hz)*, [130.37, 130.31] (s), [129.43,

129.39] (d), [128.67, 128.61] (d), [126.29, 125.76] (s), [126.05, 125.99] (d, $J = 18.6$ Hz)*, [124.24, 123.87] (d, $J = 3.6$ Hz)*, [123.79, 123.63] (s), [115.99, 115.88] (d, $J = 21.5$ Hz)*, [76.19, 75.88] (s), [71.20, 70.80] (d), [61.42, 61.22] (t), [28.09, 27.82] (q), [25.17, 24.81] (q), [14.13, 13.82] (q). *Due to C-F coupling.

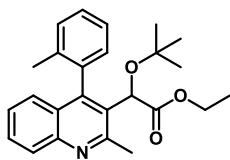


KM-1-65

Ethyl 2-(tert-butoxy)-2-(4-(2-chlorophenyl)-2-methylquinolin-3-yl)acetate (3.27c):

The product was isolated as an 1:0.97 mixture of atropisomers using the peaks at 5.11 and 5.08 ppm. Orange Oil, yield = 80.8 mg, 84% IR (thin film) 1748 cm^{-1} ; ^1H NMR (CDCl_3 , 400

MHz) δ : 8.05 (d, $J = 8.4$ Hz, 1H), 7.64 (td, $J = 6.8, 1.2$ Hz, 1H), 7.61-7.28 (m, 5H), 7.28-7.10 (m, 1H), 5.11 major, 5.08 minor (s, 1H), 4.10 (m, 2H), 3.00 major, 2.90 minor (s, 3H), 1.22 major, 1.15 minor (t, $J = 7.1$ Hz, 3H), 1.11 major, 1.05 minor (s, 9H); ^{13}C NMR (CDCl_3 , 100 MHz) δ : [172.50, 171.82] (s), [159.61, 159.55] (s), [146.67, 146.58] (s), [144.36, 144.92] (s), [137.25, 137.14] (s), [134.99, 134.96] (s), [133.84, 133.64] (d), [130.18, 129.94] (d), [129.88, 129.86] (d), [129.46, 129.37] (d), [129.43, 129.34] (s), [128.61, 128.53] (d), [126.66, 126.56] (d), [126.28, 125.95] (d), [126.11, 126.10] (d), [125.77, 127.35] (d), [76.27, 75.84] (s), [71.26, 70.84] (d), [61.34, 61.18] (t), [28.16, 27.95] (q), [25.32, 24.97] (q), [14.13, 13.99] (q).



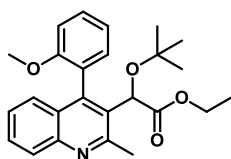
AH-3-64

Ethyl 2-(tert-butoxy)-2-(2-methyl-4-(o-tolyl)quinolin-3-yl)acetate (3.27d):

The product was isolated as an 1:0.78 mixture of atropisomers using the peaks at 5.14 and 5.12 ppm. Yellow Oil, yield = 89.8 mg, 98%. IR (thin film) 1750 cm^{-1} ; ^1H NMR (CDCl_3 , 400

MHz) δ : 8.07 (d, $J = 8.4$ Hz, 1H), 7.63 (ddd, $J = 8.3, 6.8, 1.4$ Hz, 1H), 7.48-7.28 (m, 3H), 7.25-6.98 (m, 3H), 5.14 major, 5.12 minor (s, 1H), 4.14 (m, 2H), 2.93 minor, 2.89 major

(s, 3H), 1.97 minor, 1.90 major (s, 3H), 1.22 major, 1.15 minor (t, $J = 7.1$ Hz, 3H), 1.11 minor, 1.00 major (s, 9H); ^{13}C NMR (CDCl_3 , 100 MHz) δ : [172.85, 172.48] (s), [159.94, 159.91] (s), [147.29, 146.65] (s), [146.38, 146.27] (s), [137.86, 137.41] (s), [135.68, 135.37] (s), [130.38, 130.31] (d), [129.55, 129.44] (d), [129.49, 129.33] (s), [128.79, 128.69] (d), [128.31, 128.15] (d), 126.83 (d), [126.54, 126.39] (d), [126.17, 125.81] (s), [126.13, 126.08] (d), [125.71, 125.54] (d), [76.37, 75.65] (s), [71.26, 70.69] (d), [61.29, 61.20] (t), [28.44, 27.06] (q), [24.77, 24.53] (q), [20.37, 19.85] (q), [14.11, 14.01] (q).

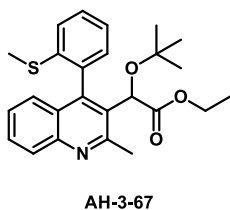


AH-3-66

Ethyl 2-(tert-butoxy)-2-(4-(2-methoxyphenyl)-2-methylquinolin-

3-yl)acetate (3.27f): The product was isolated as an 1:0.84 mixture of atropisomers using the peaks at 5.16 and 5.09 ppm. Yellow oil,

yield = 92.5 mg, 97% IR (thin film) 1744 cm^{-1} ; ^1H NMR (CDCl_3 , 400 MHz) δ : 8.03 (dd, $J = 8.4, 5.4$ Hz, 1H), 7.61 (m, 1H), 7.50 (m, 1H), 7.29 (m, 3H), 7.10 (t, $J = 7.4$ Hz, 1H), 7.04 (t, $J = 7.8$ Hz, 1H), 5.16 major, 5.14 minor (s, 1H), 4.15 (m, 2H), 3.60 minor, 3.58 major (s, 3H), 2.96 minor, 2.85 major (s, 3H), 1.21 major, 1.20 minor (t, $J = 7.1$ Hz, 3H), 1.02 minor, 0.99 major (s, 9H); ^{13}C NMR (CDCl_3 , 100 MHz) δ : [172.65, 171.72] (s), [159.82, 159.50] (s), [157.62, 156.44] (s), [146.94, 146.40] (s), [144.29, 143.93] (s), [132.28, 131.14] (d), [130.29, 130.22] (d), [129.97, 129.69] (s), [129.05, 128.95] (d), [128.44, 128.40] (d), [126.66, 126.47] (d), [126.43, 126.23] (s), 125.54 (d), [124.85, 124.66] (s), [120.44, 120.24] (d), [110.84, 110.54] (d), [76.23, 75.67] (s), [71.73, 70.94] (d), [61.25, 60.96] (t), [55.04, 54.83] (q), [28.18, 27.75] (q), [25.39, 24.80] (q), [14.13, 14.09] (q).



Ethyl 2-(tert-butoxy)-2-(2-methyl-4-(2-

(methylthio)phenyl)quinolin-3-yl)acetate (3.27g): The product was

isolated as an 1:0.84 mixture of atropisomers using the peaks at 5.16

and 5.09 ppm. Yellow-orange oil, yield = 55.5 mg, 56%. IR (thin

film) 1743 cm^{-1} ; ^1H NMR (CDCl_3 , 400 MHz) δ : 8.03 (d, J = 8.4 Hz, 1H), 7.63 (ddt, J =

8.2, 6.8, 1.4 Hz, 1H), 7.50 (tdd, J = 8.0, 3.5, 1.6 Hz, 1H), 7.42-7.2 (m, 4H), 7.13 (m, 1H),

5.09 minor, 5.08 major (s, 1H), 4.13 (m, 2H), 2.98 minor, 2.90 major (s, 3H), 2.29

minor, 2.28 major (s, 3H), 1.21 major, 1.16 minor (t, J = 7.1 Hz, 3H), 1.09 minor, 1.05

major (s, 9H); ^{13}C NMR (CDCl_3 , 100 MHz) δ : [172.69, 171.77] (s), [159.96, 159.82] (s),

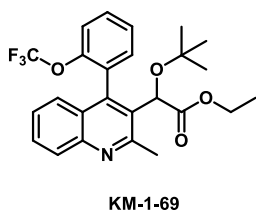
[146.80, 146.64] (s), [145.37, 144.38] (s), [139.86, 138.75] (s), 131.43 (d), [129.60,

129.29] (d), [129.52, 129.19] (s), [129.28, 129.12] (d), [128.68, 128.58] (d), 126.65 (d),

126.22 (d), [125.84, 125.58] (s), [125.79, 125.77] (d), [76.32, 75.76] (s), [71.55, 70.88]

(d), [61.19, 61.04] (t), [28.29, 27.94] (q), [25.46, 25.01] (q), [16.04, 15.41] (q), [14.10,

14.02] (q).



Ethyl 2-(tert-butoxy)-2-(2-methyl-4-(2-

(trifluoromethoxy)phenyl)quinolin-3-yl)acetate (3.27h): The

product was isolated as an 1:0.84 mixture of atropisomers using the

peaks at 5.07 and 5.01 ppm. Orange oil, yield = 78.8 mg, 73% IR (thin film) 1749 cm^{-1} ;

^1H NMR (CDCl_3 , 400 MHz) δ : 8.05 major, 8.04 minor (d, J = 8.4 Hz, 1H), 7.65 (tt, J =

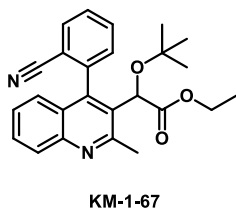
6.9, 1.5 Hz, 1H), 7.54-7.23 (m, 4H), 7.19, 7.18 (d, J = 8.2 Hz, 1H), 5.07 minor, 5.01

major (s, 1H), 4.11 (m, 2H), 2.94 major, 2.90 minor (s, 3H), 1.21 minor, 1.16 major (t, J

= 7.1 Hz, 3H), 1.04 minor, 1.03 minor (s, 9H); ^{13}C NMR (CDCl_3 , 100 MHz) δ : [172.23,

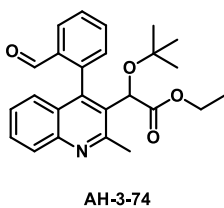
171.73] (s), [159.45, 159.37] (s), 147.83 (s), [146.74, 146.49] (s), 141.62 (s), 133.45 (d),

132.08 (d), [130.40, 130.36] (d), [129.99, 129.90] (s), [129.37, 129.35] (d), 128.94 (d), [128.58, 128.53] (d) [126.08, 125.70] (s), [126.04, 125.98, 125.92, 125.86] (q, $J = 5.6$ Hz)*, 125.47 (d), [119.62, 117.30] (d), [126.73, 126.54] (d), [126.20, 125.93] (d), [76.22, 75.84] (s), [71.25, 70.91] (d), [61.34, 61.23] (t), [28.12, 27.76] (q), [25.15, 25.00] (q), [14.67, 13.79] (q). *Due to C-F Splitting



Ethyl 2-(tert-butoxy)-2-(4-(2-cyanophenyl)-2-methylquinolin-3-yl)acetate (3.27i): The product was isolated as an 1:0.67 mixture of atropisomers using the peaks at 5.10 and 4.99. Orange oil, yield = 35.8 mg, 38% IR (thin film) 1748 cm^{-1} ; ^1H NMR (CDCl_3 , 400 MHz)

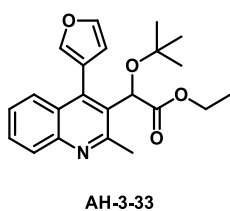
δ : 8.07 minor, 8.06 major (d, $J = 8.4$ Hz, 1H), 7.90-7.83 (m, 1H), 7.80-7.59 (m, 3H), 7.45-7.29 (m, 2H), 7.12 minor, 7.03 major (dd, $J = 8.4, 0.8$, 1H), 5.10 minor, 4.99 major (s, 1H), 4.15 (m, 2H), 2.99 major, 2.91 minor (s, 3H), 1.23 major, 1.17 minor (t, $J = 7.1$ Hz, 3H), 1.12 major, 1.05 minor (s, 9H); ^{13}C NMR (CDCl_3 , 100 MHz) δ : [172.17, 171.63] (s), [159.25, 159.62] (s), [146.76, 146.73] (s), [143.12, 142.42] (s), [140.72, 139.98] (s), [132.85, 132.45] (d), [132.44, 132.21] (d), 129.92 (d), [129.74, 129.70] (d), 129.61 (s), [129.16, 128.97] (d), [128.86, 128.77] (d), [126.59, 126.56] (d), [125.41, 125.26] (d), [177.54, 117.16] (s), [115.28, 113.90] (s), [76.75, 76.06] (s), [70.81, 70.67] (d), [61.52, 61.39] (t), [27.92, 27.91] (q), [25.12, 24.960] (q), [14.11, 14.06] (q).



Ethyl 2-(tert-butoxy)-2-(4-(2-formylphenyl)-2-methylquinolin-3-yl)acetate (3.27k): The product was isolated as an 1:0.39 mixture of atropisomers using the peaks at 5.08 and 4.98 ppm. Orange oil, yield = 66.4 mg, 70%. IR (thin film) $1751, 1698\text{ cm}^{-1}$; ^1H NMR (CDCl_3 ,

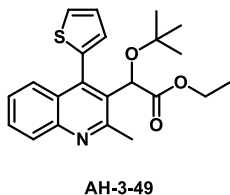
400 MHz) δ : 9.42 (s, 1H), 8.21 major, 8.17 minor (dd, $J = 7.6, 1.2$ Hz, 1H), 8.07 (d, $J =$

8.4 Hz, 1H), 7.85-7.56 (m, 3H), 7.41-7.30 (m, 2H), 7.07 (d, $J = 8.3$ Hz, 1H), 5.06 minor, 4.98 major (s, 1H), 4.27-3.98 (m, 2H), 2.94 major, 2.91 minor (s, 3H), 1.24 major, 1.10 minor (t, $J = 7.1$ Hz, 3H), 1.08 major, 0.97 minor (s, 9H); ^{13}C NMR (CDCl_3 , 100 MHz) δ : [191.07, 190.58] (d), [172.29, 171.77] (s), [159.57, 159.22] (s), [146.38, 146.22] (s), [143.04, 142.44] (s), [139.96, 139.32] (s), [135.50, 134.22] (s), [133.82, 133.50] (d), [130.36, 130.13] (s), [130.29, 130.22] (d), [129.83, 129.72] (d), [129.44, 129.36] (d), [128.81, 128.69] (d), [127.40, 127.37] (d), [126.98, 126.84] (s), [126.73, 126.54] (d), [126.20, 125.93] (d), [76.19, 75.95] (s), [70.95, 70.84] (d), [61.47, 61.38] (t), [28.18, 27.96] (q), [25.02, 24.89] (q), [14.10, 13.96] (q).



Ethyl 4,6-dihydroxy-2-methylquinoline-3-carboxylate (3.28c):

Orange oil, yield = 85.1 mg, 99% ^1H NMR (CDCl_3 , 400 MHz) δ : 8.02 (d, $J = 8.2$ Hz, 1H), 7.49 (m, 1H), 7.49 (m, 1H), 7.49 (m, 1H), 7.37 (m, 1H), 7.37 (m, 1H), 6.62 (s, 1H), 5.45 (s, 1H), 4.22 (dq, $J = 10.8, 7.2$ Hz, 1H), 4.17 (dq, $J = 10.8, 7.2$ Hz, 1H), 2.82 (s, 3H), 1.22 (t, $J = 7.1$ Hz, 3H), 1.02 (s, 9H); ^{13}C NMR (CDCl_3 , 100 MHz) δ : 172.5 (s), 159.3 (s), 146.7 (s), 143.3 (d), 132.2 (s), 130.8 (d), 129.3 (d), 128.6 (s), 128.4 (d), 126.3 (d), 125.9 (d), 119.8 (s), 113.0 (d), 76.1 (s), 70.7 (d), 61.4 (t), 28.0 (q), 24.8 (q), 14.2 (q).



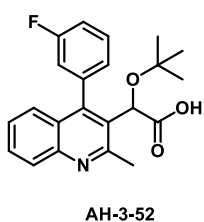
Ethyl 2-(tert-butoxy)-2-(2-methyl-4-(thiophen-2-yl)quinolin-3-yl)acetate (3.28d):

The product was isolated as an 1:0.13 mixture of atropisomers using the peaks at 2.85 and 2.83. Red-orange oil, yield = 47.4 mg, 59%. ^1H NMR (CDCl_3 , 400 MHz) δ : 8.10 (d, $J = 8.4$ Hz, 1H), 7.95 (d, $J = 8.3$ Hz, 1H), 7.67 (m, 1H), 7.67 (m, 1H), 7.54 (m, 1H), 7.46 (m, 1H), 7.33 (m, 1H), 5.93 (s, 1H), 4.18 (m, 2H), 2.85 (minor), 2.83 (major) (s, 3H), 1.28 (minor), 1.25 (major) (s,

9H), 1.18 (t, $J = 7.0$ Hz, 3H); ^{13}C NMR (CDCl_3 , 100 MHz) δ : 171.30 (s), 158.78 (s), 146.68 (s), 137.23 (s), 136.85 (s), [133.83, 133.63] (d), 133.18 (d), 133.02 (s), [132.15, 131.97] (d), 130.09 (d), 129.38 (s), [128.78, 128.70] (d), [128.57, 128.45] (d), 127.46 (d), 80.26 (s), [70.79, 70.36] (d), [61.56, 61.38] (t), [28.34, 28.11] (q), 24.69 (q), 14.08 (q).

3.6.2.2 General Procedure for Ethyl Ester Hydrolysis (3.21-3.24)

To a solution of ethyl ester quinoline (1.0 equiv) and ethanol (3.5 mL) was added aqueous 50% sodium hydroxide (3 equiv). The reaction was heated to 60 °C and was stirred until 100% conversion was observed by HPLC. The solution was cooled to ambient temperature and was neutralized with 1N HCl to pH 5. The solution was extracted with chloroform- d_6 (two 0.5-mL portions) and the combined organic phase was dried over magnesium sulfate, filtered, and examined via ^1H -NMR. Carboxylic acid products requiring purification were chromatographed over 4 g of silica gel eluted with 0-5-10% dichloromethane-methanol. Product rich fractions were pooled and evaporated to afford desired acids (3.21-3.24).



2-(tert-Butoxy)-2-(4-(3-fluorophenyl)-2-methylquinolin-3-yl)acetic acid (3.22b):

The product was isolated as an indistinguishable mixture of atropisomers. White solid, yield = 24.1 mg, 35%. mp 110-115°C; IR

(thin film) 1730 cm^{-1} ; ^1H NMR ($\text{MeOH-}d_4$, 400 MHz) δ : 8.06 (d, $J =$

8.4 Hz, 1H), 7.68 (t, $J = 6.9$ Hz, 1H), 7.61-7.18 (m, 5H), 7.09 (m, 1H), 5.24 (s, 1H), 2.84

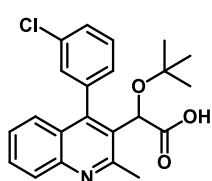
(s, 3H), 1.00 (s, 9H); ^{13}C NMR ($\text{MeOH-}d_4$, 100 MHz) δ : 177.26 (s), [158.95, 157.20] (s),

[146.05, 144.62] (s), 137.05 (s), 132.68 (s), [132.13, 132.08, 132.06, 132.03] (d),*

[131.83, 131.51, 131.65] (s),* [130.11, 129.78] (s) 129.87 (d), 129.87 (s), [129.15,

129.00] (d), [128.63, 128.17] (d), 126.71 (d), [125.36, 125.35, 125.30] (s),* 119.04 (d),

116.20 (d), 116.16 (d) [75.71, 75.60] (s), 72.83 (d), [27.91, 27.79] (q), 24.66 (q); Exact mass calcd for $C_{23}H_{22}FNO_4$ $[M+H]^+$, 368.165648. Found 368.165782. *C-F coupling could not be determined for this sample, and so all peaks were reported.

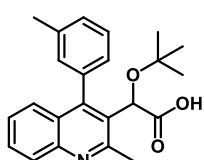


NGJ-9-024

2-(tert-Butoxy)-2-(4-(3-chlorophenyl)-2-methylquinolin-3-yl)acetic acid

acid (3.22c): The product was isolated as an 1.0:0.9 mixture of atropisomers using the peaks at 5.20 and 5.17 ppm ppm; Yellow oil, yield = 67.5 mg, 92%. IR (thin film) 1640 cm^{-1} ; ^1H NMR (CDCl_3 , 400

MHz) δ : 10.00 (s, 1H, OH) 8.13 (d, $J = 8.4\text{ Hz}$, 1H), 7.78 (s, 1H), 7.69-7.61 (m, 2H), 7.54-7.46 (m, 2H), 7.43-7.30 (m, 2H), 7.22 (d, $J = 7.3\text{ Hz}$, 1H), 5.2 major, 5.17 minor (s, 1H), 2.94 major, 2.90 minor (s, 3H), 0.99 (s, 9H); ^{13}C NMR (CDCl_3 , 100 MHz) δ : 173.7 (s), [158.9, 158.8] (s), [146.6, 146.5] (s), [145.5, 145.4] (s), [137.6, 137.5] (s), 134.0 (s), 131.2 (d), [130.3, 129.9] (s), [130.2, 129.2] (d), [130.1, 130.0] (d), [129.6, 129.5] (d), [129.0, 128.9] (d), 127.9 (d), [127.4, 127.3] (d), [126.6, 126.5] (d), 126.4 (d), [126.1, 125.9] (s), [77.2, 76.9] (s), 70.7 (d), [28.14, 28.07] (q), [23.8, 23.7] (q). Exact mass calcd for $C_{22}H_{22}ClNO_3$ $[M+H]^+$, 384.136098. Found 384.136358.

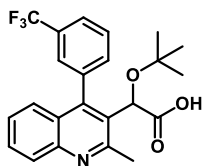


AH-3-61

2-(tert-Butoxy)-2-(2-methyl-4-(m-tolyl)quinolin-3-yl)acetic acid

(3.22d): The product was isolated as a 1:0.79 mixture of atropisomers using the peaks at 5.33 and 5.32 ppm. Yellow oil, yield = 8.3 mg, 11%.

IR (thin film) 1726 cm^{-1} ; ^1H NMR (CDCl_3 , 400 MHz) δ : 8.06 (d, $J = 8.4\text{ Hz}$, 1H), 7.67 (ddt, $J = 2.2, 6.6, 8.4\text{ Hz}$, 1H), 7.52-7.30 (m, 5H), 7.15-7.08 (m, 1H), [5.33, 5.32] (s, 1H), 2.84 (s, 3H), 2.44 (s, 3H), [1.01, 1.00] (s, 9H); Exact mass calcd for $C_{23}H_{25}NO_3$ $[M+H]^+$, 364.190720. Found 364.190736.

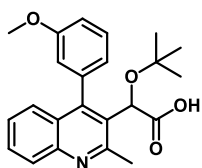


AH-3-53

2-(tert-Butoxy)-2-(2-methyl-4-(3-(trifluoromethyl)phenyl)quinolin-

3-yl)acetic acid (3.22e): The product was isolated as a 1:0.73 mixture of atropisomers using the peaks at 4.99 and 4.92 ppm. Yellow oil, yield = 36.1 mg, 51%. ¹H NMR (MeOH-d₄, 400 MHz) δ: 8.18 (d, *J* = 7.6

Hz, 1H), 7.99 (dd, *J* = 2.7, 8.0 Hz, 1H), 7.87 (t, *J* = 7.2 Hz, 1H), 7.78 (d, *J* = 7.0 Hz, 1H), 7.68 (m, 1H), 7.65 (m, 1H), 7.43 (m, 1H), 7.32 (m, 1H), 4.99 minor, 4.91 major (s, 1H), 2.92 (s, 3H), 0.93 (s, 9H); ¹³C NMR (MeOH-d₄, 100 MHz) δ: [177.65, 177.42] (s), [160.20, 160.13] (s), 145.62 (s), [144.59, 144.55] (s), 137.49 (s), [135.14, 134.04] (d), [133.88, 133.82] (s), [132.36, 132.41,] (q, *J* = 3.5 Hz)*, [130.71, 130.39] (s), 129.85 (d), 129.61 (s), [129.06, 128.77] (q, *J* = 21.5 Hz)*, [128.16, 128.07,] (q, *J* = 5.4 Hz)*, [126.93, 126.66] (q, *J* = 3.7 Hz)*, [126.06, 125.99] (s), [125.95, 125.66] (d), [124.89, 124.66] (q, *J* = 3.7 Hz)*, [74.81, 74.75] (s), [72.16, 72.03] (d), [27.20, 27.16] (q), 20.46 (q). *Due to C-F coupling.



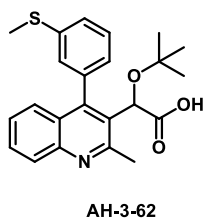
AH-3-42

2-(tert-Butoxy)-2-(4-(3-methoxyphenyl)-2-methylquinolin-3-

yl)acetic acid (3.22f): The product was isolated as a 1:0.72 mixture of atropisomers using the peaks at 3.84 and 3.83 ppm. Yellow oil, yield = 33.7 mg, 54%. ¹H NMR (CDCl₃, 400 MHz) δ: 8.22 (m, 1H), 7.71 (t, *J*

= 7.6 Hz, 1H), 7.45 (m, 3H), 7.29 (m, 1H), 7.08 (dtd, *J* = 0.8, 3.5, 8.3 Hz, 1H), 6.90 (m, 1H), 5.33 minor, 5.32 major (s, 1H), 3.84 minor, 3.83 major (s, 3H), 2.91 (s, 3H), 1.02 minor, 1.01 major (s, 9H); ¹³C NMR (CDCl₃, 100 MHz) δ: [172.35, 172.25] (s), [159.81, 159.04], [158.31, 158.18] (s), 149.11 (s), [136.52, 136.44] (s), [132.17, 132.12] (d), [130.37, 130.12] (d), 129.09 (s), [128.62, 128.50] (d), 126.93 (d), 126.68 (d), 126.15 (s),

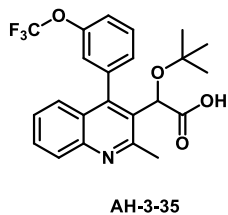
[123.58, 121.69] (d), 115.86 (s), 115.34 (d), [115.60, 114.49] (d), [77.90, 77.72] (s), [70.68, 70.50] (d), [55.43, 55.21] (q), 28.13 (q), 23.79 (q).



2-(tert-Butoxy)-2-(2-methyl-4-(3-(methylthio)phenyl)quinolin-3-

yl)acetic acid (3.22g): The product was isolated as a 1:0.78 mixture of atropisomers using the peaks at 5.30 and 5.27 ppm. Yellow oil, yield = 34.4 mg, 53%. IR (thin film) 1729 cm^{-1} ; ^1H NMR (CDCl_3 , 400 MHz) δ :

8.13 (m, H), 7.66 (m, 1H), 7.52-7.29 (m, 5H), 7.16-7.02 (m, 1H), 5.31 minor, 5.28 major (s, 1H), 2.89 (s, 3H), 2.48 major, 2.44 minor (s, 3H), 1.02 major, 1.00 minor (s, 9H); ^{13}C NMR (CDCl_3 , 100 MHz) δ : [173.01, 172.81] (s), [158.48, 158.45] (s), [148.92, 148.90] (s), [145.89, 145.82] (s), [138.64, 137.55] (s), [136.30, 135.39] (s), 131.74 (d), [129.97, 129.95] (d), [129.57, 128.74] (s), 129.30 (s), [128.27, 128.08] (d), [127.83, 127.78] (d), [127.67, 127.59] (d), [126.72, 126.64] (d), 126.10 (s), 125.75 (d), [77.56, 77.42] (s), 70.69 (d), [28.75, 28.06] (q), [24.01, 23.81] (q), [21.57, 21.42] (q); Exact mass calcd for $\text{C}_{23}\text{H}_{25}\text{NO}_3\text{S}$ $[\text{M}+\text{H}]^+$, 396.162791. Found 396.163160.



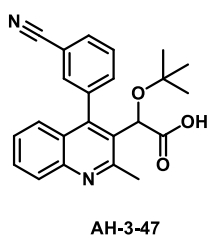
2-(tert-Butoxy)-2-(2-methyl-4-(3-

(trifluoromethoxy)phenyl)quinolin-3-yl)acetic acid (2.22h): The

product was isolated as a 1:0.53 mixture of atropisomers using the peaks at 5.20 and 5.19 ppm. Yellow oil, yield = 63.1 mg, 86%. ^1H

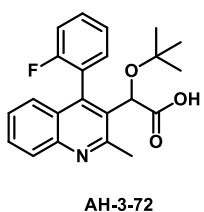
NMR (CDCl_3 , 400 MHz) δ : 8.69 (s, 1H, O-H), 7.87 (tt, $J = 7.1, 1.4$ Hz, 1H), 7.73-7.52 (m, 4H), 7.52-7.42 (m, 2H), 7.22 (s, 1H), 5.20 (minor), 5.19 (major) (s, 1H), 3.14 (minor) 3.11 (major) (s, 3H), 0.99 (s, 9H); ^{13}C NMR (CDCl_3 , 100 MHz) δ : [172.33, 172.14] (s), 158.65 (s), 149.59 (s), 148.84 (s), 135.86 (s), 132.56 (q)*, [132.28, 132.18,] (s), 132.01 (s), 131.51 (s), 131.06 (d), [129.92, 129.33] (d), [128.66, 128.54] (d), [126.78, 126.67]

(d), 126.27 (s), 123.46 (d), 122.42 (d), [77.59, 77.44] (s), [70.04, 69.98] (d), [27.90, 27.85] (q), 21.47 (q); Exact mass calcd for $C_{23}H_{22}F_3NO_4$ $[M+H]^+$, 434.157369. Found 434.157945. * C-F coupling could not be determined for this sample, and so all peaks were reported.



2-(tert-Butoxy)-2-(4-(3-cyanophenyl)-2-methylquinolin-3-yl)acetic acid (3.22i):

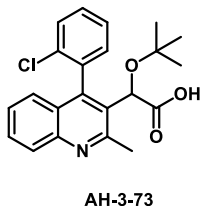
The product was isolated as a 1:0.95 mixture of atropisomers using the peaks at 5.06 and 4.97 ppm. Yellow oil, yield = 31.4 mg, 49%. 1H NMR (MeOH- d_4 , 400 MHz) δ : 8.16-7.90 (m, 3H), 7.71-7.29 (m, 5H), 5.06 major, 4.97 minor (s, 1H), 2.90 minor, 2.87 major (s, 3H), 0.92 minor, 0.89 major (s, 9H); ^{13}C NMR (MeOH- d_4 , 100 MHz) δ : 178.09 (s), 160.13 (s), [146.45, 145.61] (s), [145.55, 145.48] (s), [137.11, 136.73] (s), [135.93, 135.73] (s), [133.88, 133.81] (s), 133.04 (d), 132.83 (s), 131.30 (d), [128.91, 128.75] (d), [128.53, 128.30] (d), [127.46, 127.12] (d), 126.77 (d), 126.55 (d), 126.40 (s), [125.73, 125.49] (d), 74.75 (s), [72.40, 72.32] (d), [27.33, 27.25] (q), [23.44, 23.39] (q); Exact mass calcd for $C_{23}H_{22}N_2O_4 \cdot H_2O$ $[M+Na]^+$, 415.162828. Found 415.163184.



2-(tert-Butoxy)-2-(4-(2-fluorophenyl)-2-methylquinolin-3-yl)acetic acid (3.23b):

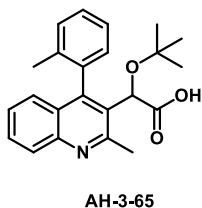
The product was isolated as a 1:0.56 mixture of atropisomers using the peaks at 2.93 and 2.85 ppm. White solid, 35.9 mg, 54%. mp 140-144 °C; IR (thin film) 1722 cm^{-1} ; 1H NMR ($CDCl_3$, 400 MHz) δ : 8.02 (d, J = 8.4 Hz, 1H), 7.80-7.71 (m, 1H), 7.71-7.57 (m, 2H), 7.52-7.22 (m, 4H), 5.23 minor, 5.21 major (s, 1H), 2.93 minor 2.85 major (s, 3H), 1.08 minor, 0.99 major (s, 9H); ^{13}C NMR (CD_3OD , 100 MHz) δ : [174.14, 173.50] (s), [161.69, 159.27] (d, J = 119.4 Hz)*, 158.99 (s), [145.38, 142.68] (d, J = 272.8 Hz) *, [132.50, 132.47] (d),

[131.49, 131.41] (d), 131.27 (d), [131.00, 130.91] (d), 130.85 (d), [129.95, 129.92] (d), [126.61, 126.50] (d, $J = 1.4$ Hz)*, [125.87, 125.70] (d), 125.77 (s), [124.39, 123.94] (d, $J = 3.7$ Hz)*, 123.63 (s), [123.06, 123.90] (s), [115.80, 115.71] (d, $J = 21.5$ Hz)*, [76.15, 75.77] (s), [70.57, 70.34] (d), [26.97, 26.77] (q), [23.12, 22.77] (q). Exact mass calcd for $C_{23}H_{22}FNO_4$ $[M+H]^+$, 368.165648. Found 368.165878.



2-(tert-Butoxy)-2-(4-(2-chlorophenyl)-2-methylquinolin-3-yl)acetic acid (3.23c):

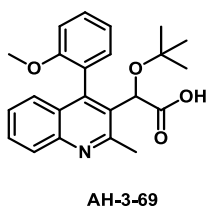
The product was isolated as a 1:0.97 mixture of atropisomers using the peaks at 5.34 and 5.19 ppm. White solid, 66.9 mg, 96%. mp 109-115 °C; IR (thin film) 1729 cm^{-1} ; 1H NMR ($CDCl_3$, 400 MHz) δ : 8.13 (d, $J = 8.5$ Hz, 1H), 7.73-7.62 (m, 2H), 7.81-7.50 (m, 1H), 7.50-7.32 (m, 3H), 7.22-7.15 (m, 1H), 5.34 major, 5.19 minor (s, 1H), 3.04 major, 2.93 minor (s, 3H), 1.16 major, 1.08 minor (s, 9H); ^{13}C NMR ($CDCl_3$, 100 MHz) δ : [173.68, 172.97] (s), [159.35, 158.43] (s), [145.98, 145.54] (s), [145.24, 145.08] (s), [135.64, 134.64] (s), [134.57, 133.53] (s), 133.35 (d), [132.18, 132.08] (d), [130.57, 130.33] (d), 130.04 (s), [129.82, 129.72] (d), [128.59, 128.47] (d), [127.84, 127.70] (d), [126.95, 126.66] (d), [126.41, 125.89] (d), [126.24, 125.41] (s), 76.51 (s), [70.72, 70.39] (d), [28.04, 27.80] (q), [24.32, 24.09] (q); Exact mass calcd for $C_{22}H_{22}ClNO_3$ $[M+H]^+$, 384.136098. Found 384.136256.



2-(tert-Butoxy)-2-(2-methyl-4-(o-tolyl)quinolin-3-yl)acetic acid (3.23d):

The product was isolated as a 1:1 mixture of atropisomers using the peaks at 5.34 and 5.24 ppm. White solid, yield = 75.8 mg, 93% mp 220-226 °C; 1H NMR ($CDCl_3$, 400 MHz) δ : 8.13 (d, $J = 8.4$ Hz, 1H), 7.64 (m, 1H), 7.50-7.28 (m, 4H), 7.24 (m, 2H), 5.34, 5.24 (s, 1H), 2.92, 2.90 (s, 3H), 2.06, 1.91 (s, 3H), 1.15, 1.05 (s, 9H); ^{13}C NMR ($CDCl_3$, 100 MHz) δ : [173.97,

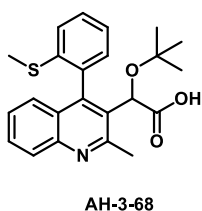
173.33] (s), [159.25, 159.01] (s), [148.92, 148.33] (s), [145.29, 144.92] (s), 136.12 (s)
 [135.23, 134.67] (s), [130.94, 130.62] (d), [130.38, 130.11] (d), 129.95 (s) [128.92,
 128.86] (d), [127.15, 126.98] (d), [126.68, 126.62] (d), [126.55, 126.42] (d), 126.40 (s),
 125.41 (d), 120.28 (d), 76.64 (s), [71.05, 70.62] (d), [28.38, 27.98] (q), [23.89, 23.65] (q),
 [20.44, 20.05] (q); Exact mass calcd for C₂₃H₂₅NO₃ [M+H]⁺, 364.190720. Found
 364.191025.



2-(tert-Butoxy)-2-(4-(2-methoxyphenyl)-2-methylquinolin-3-

yl)acetic acid (3.23f): The product was isolated as a 1:0.38 mixture of atropisomers using the peaks at 3.67 and 3.61 ppm. Yellow solid, yield

= 12.1 mg, 14%. mp 115-120 °C; ¹H NMR (CDCl₃, 400 MHz) δ: 8.37 (m, 1H), 7.72 (m, 1H), 7.62-7.49 (m, 2H), 7.42 (m, 1H), 7.34 (m, 1H), 7.22-7.03 (m, 2H), 5.28 major, 5.08 minor (s, 1H), 3.67 minor, 3.61 major (s, 3H), 3.07 minor, 3.02 major (s, 3H), 1.02 minor, 1.01 major (s, 9H); Exact mass calcd for C₂₃H₂₅NO₄ [M+H]⁺, 380.185635. Found 380.185964.

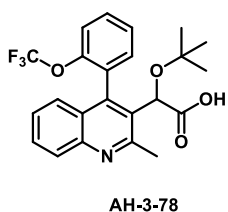


2-(tert-Butoxy)-2-(2-methyl-4-(2-(methylthio)phenyl)quinolin-3-

yl)acetic acid (2.23g): The product was isolated as a 1:0.64 mixture of atropisomers using the peaks at 1.10 and 1.03 ppm. Yellow oil, yield =

5.6 mg, 12%. IR (thin film) 1734 cm⁻¹; ¹H NMR (CDCl₃, 400 MHz) δ: 7.97 minor, 7.96 major (d, *J* = 8.0 Hz, 1H), 7.72 (m, 1H), 7.60-7.10 (m, 6H), 5.14 minor, 5.19 major (s, 1H), 2.99 minor 2.89 major (s, 3H), 2.32 major, 2.31 minor (s, 3H), 1.10 minor, 1.03 major (s, 9H); ¹³C NMR (CDCl₃, 100 MHz) δ: [175.06, 173.60] (s), [159.66, 159.54] (s), [147.03, 146.41] (s), [145.04, 144.92] (s), 138.83 (s) [134.77, 133.54] (s), 131.10 (d), [129.69, 129.62] (d), 129.44 (d) [129.19, 129.12] (d), [126.88,

126.43] (d), [126.35, 126.30] (d), [126.23, 125.83] (d), [124.49, 124.20] (d), [76.17, 75.49] (s), [71.07, 70.71] (d), [27.21, 27.09] (q), [23.61, 22.99] (q), [14.23, 14.27] (q); Exact mass calcd for C₂₃H₂₅NO₃S [M+H]⁺, 396.162791. Found 396.163143.



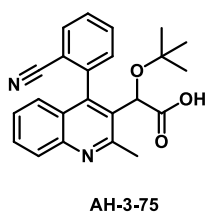
2-(tert-Butoxy)-2-(2-methyl-4-(2-

(trifluoromethoxy)phenyl)quinolin-3-yl)acetic acid (3.23h): The

product was isolated as a 1:0.94 mixture of atropisomers using the

peaks at 5.25 and 5.15 ppm. Colorless oil; IR (thin film) 2904, 1704

cm⁻¹; ¹H NMR (CDCl₃, 400 MHz) δ: 8.10 (d, *J* = 8.4 Hz, 1H), 7.40-7.30 (m, 6H), 7.19 (t, *J* = 9.1 Hz, 1H), 5.25 major, 5.15 minor (s, 1H), 2.99 major, 2.92 minor (s, 3H), 1.07 major, 1.00 minor (s, 9H); ¹³C NMR (CDCl₃, 100 MHz) δ: [173.88, 173.25] (s), [159.49, 158.77] (s), [147.78, 146.72] (s), [146.32, 145.67] (s), [143.05, 142.07] (s), 133.94 (d), 131.64 (d), [130.36, 130.07] (s) [130.44, 130.25] (d), [129.82, 129.75] (d), 128.57 (s), [128.02, 127.84] (d), [126.11, 126.07] (d), [126.36, 125.92] (q, *J* = 11.6 Hz)*, [125.67, 125.76] (d), 116.61 (d), 76.30 (s), [71.21, 70.99] (d), [28.13, 27.83] (q), [24.45, 24.29] (q); Exact mass calcd for C₂₃H₂₂F₃NO₄ [M+H]⁺, 434.157369. Found 434.157785. *Due to C-F coupling



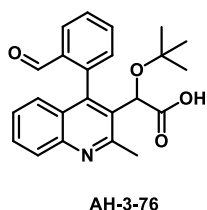
2-(tert-Butoxy)-2-(4-(2-cyanophenyl)-2-methylquinolin-3-yl)acetic

acid (2.23i): The product was isolated as a 1:0.63 mixture of

atropisomers using the peaks at 5.30 and 5.06 ppm. White solid, yield

= 18.6 mg, 56 %. mp >260 °C; IR (thin film) 2904, 1704 cm⁻¹; ¹H NMR (CDCl₃, 400 MHz) δ: 8.14 (t, *J* = 7.7 Hz, 1H), 7.93-7.82 (m, 2H), 7.79-7.56 (m, 3H), 7.40 (m, 1H), 7.18-7.06 (m, 1H), 5.37 major, 5.06 minor (s, 1H), 3.04 major 2.91 minor (s, 3H), 1.17 major, 1.06 minor (s, 9H); ¹³C NMR (CDCl₃, 100 MHz) δ: [173.41, 172.83] (s), [158.84,

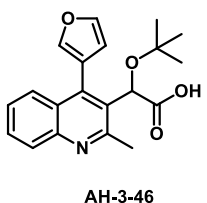
156.73] (s), [146.16, 145.84] (s), [143.96, 143.81] (s), [140.39, 139.30] (s), [132.98, 132.94] (d), [132.61, 132.52] (d), [132.18, 132.09] (d), [130.26, 129.45] (d), 130.14 (s), 129.93 (d), [128.24, 128.09] (d), [127.07, 126.97] (d), [126.41, 125.33] (s), [125.54, 125.11] (d), [117.91, 117.24] (s), [115.04, 113.65] (s), [77.72, 77.57] (s), [70.66, 69.96] (d), [28.07, 27.62] (q), [24.25, 24.09] (q); Exact mass calcd for $C_{23}H_{22}N_2O_3$ $[M+H]^+$, 375.170319. Found exact mass not observed.



2-(tert-Butoxy)-2-(4-(2-formylphenyl)-2-methylquinolin-3-yl)acetic acid

acid (3.23k): The product was isolated as a 1:0.51 mixture of atropisomers using the peaks at 9.50 and 9.48. Black oil, yield = 6.2

mg, 10%. IR (thin film) 2904, 1704 cm^{-1} ; 1H NMR ($CDCl_3$, 400 MHz) δ : 9.50 major, 9.48 minor (s, 1H), 8.18 (t, $J = 7.8$ Hz, 1H), 8.13 (d, $J = 8.5$ Hz, 1H), 7.82-7.59 (m, 3H), 7.39-7.26 (m, 2H), 7.08 (t, $J = 8.4$ Hz, 1H), 5.12, 5.10 (s, 1H), 3.00 major, 2.95 minor (s, 3H), 1.08 major, 0.97 minor (s, 9H); ^{13}C NMR ($CDCl_3$, 100 MHz) δ : [191.08, 190.45] (s), [174.05, 173.60] (s), [159.57, 158.95] (s), [145.11, 144.10] (s), [139.24, 138.35] (s), [135.35, 133.99] (s), 133.46 (d), 131.51 (s), 130.00 (d), [129.71, 129.47] (d), [127.96, 127.73] (d), [127.63, 127.05] (d), [126.93, 126.87] (d), [126.19, 125.95] (d), [76.74, 76.47] (s), [70.88, 70.77] (d), [28.17, 28.04] (q), [23.68, 23.36] (q); Exact mass calcd for $C_{23}H_{23}NO_4$ $[M+H]^+$, 378.169985. Found 378.170217.

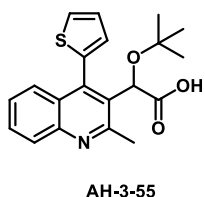


2-(tert-Butoxy)-2-(4-(furan-3-yl)-2-methylquinolin-3-yl)acetic acid

(3.24c): Yellow solid, yield = 77.8 mg, 99% mp >260 °C; IR (thin film)

3352, 1595 cm^{-1} ; 1H NMR ($CDCl_3$, 400 MHz) δ : 7.93 (d, $J = 8.4$ Hz, 1H), 7.79 (d, $J = 9.0$ Hz, 1H), 7.78 (s, 1H), 7.69-7.50 (m, 3H), 7.44 (t, $J = 7.8$ Hz, 1H), 5.35 (s, 1H), 2.86 (s, 3H), 0.97 (s, 9H); ^{13}C NMR ($CDCl_3$, 100 MHz) δ

177.99 (s), 169.06 (d), 159.97 (s), 145.43 (s), 143.03 (d), 138.35 (s), 134.84 (s), [132.44, 132.41] (d), [131.72, 131.62] (d), [128.63, 128.54] (d), 126.74 (d), 126.50 (s), [125.91, 125.59] (d), 119.90 (s), 74.75 (s), 72.14 (d), 27.22 (q), 23.38 (q).



2-(tert-Butoxy)-2-(2-methyl-4-(thiophen-2-yl)quinolin-3-yl)acetic acid (3.24d):

The product was isolated as an 1:0.42 mixture of atropisomers using the peaks at 6.02 and 5.32 ppm. Red-orange solid, yield = 25.9 mg, 59%. mp >260 °C: IR (thin film) 1732 cm⁻¹; ¹H NMR (CDCl₃, 400 MHz) δ: 8.09 (d, *J* = 8.4 Hz, 1H), 7.96 (d, *J* = 8.3 Hz, 1H), 7.72-7.56 (m, 2H), 7.54 (m, 1H) 7.49-7.38 (m, 2H), 6.02 (major), 5.32 (minor) (s, 1H), 2.88 (minor), 2.83 (major) (s, 3H), 1.25 (s, 9H); ¹³C NMR (CDCl₃, 100 MHz) δ: [173.15, 173.38] (s), [157.97, 156.24] (s), 137.16 (s), 134.19 (s), 133.35 (s), [132.24, 132.21, 132.16, 132.06] (d), 131.10 (d), 130.89 (s), 129.57 (d), [128.66, 128.59] (s), 128.11 (d), 127.38 (d), 127.01 (d), 123.46 (d), [77.58, 76.91] (s), [80.26, 70.52] (d), [28.37, 28.12] (q), [23.72, 20.57] (q); Exact mass calcd for C₂₀H₂₁NO₃S [M+H]⁺, 356.131491. Found 356.131781.

3.6.2.3 Recombinant Proteins and IN Multimerization Assay.

Recombinant wild type HIV-1 IN proteins containing either a N-terminal 6xHis or a FLAG tag were expressed in *E. coli* and purified as previously described.⁸ The HTRF-based assay used to monitor the inhibitor induced aberrant multimerization of IN was performed as previously reported.^{i,ii} Briefly, two separate preparations of His-tagged and FLAG-tagged IN proteins were mixed in presence of increasing concentration of the test compounds and incubated for 2.5 h at room temperature. Anti-His6-XL665 and anti-FLAG-EuCryptate antibodies (Cisbio, Inc., Bedford, MA) were then added to the

reaction and incubated at room temperature for 3 h. The IN multimerization HTRF signal was recorded using a PerkinElmer EnSpire multimode plate reader and dose-response curves were fitted using Origin software (v9.4).

CHAPTER IV – A Foray into Organocatalyzed Carbon-Carbon Bond Forming Reactions

4.1 Introduction

4.1.1 Catalysis in Chemistry

Over 80% of industrial chemical manufacturing processes make use of catalysts to increase the rate of a desired reaction.¹²⁷ A catalyst is a substance that decreases the activation energy of a reaction, reduces the overall reaction time, and regenerates at the end of the reaction. Catalysts can be classified according to the phases in which the catalysts, reactants, and products are present and includes homogeneous, heterogeneous, or biological. Traditionally, catalysts have included a transition metal which undergoes a redox cycle to synthesize the desired product while also regenerating the catalyst. Common transition metal catalysts include palladium, platinum, iridium, and rhodium, which are also some of the most expensive metals within the periodic table. The most common catalysts used in industry utilize these precious metals for their inherent activity.¹²⁷⁻¹²⁹ As these catalysts can be extremely difficult to use, are toxic, and are typically non-recoverable, chemists have been developing other catalytic pathways from the traditional redox cycle, which are of great interest to the synthetic community.

4.1.2 Rise of Organocatalysis

New advancements in organic synthesis have led to exchanging these precious metal catalysts for organocatalysts. While documented examples have been sporadic over the last century using small molecules as organocatalysts, it was not until the late 1990's that the field of organocatalysis was born from a small number of inspiring articles.¹³⁰

Approximately 1,500 manuscripts were prepared on the subject between 1998 and 2008, which has led to developing one of the main branches of enantioselective synthesis.

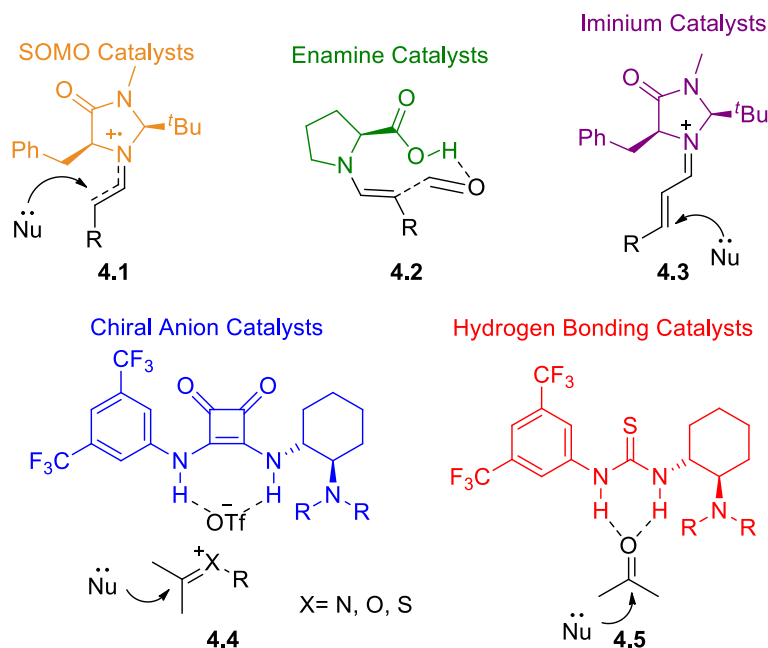


Figure 4.1 Some examples of organocatalysts

There are 5 main binding types of organocatalysts (Figure 4.1): enamine catalysis, hydrogen-bonding catalysis, iminium catalysis, singly occupied molecular orbital (SOMO) catalysis, and chiral anion catalysis.¹³¹ These catalysts have many benefits over their predecessors in that they are stable in air and water, inexpensive and easy to prepare, do not require the use of a glove box, and are non-toxic.

4.1.3 Hydrogen Bonding and Chiral Anion Organocatalysts

Of the previously listed catalysts, squaramide and thiourea catalysts can both be used as hydrogen bonding catalysts, as well as chiral anion catalysts. They typically contain an acidifying group on one arm, a chiral diamine controller on the other, and a central squarate or thiourea group where the hydrogen bond donating (HBD) site is

located (Figure 4.3). The acidifying group contains an aromatic ring with electron withdrawing substituents such as a trifluoromethyl. The purpose of the acidifying group is to decrease the pK_a value of the hydrogens in the HBD site leading to an increased bonding capacity. The chiral diamine controller changes the size and shape of the catalytic pocket and acts as a base in the reaction to deprotonate and place the nucleophile for a selective addition. The center of the catalyst will contain either a squarate or thiourea group with two nitrogens bearing acidic protons. These protons will act as a HBD which will lock in a substrate allowing for selective addition to occur through the assistance of the chiral diamine controller.

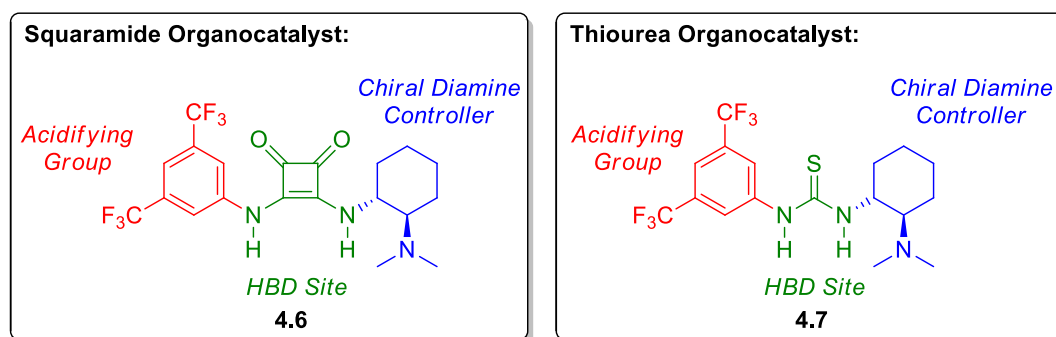


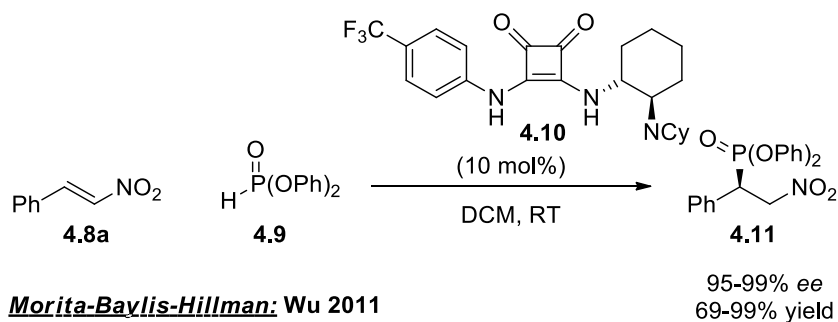
Figure 4.2 General structure of squaramide and thiourea organocatalysts

Thiourea organocatalysts were initially used by Jacobson as HBD catalysts for an asymmetric variant of the Strecker reaction.¹³² Additionally, Jacobson showed the versatility of thiourea catalysts by successfully and enantioselectively coupling imines with silyl enol ethers via a Mannich reaction.¹³³ This led the way for the use of HBD catalysis in the following reactions: Michael addition,¹³⁴⁻¹³⁶ Henry reaction,¹³⁷ and addition to oxonium ions.¹³⁸

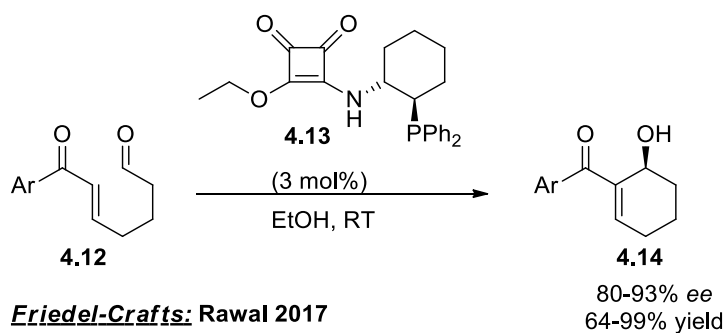
In 2008, Rawal published the first paper using a new class of HBD catalysts with a squarate center.¹³⁹ This new type of organocatalyst quickly became popular in

enantioselective organic reactions such as the Michael addition,¹⁴⁰⁻¹⁴⁴ Friedel-Crafts,¹⁴⁵⁻¹⁴⁶ and Morita-Baylis-Hillman.¹⁴⁷ A summary of these reaction types can be seen in Scheme 4.1.

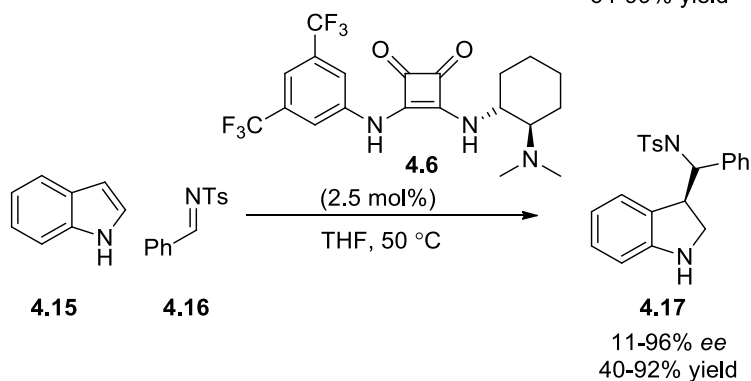
Michael Addition: Rawal 2010



Morita-Baylis-Hillman: Wu 2011



Friedel-Crafts: Rawal 2017



Scheme 4.1 Examples of squaramide catalyzed organic reactions

4.1.4 Structure Activity Relationships of Thiourea and Squaramide Subunits

Recently, squaramide organocatalysts have surpassed the use of thiourea in terms of the number of citations. Delving into the structure activity relationships between the

two systems, it is obvious why squaramides have preference and superior conversion rates and enantioselectivities over their thiourea counterparts. Activation by the catalysts depends on the central nitrogen being in alignment. While both thiourea and the squarate centers have planes of rotation, thiourea substituents have lower energy conformers that rotate the S-C-N-H system out of the desired alignment (Figure 4.4).¹⁴⁸ Substrate **4.7a** is predicted to be 1.5 kcal more stable than **4.7c** due to the weak N-H-S bond and **4.7b** is slightly more stable than **4.7c** by 0.8 kcal due to its intramolecular hydrogen bonding. Additionally, with these intramolecular HBD interactions present, it leads to an increase in the pK_a and decrease in the efficiency of the catalyst. Squaramide catalysts also have the potential to rotate and exploit alternative intramolecular HBD interactions. However, with the rigidity of the squarate center, it makes the distance much greater, and less favorable to access these non-favorable conformers.

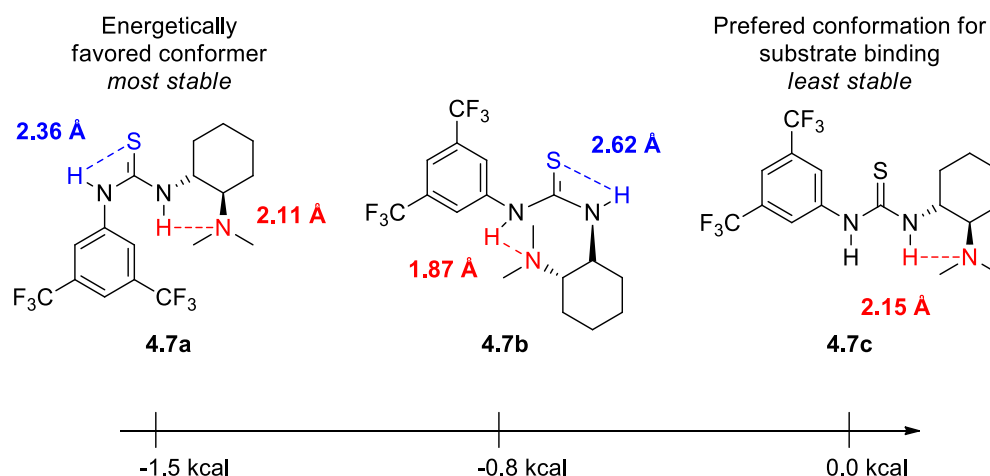


Figure 4.3 Competing conformations of thiourea catalysts

With these considerations in mind, it is not surprising that squaramides typically have pK_a values 0.13-1.97 lower than their thiourea counterparts in DMSO.¹⁴⁹⁻¹⁵⁰ Ultimately the difference in pK_a is strongly dependent on the parent structure and the two

groups attached to the nitrogens. Manipulation of the acidifying group can greatly affect the pK_a as shown in Figure 4.5, more so than the chiral diamine group.

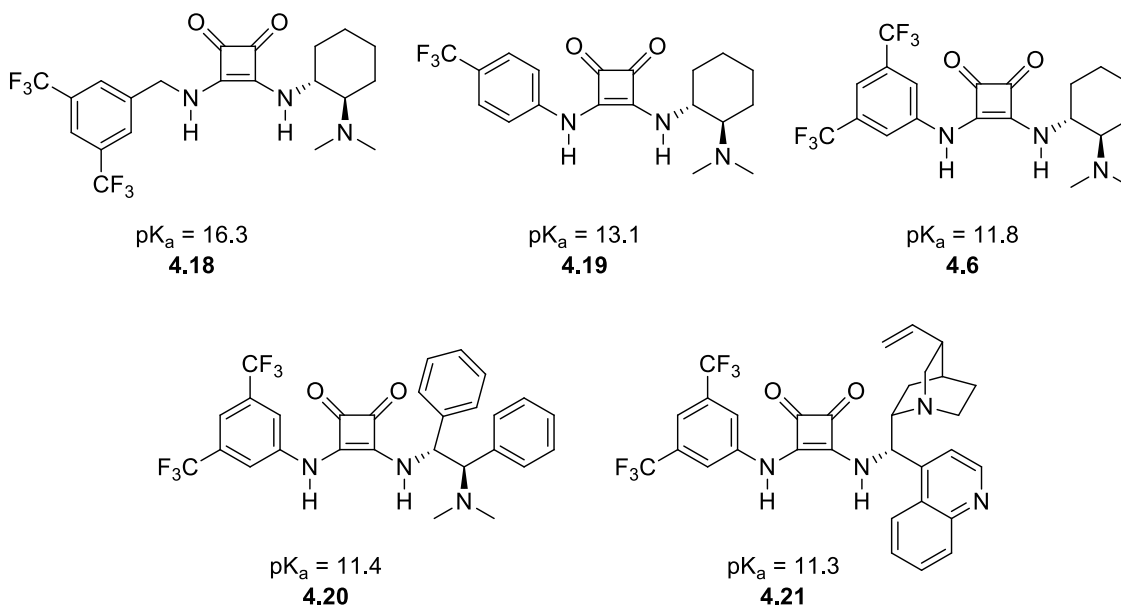


Figure 4.4 Comparison of pK_a values of common squaramide organocatalysts

Although catalyst **4.18** has the highest pK_a , it cannot be assumed that it has the worst activity. In fact, Rawal used a benzyl acidifying group in his initial work with squaramide organocatalysts for the addition of β -diketones to β -nitrostyrenes,¹³⁹ as well as Pedrosa for the synthesis of chromenes and spirochromanes¹⁵¹ and both achieved excellent conversions and enantioselectivity. There are other stabilization factors to consider, including noncovalent interactions between the substrate and catalyst, which factor into the choice of catalyst.

4.2 Research Hypothesis

Manipulation of noncovalent interactions can be used as a tool to guide the development of thiourea and squaramide organocatalysts. This project will have three

components: 1) computational calculation of organocatalyst-substrate binding to better understand the important noncovalent interactions, 2) the synthesis of new organocatalysts utilizing this knowledge, and 3) exploration of new reactions that can be catalyzed through the use of organocatalysts. While the results in the first two areas are very preliminary and will not be discussed here, the results of the third area and a new organocatalyzed reaction will be described.

4.3 Research Design and Methods

4.3.1 Probing New Organocatalyzed Reactions

Since organocatalysis is a new area of research in the group, the first task will be to screen a known Michael addition using purchased squaramide and thiourea organocatalysts.^{136, 139-140, 152} All reactions will be completed by adding the substrate to a 4 mL vial and dissolving in CDCl₃. The use of CDCl₃ will allow the reaction progress to be monitored by ¹H NMR and spectra will be taken at regular intervals. The nucleophile will then be added to the vial followed by the catalyst. The reactions will then be transferred to NMR tubes and left to react.

4.4 Results and Discussion

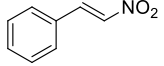
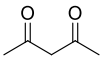
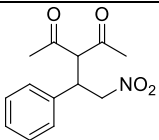
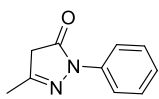
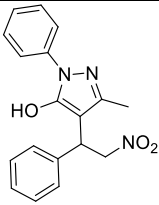
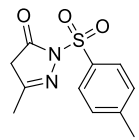
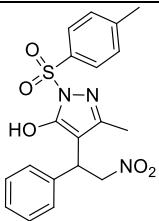
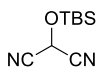
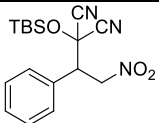
4.4.1 Reaction Screen for Enantioselective Additions

Initial screening with β -nitrostyrenes were chosen due to their prevalence in the literature in Michael additions (Table 4.6, entry 1-5). Both addition of diketones¹³⁹ and pyrazolinones^{135, 141, 152-153} were of interest as they had been done before and gave important information into the design and work up of these enantioselective additions

(entries 1 and 2). To extend the substrate scope for the pyrazolinones, a tosyl substitution on the nitrogen was attempted using squaramide **4.34b** (Table 4.6, entry 3).

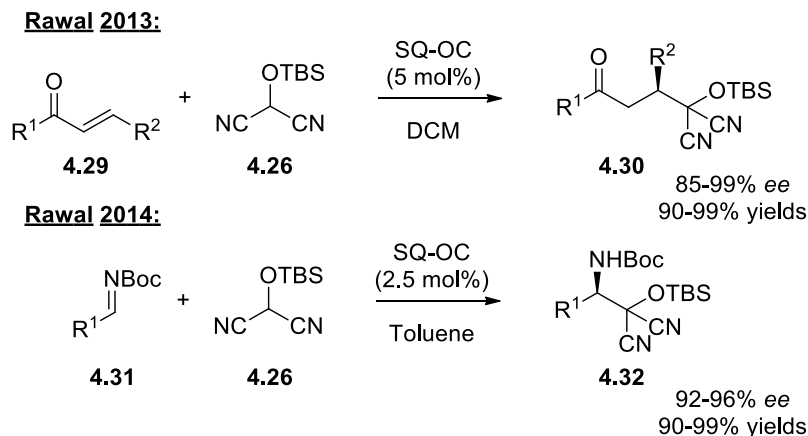
Disappointingly, conversion rates were extremely slow, and the product was unable to be purified by column chromatography.

Table 4.1 Reaction screening for enantioselective Michael addition to β -nitrostyrene

Entry	Electrophile	Nucleophile	Time (hr)	Conversion ^a (%)	Yield ^b (%)	% ee ^c	Substrate	Product
1	 4.8a	 4.22	24	86	--	--	4.27a	
2		 4.23	24	100	95	77	4.27b	
3		 4.24	72 24	66.7 8	--	--	4.27c	
4		NO₂Me 4.25	24	0	--	--	4.27d	No product
5		 4.26	8	100%	77	77	4.28a	

Note: a) conversion is based on ¹H NMR integration of product relative to any remaining starting material. b) yields are of pure products after chromatography. c) Enantioselectivities were determined by chiral HPLC as compared to the racemic entry.

The final nucleophile that was tried with β -nitrostyrene was a masked acyl cyanide (MAC), which has been used previously in the enantioselective addition to imines and enones using a quinine-based squaramide organocatalysts (Scheme 4.2).^{142, 154} MAC reagents are unique acyl anion equivalents that can be unmasked at a later stage as the ester, amide, or carboxylic acid, for example.¹⁵⁵



Scheme 4.2 Enantioselective addition of MAC to π -bonds

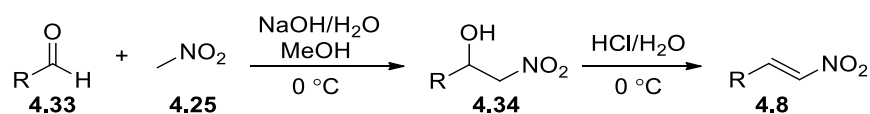
The addition of MAC **4.26** to β -nitrostyrene **4.8a** fully converted to product **4.28a** within 8 hours with a yield of 77% and 77 % *ee*. The addition of MAC to β -nitrostyrene surprisingly has not been accomplished prior. The results leading from this reaction will be discussed further in the following section.

4.4.2 Enantioselective Addition of Masked Acyl Cyanides to β -Nitrostyrenes

4.4.2.1 Synthesis of β -Nitrostyrenes to Fulfill Substrate Scope

To explore the scope of the reaction, multiple β -nitrostyrenes substrates were synthesized using one of three condensation reactions followed by an E2 elimination. The second step either utilized NaOH as the base in cold temperatures¹⁵⁶ or refluxing with ammonium acetate.¹⁵⁷⁻¹⁵⁸ Initially, reactions were tried with NaOH as the base. However,

it was found that the E2 elimination was not occurring if the reaction temperature became too warm, leaving behind the initial condensation adduct **4.34**. Even with the careful addition, the reactions were typically low yielding (10-40%), and some substrates that were tried at lower temperatures also did not progress beyond alcohol **4.34**. Ammonium acetate was also tried, with and without acetic acid, which led to the synthesis of pure material, however there was not an improvement in the yields.



Scheme 4.3 Synthesis of β -nitrostyrenes with byproduct formation

Regardless of the low yields, a range of β -nitrostyrenes were synthesized (Figure 4.8) with both electron withdrawing (**4.8c**, **4.8d**, and **4.8g**) and electron donating groups (**4.8b**, **4.6e**, and **4.8f**), as well as heteroaromatic derivatives (**4.8h** – **4.8j**) and one alkyl variant (**4.8k**). This provided a broad substrate scope for the ensuing Michael addition.

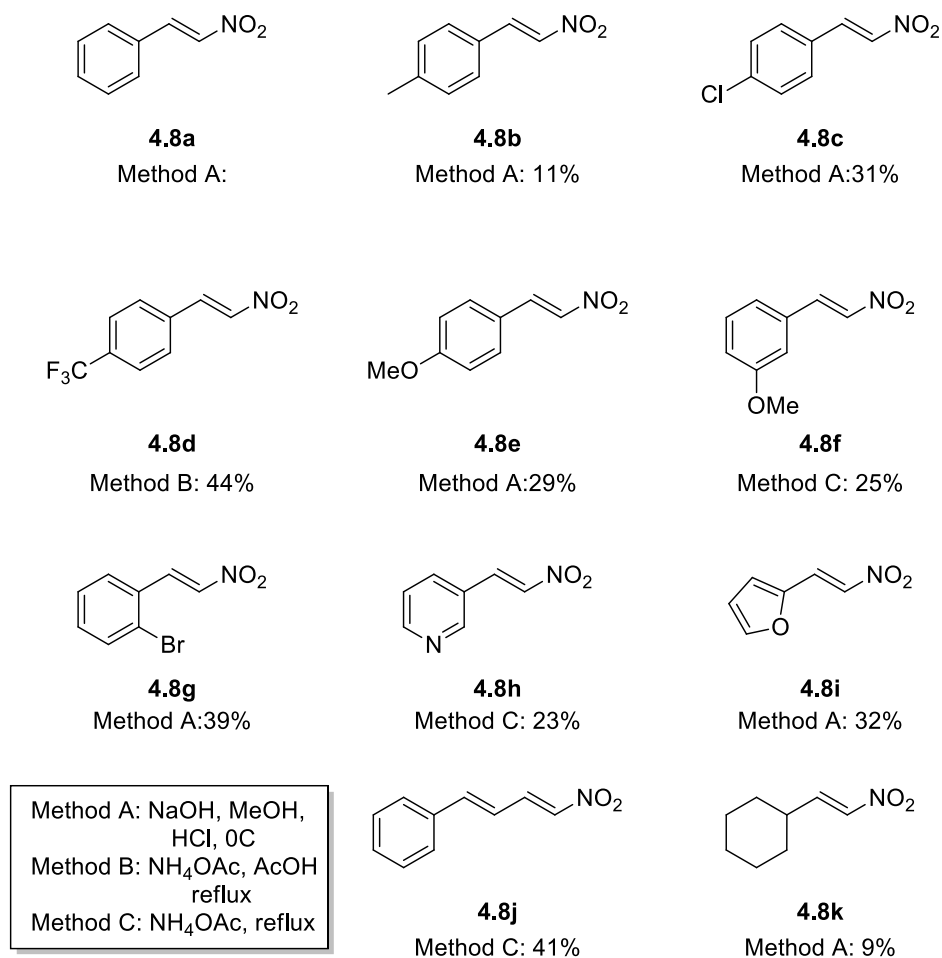


Figure 4.5 Substrate scope of β -nitrostyrenes via aldehyde condensation with nitromethane

4.4.2.2 Enantioselective Addition of Masked Acyl Cyanide to β -Nitrostyrenes

The addition of MAC to β -nitrostyrenes started with an organocatalyst screen using nitrostyrene **4.8a** as the model system. No background reaction was observed without the presence of a catalyst. Each catalyst contained a thiourea or squaramide center with an array of acidifying groups and chiral diamine controllers. MAC **4.26** and β -nitrostyrene **4.8a** were dissolved in CDCl₃ and cooled to 0 °C before catalyst was added. Monitoring the reaction by TLC was difficult as the starting material and product

had similar R_f values. The best solvent system that was determined was using 1:4 DCM in hexanes and running the plate 3 times to see separation. Also, a PAA stain could be used to differentiate between both UV active products as it only stained the desired product. It was much easier to monitor the reactions via ^1H NMR. Therefore, ^1H NMR was taken at 1, 4, 8, and 24 hour increments. Table 4.8 is a summary of the results. It became apparent that the catalysts containing the squarate centers (entries 1-6) were superior to the thioureas (entries 7-14), which is most likely due to the more acidic protons binding the substrates within the catalytic pocket and the more rigid structure of squaramides (Figure 4.6).^{149-150, 159} Additionally, one urea was screened which showed no reaction at all (entry 15).

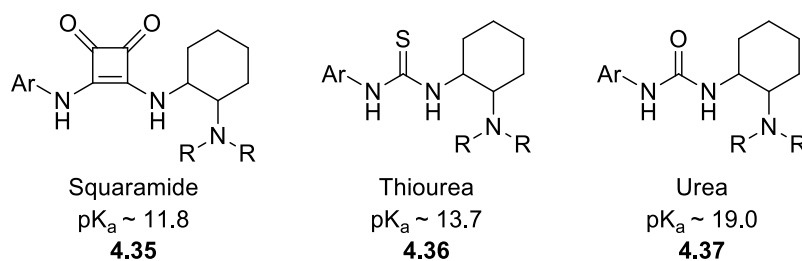


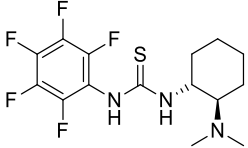
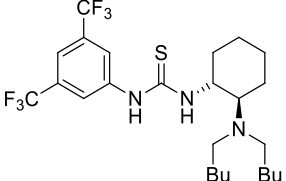
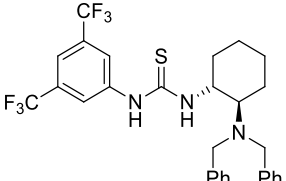
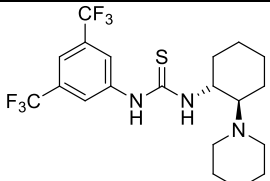
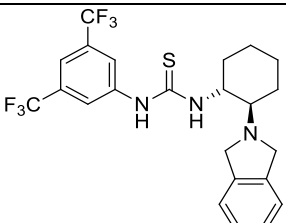
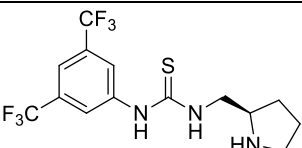
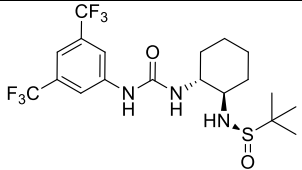
Figure 4.6 pK_a comparison of organocatalysts

Looking more closely at the differences of the catalytic systems, it was found that the reaction favored the chiral cyclohexyl diamines with a slight amount of bulk situated off the basic amine for both the squarate and thiourea series (entries 5, 6, 9, and 12). This resulted in the highest enantioselectivities of both series: 75, 79, 70, and 66% *ee*, respectively. Typically, reactions had complete conversion of the starting materials within 24 hours. Those that did not convert fully include catalysts **4.38d** and **4.38f**, which both contained the largest substituents and are unable to activate MAC. This led to using

catalyst **4.38f** as the chosen catalyst, as it fully converted the desired material within 24 hours with 79% *ee*.

Table 4.2 Organocatalyst Screen

Entry	Substrate	Organocatalyst	Time (h)	Conversion (%)	<i>ee</i> ^b (%)
1	4.38a		24	100	50
2	4.38b		8	100	72
3 ^a	4.38c		24	100	69
4	4.38d		24	100	51
5	4.38e		24	100	75
6	4.38f		24	100	79
7 ^a	4.39a		24	100	56

8	4.39b		8	100	28
9	4.39c		5	100	70
10 ^c	4.39d		96	87	--
12	4.39e		8	100	66
13	4.39f		24	77	17
14	4.39g		24	100	12
15	4.40a		24	0	--
16	--	No catalyst	120	0	--

Note: a) Substrates synthesized in the Donahue Research Group. b) enantioselectivity was determined by chiral HPLC. c) Due to the length of conversion, the %ee was not obtained.

With the best identified catalyst **4.38f** determined, the next steps involved an extensive solvent screen (Table 4.9). Common organic solvents used in Michael additions were screened first (entries 1-6). Solvent had a large effect on the enantioselectivity and

yield of the reaction. In general, non-polar, polar protic, and polar aprotic solvents, were all tolerated, although there were several solvents that had very low conversions (entries 12-14, and 21). This could be due to the higher dielectric strengths of those solvents [acetone (20.7 k) and acetonitrile (11.1 k)]. THF, though, had similar dielectric constants to other solvents that fully converted such as DCM, therefore other factors must be present, such as the ability of THF to serve as a hydrogen bond acceptor via its lone pair electrons on oxygen.

Table 4.3 Solvent screen with organocatalyst **4.38f**

Entry	Solvent	ee ^a (%)	Yield ^b (%)	Conversion (%)
1	DCM	79	74	100
2	CHCl₃	88	96	100
3	hexanes	77	67	100
4	toluene	77	79	100
5	Et ₂ O	61	85	100
6	THF	47	43	60
7	CDCl₃	87	87	100
8	CCl ₄	78	76	100
9	toluene-D ₈	74	83	100
10	toluene-F ₈	79	86	100
11	trifluorotoluene	82	86	100
12	acetone	10	15	13
13	acetonitrile	5	23	38
14	ethyl acetate	48	50	75
15	cyclopentyl methyl ether	63	73	91
16	2-MeTHF	55	89	100
17	MTBE	43	77	91
18	nitromethane	45	54	88
19	perfluorodecalin	52	72	91
20	hexafluoroisopropanol	58	89	97
21	trifluoroethanol	44	71	68

Note: a) enantioselectivity was determined by chiral HPLC. b) yields are of compounds purified by chromatography.

The best solvent was CHCl_3 providing the desired product in 96% yield and 88% *ee*. CDCl_3 was a close second, followed by trifluorotoluene with enantioselectivities of 87% and 82%, respectively. Using halogenated solvents also clearly led to higher enantioselectivities (78-88%) as well as non-polar solvents such as hexanes and toluene (each 77% *ee*). Polar ether solvents such as THF and Et_2O gave lower enantioselectivities.

With the reaction parameters defined, they were then applied to the variety of β -nitrostyrenes that had been previously synthesized. Initially, catalyst loading started at 0.5 mol% of **4.38f** as it converted the model system with good enantioselectivity. However, when this was applied to substrates with substitution at the 4-position, full conversion was not occurring as was expected after 24 hours (Table 4.10, entries 2 and 5). Therefore, the catalyst load was increased to 2 and 5 mol% with **4.28b** which resulted in 95% conversion within 24 hours (entries 3 and 4). Since the results were similar between these two catalyst loadings, all substrates were carried through using 2 mol% of catalyst (Table 4.10).

All β -nitrostyrene derivatives **4.28a-k** converted to the desired product within 24 hours with $\geq 95\%$ conversion. Most of the substrates also converted with enantioselectivities greater than 85%, with two converting with enantioselectivities in the 70's (entry 7 and 12), one in the 60's (entry 14), and the last at 50% *ee* (entry 11). Pyridyl **4.28h** had the lowest enantioselectivity at 50% *ee*, which is unsurprising due to the ability of the nitrogen to participate as a base, enabling the substrate to self-catalyze the racemic reaction. A separate background reaction was carried out using **4.28h** without catalyst to see if a reaction would occur on its own. The reaction was left in an NMR tube

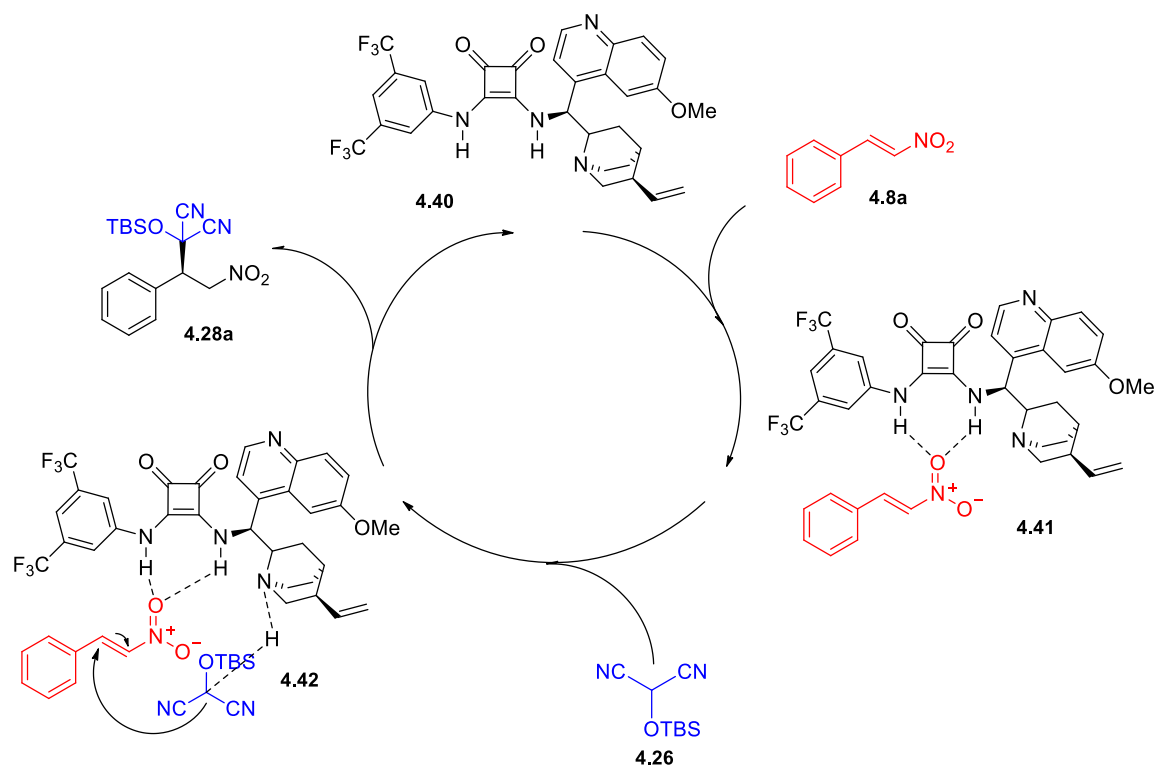
at room temperature for 72 hours. After being checked, there was approximately 5% conversion of starting material to product, conforming the background reaction had occurred. Substrate **4.28k** was the only non-aromatic nitroolefin that was screened and although it did convert to the desired material, it also produced a by-product that led to a decreased yield and *ee* (entry 14).

Table 4.4 Enantioselective substrate scope

<p style="text-align: center;"> $\text{R}-\text{CH}=\text{CH}-\text{NO}_2$ (4.8a) + $\text{NC}-\text{CH}(\text{OTBS})-\text{CN}$ (4.26) $\xrightarrow[\text{0 } ^\circ\text{C, 24h}]{\text{4.38f (0.5 mol\%), CHCl}_3 \text{ (0.3 M)}}$ $\text{R}-\text{CH}(\text{CN})-\text{CH}(\text{NO}_2)-\text{CN}$ (4.28a) </p>						
Entry	Substrate	R	Catalyst Load (mol %)	Conversion ^a (%)	Yield ^b (%)	<i>ee</i> ^c (%) ^a
1	4.28a	Ph	0.05	100	96	88
2	4.28b	4-Me	0.05	87	--	--
3	4.28b	4-Me	0.2	95	74	88
4	4.28b	4-Me	0.5	95	88	88
5	4.28c	4-Cl	0.05	52	--	--
6	4.28c	4-Cl	0.2	95	78	84
7	4.28d	4-CF ₃	0.2	95	49	72
8	4.28e	4-OMe	0.2	95	65	86
9	4.28f	3-OMe	0.2	100	69	87
10	4.28g	2-Br	0.2	98	90	85
11	4.28h	3-pyridyl	0.2	100	65	50
12	4.28i	2-furyl	0.2	100	72	76
13	4.28j	cinnamoyl	0.2	100	99	87
14	4.28k	cyclohexyl	0.2	100	47	67

Note: a) Conversions were determined by ¹H NMR integration of product to remaining starting material. b) Yield is recorded for compounds purified by column chromatography. c) Enantioselectivities were calculated from HPLC integration after the peaks had been compared to the racemic mixtures. A table of retention times and absorbances can be seen in section 4.7.2.3 Table 4.5.

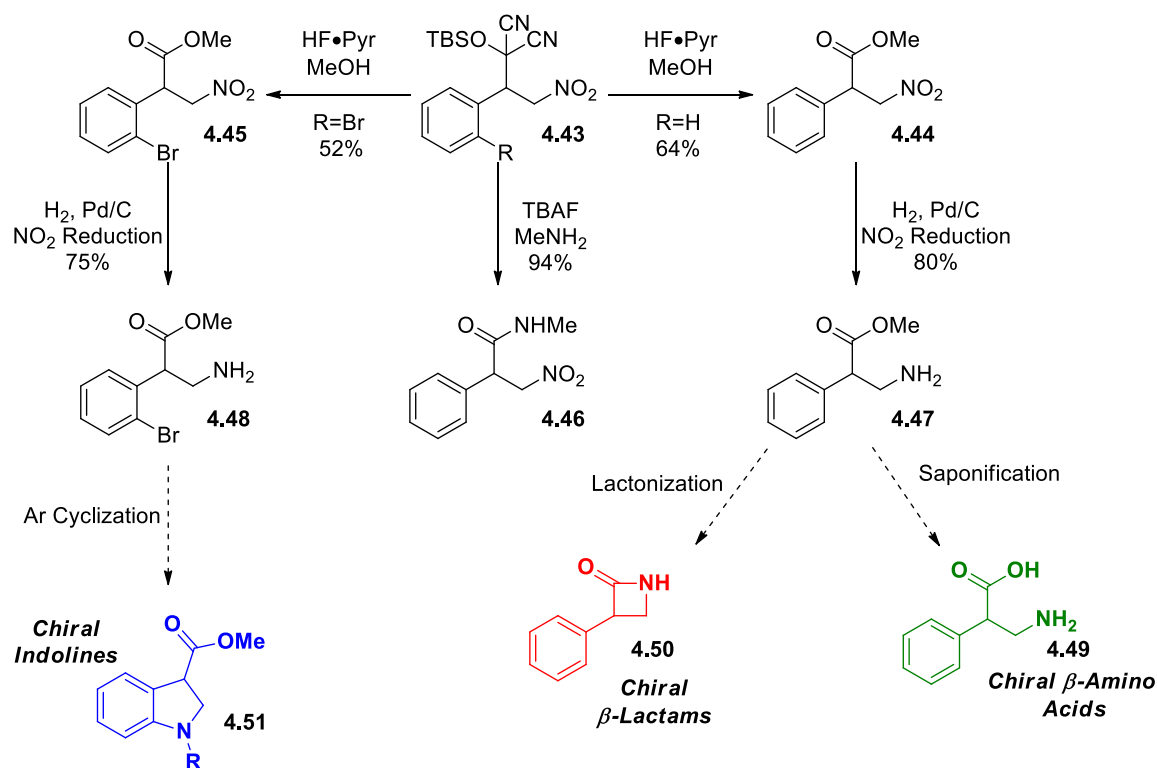
The proposed mechanism uses squaramide organocatalysts to bind to the nitro group of **4.8a** and dock via hydrogen bonding to form complex **4.41**. MAC (**4.26**) has a *pK_a* of ~ 10, enabling deprotonation through the basic nitrogen of the quinine ring, and bringing it within 5 Å of **4.8a** allowing addition to occur (**4.42**) producing **4.28a**.



Scheme 4.4 Catalytic cycle for the addition of MAC to β-nitrostyrene

4.4.2.3 Derivatization of Nitro-MAC Analogs

The products were then converted to desirable natural product synthons including β-amino acids, β-lactams, and indolines (Scheme 4.11). Silyl deprotection of **4.28a** using TBAF in the presence of N-methylamine converted the MAC group to nitroamide **4.46** with a 94% yield. Also, HF·Pyr in the presence of MeOH converted the MAC group to nitroesters **4.44** and **4.45** with yields of 64 and 52%, respectively. Reduction of the nitro group was accomplished via H₂ and Pd/C to synthesize amines **4.47** and **4.48** with yields of 80 and 75%, respectively.



Scheme 4.5 Derivatization of β -nitrostyrenes to for desirable natural product synthons

The remaining derivatizations shown in Scheme 4.5 have yet to be completed.

Chiral β -amino acids can be produced from **4.44** using LiOH in $\text{THF}/\text{H}_2\text{O}$.¹⁶⁰ The rotation of **4.46** will be measured and compared to a known amino acid to determine the exact configuration of the stereocenter. Based on the proposed catalytic cycle, the *R*-enantiomer is predicted. Exposure of **4.44** to MeMgBr and Et_2O will trigger lactonization to form chiral β -lactams.¹⁶¹ Additionally amine **4.45** can undergo a reductive cyclization using Bu_3SiH and AIBN to synthesize indoline **4.48**.¹⁶² These remaining reactions serve to both identify the enantiomer formed in the addition of MAC reagents to β -nitrostyrenes and to highlight the utility of the method by forming useful natural product synthons.

4.5 Summary and Conclusion

The understanding of the important noncovalent interactions within organocatalyzed reactions is undoubtedly an underexplored area of research, providing new avenues of catalyst design and reaction development. The research group is interested in squaramide and thiourea catalysts that serve as dual catalysts able to both hydrogen bond to activate the substrate and to deprotonate a nucleophile. With these properties in mind, an initial screen of new Michael addition reactions was undertaken and the addition of a masked acyl cyanide (MAC) reagent to β -nitrostyrene was realized. MACs are unique one carbon nucleophiles providing the synthetic equivalent of an acyl anion addition to a substrate. Squaramide and thiourea organocatalysts contain tertiary amines that are basic enough to deprotonate the MAC. The products are enantiopure nitroolefins with a chiral center adjacent to an aromatic ring. A catalyst screen identified a quinine-derived squaramide organocatalyst as the ideal catalyst and a solvent screen identified chloroform as the solvent that provided the best conversions and enantioselectivity. A variety of substituted β -nitrostyrenes were synthesized to demonstrate the substrate scope. Using only 2 mol% of catalyst, all substrates converted in $\geq 95\%$ within 24 hours. Product yields ranged from 50-96% with 50-88% *ee*. Additionally, a route to desirable natural product synthons such as β -amino acids, β -lactams, and 2-substituted indolines is in progress and demonstrates the utility of the products.

4.6 Experimental

4.6.1 General Methods

4.6.1.1 Experimental Techniques

Starting materials were purchased from commercial vendors and used without purification unless noted. Unless otherwise noted, all reactions were carried out using flame-dried glassware and standard syringe, cannula, and septa techniques, when necessary.⁶⁷ Tetrahydrofuran (THF), diethyl ether (Et₂O), hexanes, dichloromethane (CH₂Cl₂), and toluene (PhCH₃) were dried by passage through a column of activated alumina on an mBraun SPS.⁶⁸ Acetonitrile (ACN) was dried by passage through a column of activated alumina on an Innovative Technologies system. Analytical thin layer chromatography was performed using Sorbent Technologies 250 μm glass-backed UV254 silica gel plates. The plates were first visualized by fluorescence upon 254 nm irradiation then by iodine chamber. The plates were then dipped in one of the following stains followed by heating: *p*-anisaldehyde, phosphomolybdic acid, vanillin, ceric ammonium molybdate, potassium iodoplatinate, ninhydrin or bromocresol green. Flash column chromatography was performed using Sorbent Technologies 40-63 μm, pore size 60 Å silica gel with solvent systems indicated. Solvent removal was affected using a Buchi R3 rotary evaporator with a V900 diaphragm pump (~10 mmHg). All yields refer to isolated material that is chromatographically (TLC or HPLC) and spectroscopically (¹H NMR) homogenous.

4.6.1.2 Characterization

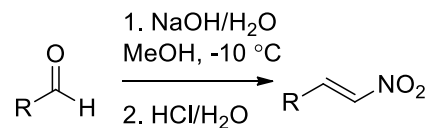
All melting points were taken with a Thomas Hoover melting point apparatus and are uncorrected. Infrared spectra were recorded on a Nicolet Nexus 470 FTIR spectrometer as neat liquids, oils, solids or as thin films formed from evaporation of NMR solvent over the ATR plate. HPLC were recorded on an Agilent 1260 Infinity using a CHIRALPAK IC (4.6 x 250 mm, 5 micron) column with a isocratic gradient of 5% iPrOH in hexanes monitoring at 214 nm. High-resolution mass spectra were recorded at the Old Dominion University College of Science Major Instrumentation Center (COSMIC) on a Bruker 12 Tesla APEX-Qe FTICR-MS with an Apollo II ion source. Combustion analysis was performed at Atlantic Microlabs on samples taken from the bulk of the material. Optical rotation analysis was done with a Rudolph Research Analytical Autopol IV Automatic Polarimeter.

4.6.1.3 NMR Parameters

Proton nuclear magnetic resonance spectra were recorded on a Bruker UltraShield Plus 400 MHz spectrometer and are recorded in parts per million from internal chloroform (7.26 ppm), methanol, benzene, or dimethylsulfoxide on the δ scale and are reported as follows: chemical shift [multiplicity (s=singlet, d=doublet, t=triplet, q=quartet, qu=quintet, m=multiplet, and derivatives thereof), coupling constant(s) in hertz, integration, interpretation]. ⁶⁹ ¹³C NMR data were recorded on a Bruker UltraShield Plus 100 MHz spectrometer and are reported as follows: chemical shift (multiplicity as determined from DEPT (CH, CH₃ up and CH₂ down) and/or HSQC experiments).

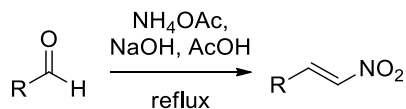
4.6.1.4 General Procedures for the Synthesis of β -Nitrostyrene Derivatives

Method 1:¹⁵⁶

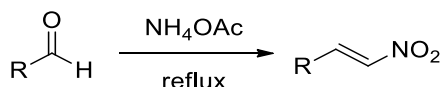


To a flask fitted with a thermometer in an ice salt water bath, aldehyde (16.65 mmol, 1 eq) followed by methanol (16.65 mmol, 5 M) and nitromethane (16.65 mmol, 1 eq) were added. The solution cooled to -10 °C and sodium hydroxide (16.65 mmol, 25 M) was added dropwise via syringe keeping the temperature between 0 – 10 °C. A white precipitant formed. If the solution became too thick to stir properly, 1-2 mL of methanol was added. The slurry stirred for fifteen minutes. To this, 6-7 mL of ice water was added slowly, and was added dropwise via pipette to a solution of hydrochloric acid (16.65 mmol, 1.67 M) that was in an ice and salt water bath. The temperature was kept below 10 °C. This stirred for 30 minutes at 10 °C. The resulting solid or oil was purified as needed.

If solid formed, it is filtered out by suction and washed with ice water. The resulting solid is recrystallized with cold ethanol producing a pure product. If an oil formed, it was extracted with Et₂O (20 mL x 3). The combined organic phase was washed with brine, dried over sodium sulfate, filtered, and condensed to a crude oil which was purified by column chromatography.

Method 2:¹⁵⁸

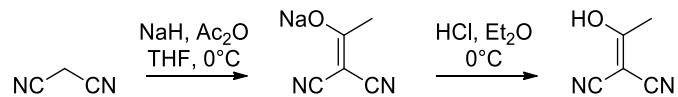
An aldehyde (2.87 mmol, 1 eq) was added dropwise via syringe into a solution of ammonium acetate (6.80 mmol, 2.4 eq), nitromethane (2.87 mmol, 0.5 M), and acetic acid (2.87 mmol, 0.25 M) that was refluxing at 90 °C. The reaction refluxed for 5 hours and then was poured into water and extracted with EtOAc (20 mL x 3). The combined organic layers were washed with brine, dried over sodium sulfate, filtered and concentrated into a crude oil. The crude was purified by column chromatography.

Method 3:¹⁵⁷

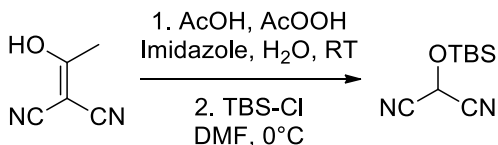
Aldehyde (15.13 mmol, 1 eq) and nitromethane (15.13 mmol, 0.33 M) were added to a flask followed by ammonium acetate (4.54 mmol, 0.3 eq) and stirred for 5 hours at 100 °C. The reaction cooled and ethyl acetate (30 mL) and water (30 mL) were added to the reaction flask. The reaction was extracted by EtOAc (60 mL) three times. The combined organic layers were washed with brine, dried over sodium sulfate and filtered. The resulting crude was either purified by column chromatography or recrystallization with cold ethanol.

Characterization data can be found at the provided references for substrates **4.8a-k**.

4.6.1.5 General Procedure for the Synthesis of TBS protected Masked Acyl Cyanide



Part A:¹⁶³ NaH (0.17 mol) was added to a flame dried, 250 mL, two-necked, round bottom flask. The flask was capped with a rubber septum and then purged with N_2 for 5 minutes. THF (90 mL) was added to the flask via syringe, and the reaction was cooled to 0°C for 10 minutes. Malononitrile (5.0 g, 0.076 mol) was added to a separate flamed dried 50 mL recovery flask and fully dissolved in THF (5 mL) before it was transferred via syringe to the 250 mL round bottom flask. The reaction stirred for 30 minutes before acetic anhydride (0.076 mol) was added dropwise via syringe before stirring for an additional 60 minutes. The reaction was then warmed to room temperature and the solvent removed in vacuo. The resulting solid is then slurried with acetone before being filtered. The filter cake is collected, slurried again with acetone and filtered an additional two times. The brown filtrate is then collected and concentrated to produce a light tan solid. The solid is then transferred to a flame dried 250 mL round bottom flask and dissolved in diethyl ether (40 mL). The reaction is then cooled to 0°C before a solution of 2 M HCl in diethyl ether (40 mL) is added. The reaction is then warmed to room temperature over a 2-hour period, before the solid is filtered and rinsed with DCM (25 mL). The brown solid is then collected and dried over night to produce acetyl malononitrile as a tacky brown solid. (7.56 g, 98% yield)



Part B:¹⁴² Acetyl malononitrile (1.3g, 12 mmol) was added to a 200 mL round bottom flask and dissolved in H₂O (10 mL). AcOOH (10 mL) and AcOH (20 mL) were mixed together in a secondary container before being added to the acetyl malononitrile. The reaction stirred at room temperature for 2 hours before the solvents were removed in vacuo to produce a white oil. The oil was then dissolved in DMF (20 mL) and cooled to 0 °C. TBS-Cl (3.07g, 20.4 mmol) was added followed by imidazole (1.23g, 18 mmol). The reaction stirred for 30 minutes at 0 °C and then 30 minutes at room temperature. The reaction as diluted with Et₂O (40 mL) and H₂O (30 mL) and extracted 3 times with Et₂O (20 mL). The organic layer was collected washed with saturated NaHCO₃ (20 mL) and Brine (20 mL) before being dried over Na₂SO₄. The resulting solution was concentrated and purified on SiO₂ (0%, 3%, 6% EtOAc/Hex). Pale Yellow Oil.

4.6.1.6 General Procedure for the Racemic Base Catalyzed Addition of Masked Acyl Cyanides to β -Nitrostyrenes



To a flame dried 4 mL vial fitted with a stir bar, 2-((tert-butyldimethylsilyl)oxy)-malononitrile (MAC) (43 mg, 1.1 eq) was added and dissolved in deuterated chloroform (0.670 mL, 0.3 M). β -Nitrostyrene (30 mg, 1.0 equiv) was added followed by base (0.1 eq). The reaction was monitored by ¹H NMR until complete. The crude material was

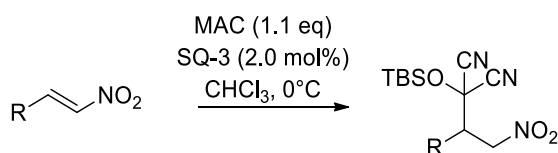
purified by SiO₂ (5-10% EtOAc/hexanes), and analyzed by HPLC Chiralpak IC 95% hexanes/iPrOH, flow rate 1 mL/min.

Table 4.5 Racemic synthesis of the MAC addition to β -nitrostyrenes

Entry	R ₁	R ₂	Base (0.1 eq)	Conversion (%)	Yield (%)	Peak 1 (min)	Peak 2 (min)
1a	Ph	H	TEA	0	---	---	---
1b	Ph	H	Pyridine	32	---	---	---
1c	Ph	H	DMAP	0	--	---	---
1d	Ph	H	Imidazole	51	---	---	---
1e	Ph	H	NaOH	100		5.374	6.549
2	4-MePh	H	NaOH	100	54.7	5.289	6.743
3	4-ClPh	H	NaOH	100	33.5	6.305	7.713
4	4-CF ₃ Ph	H	NaOH	100	51.0	5.110	6.468
5	4-OMePh	H	NaOH	100	95.0	7.197	8.757
6	3-OMePh	H	NaOH	100	52.8	6.696	7.721
7	2-BrPh	H	NaOH	100	65.0	5.450	6.376
8	3-Pyridine	H	NaOH	100	30.3	3.484	4.130
9	Furan	H	NaOH	100	28.2	5.227	6.161
10	Cinnamoyl	H	NaOH	100	72	5.797	6.462
11	Cyclohexyl	H	NaOH	100	30	4.241 (6.218)	4.580 (6.603)

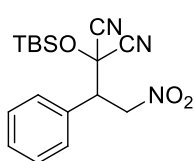
4.6.1.7 General Procedure for the Organocatalyzed addition of Masked Acyl

Cyanides to β -Nitrostyrenes



To a flame dried 4 mL vial fitted with a stir bar was added 2-((tert-butyldimethylsilyl)oxy)malononitrile (MAC) (43 mg, 1.1 eq). Chloroform (0.670 mL, 0.3 M) was added followed by β -nitrostyrene (30 mg, 1.0eq). The reaction was then placed in the freezer to stir for 10 minutes while cooling to 0 °C before organocatalyst (0.4 mg, 0.005 eq) was added. The reaction was left to stir at 0 °C for 24 hours before the solvent

was removed. The crude material was purified on SiO₂ (5%-10% EtOAc/hexanes) and analyzed by HPLC Chiralpak IF 95% hexanes/iPrOH at a flow rate of 1 mL/min.

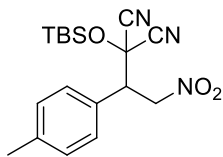


2-((tert-Butyldimethylsilyl)oxy)-2-(2-nitro-1-

phenylethyl)malononitrile (4.28a): Following the general procedure

for the enantioselective addition of MAC to β -nitrostyrenes., **4.8a** was

isolated as a white solid (67.0 mg, 96% yield, 88% *ee*). R_f = 0.41 (20% EtOAc/Hex). mp 63-65 °C; IR (thin film) 3020, 2932, 2859, 2246, 1558, 1379, 1129 cm⁻¹; ¹H NMR (CDCl₃, 400 MHz) δ 7.47-7.39 (m, 5H), 5.07 (dd, J = 13.8, 5.8 Hz, 1H), 4.93 (dd, J = 13.8, 8.4, Hz, 1H), 4.26 (dd, J = 8.4, 5.8 Hz, 1H), 0.93 (s, 9H), 0.37 (s, 3H), 0.32 (s, 3H); ¹³C NMR (CDCl₃, 100 MHz) δ 130.5 (d), 130.4 (s), 129.5 (d, 2C), 113.8 (s), 113.4 (s), 74.8 (t), 66.9 (s), 53.4 (d), 25.3 (q), 18.2 (s), -4.59 (q), -4.62 (q); HPLC: R_t 7.29 min (major), 5.81 min (minor); $[\alpha]_D^{25}$ = +7.5 (c = 1.0, CHCl₃); HRMS ESI: Exact mass calcd for C₁₇H₂₃N₃O₃SiNa [M+Na]⁺, 368.1400. Found 368.1402.



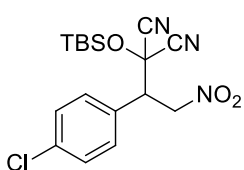
2-((tert-Butyldimethylsilyl)oxy)-2-(2-nitro-1-(p-

tolyl)ethyl)malononitrile (4.28b): Following the general procedure

for the enantioselective addition of MAC to β -nitrostyrenes, **4.8b** was

isolated as a pale yellow oil (48.2 mg, 73% yield, 88% *ee*). R_f = 0.43 (20% EtOAc/Hex). IR (thin film) 2931, 2860, 2240, 1562, 1375, 1128 cm⁻¹; ¹H NMR (CDCl₃, 400 MHz) δ 7.30 (d, J = 8.2 Hz, 2H), 7.23 (d, J = 8.2 Hz, 2H), 5.04 (dd, J = 13.6, 5.8 Hz, 1H), 4.90 (dd, J = 13.6, 8.4 Hz, 1H), 4.22 (dd, J = 8.4, 5.8 Hz, 1H), 2.37 (s, 3H), 0.94 (s, 9H), 0.38 (s, 3H), 0.32 (s, 3H); ¹³C NMR (CDCl₃, 100 MHz) δ 140.5 (s), 130.1 (d), 129.2 (d), 127.1 (s), 113.8 (s), 113.3 (s), 74.2 (t), 67.0 (s), 53.0 (d), 25.2 (q), 21.3 (q), 18.1 (s), -4.72 (q), -

4.74 (q); HPLC: R_t 6.59 min (major), 5.24 min (minor); $[\alpha]^{25}_D = +6.5$ ($c = 1.0$, CHCl_3); HRMS ESI: Exact mass calcd for $\text{C}_{18}\text{H}_{25}\text{N}_3\text{O}_3\text{SiNa}$ $[\text{M}+\text{Na}]^+$, 382.1557. Found 382.1559.

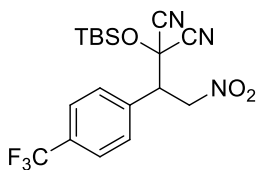


2-((tert-Butyldimethylsilyl)oxy)-2-(1-(4-chlorophenyl)-2-

nitroethyl)malononitrile (4.28c): Following the general procedure

for the enantioselective addition of MAC to β -nitrostyrenes, **4.8c** was

isolated as a yellow oil (48.4 mg, 78% yield, 84% *ee*). $R_f = 0.46$ (20% EtOAc/Hex). IR (thin film) 2931, 2860, 2237, 1562, 1375, 1130 cm^{-1} ; ^1H NMR (CDCl_3 , 400 MHz) δ 7.43 (d, $J = 8.5$ Hz, 2H), 7.36 (d, $J = 8.5$ Hz, 2H), 5.05 (dd, $J = 13.8, 5.5$ Hz, 1H), 4.89 (dd, $J = 13.8, 8.8$ Hz, 1H), 4.23 (dd, $J = 8.8, 5.5$ Hz, 1H), 0.94 (s, 9H), 0.38 (s, 3H), 0.33 (s, 3H); ^{13}C NMR (CDCl_3 , 100 MHz) δ : 136.6 (s), 130.7 (d), 129.7 (d), 128.7 (s), 113.5 (s), 113.1 (s), 73.9 (t), 66.4 (s), 52.7 (d), 25.2 (q) 18.1 (s), -4.71 (q), -4.75 (q); HPLC: R_t 7.55 min (major), 6.20 min (minor); $[\alpha]^{25}_D = -0.03$ ($c = 1.0$, CHCl_3); HRMS ESI: Exact mass calcd for $\text{C}_{17}\text{H}_{22}\text{ClN}_3\text{O}_3\text{SiNa}$ $[\text{M}+\text{Na}]^+$, 402.1011. Found 402.1013.



2-((tert-Butyldimethylsilyl)oxy)-2-(2-nitro-1-(4-

(trifluoromethyl)phenyl)ethyl)malononitrile (4.28d): Following

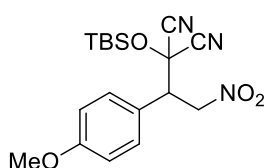
the general procedure for the enantioselective addition of MAC to

β -nitrostyrenes, **4.8d** was isolated as a yellow oil (28.0 mg, 49% yield, 72% *ee*). $R_f = 0.20$ (5% EtOAc/Hex). IR (thin film) 2955, 2933, 2860, 2237, 1562, 1325, 1119 cm^{-1} ; ^1H NMR (CDCl_3 , 400 MHz) δ 7.72 (d, $J = 8.2$ Hz, 2H), 7.57 (d, $J = 8.2$ Hz, 2H), 5.09 (dd, $J = 13.9, 5.4$ Hz, 1H), 4.95 (dd, $J = 13.9, 8.9$ Hz, 1H), 4.33 (dd, $J = 8.9, 5.4$ Hz, 1H), 25.1 (s, 9H), 18.1 (s), -4.72 (s, 3H), -4.77 (s, 3H); ^{13}C NMR (CDCl_3 , 100 MHz) δ 134.2 (s), 132.4 (q, $J = 33.0$ Hz)*, 129.9 (d), 126.4 (q, $J = 3.6$ Hz)*, [127.5, 124.8, 122.1, 119.4] (s), 113.4 (s), 113.0 (s), 73.8 (t), 66.2 (s), 59.2 (d), 25.1 (q), 18.1 (s), -4.72 (q), -4.77 (q);

HPLC: R_t 6.27 min (major), 5.02 min (minor); $[\alpha]^{25}_D = -20.2$ ($c = 0.63$, CHCl_3); HRMS

ESI: Exact mass calcd for $\text{C}_{18}\text{H}_{22}\text{F}_3\text{N}_3\text{O}_3\text{SiNa}$ $[\text{M}+\text{Na}]^+$, 436.1274. Found 436.1277.

*Due to C-F coupling.



2-((tert-Butyldimethylsilyl)oxy)-2-(1-(4-methoxyphenyl)-2-

nitroethyl)malononitrile (4.28e): Following the general

procedure for the enantioselective addition of MAC to β -

nitrostyrenes, **4.8e** was isolated as a pale-yellow oil (54.1 mg, 86% yield, 86% *ee.*). $R_f =$

0.20 (5% EtOAc/Hex). IR (thin film) 2932, 2860, 2245, 1262, 1515, 1376, 1255, 1128

cm^{-1} ; ^1H NMR (CDCl_3 , 400 MHz) δ 7.34 (d, $J = 8.7$ Hz, 1H), 6.94 (d, $J = 8.7$ Hz, 1H),

5.03 (dd, $J = 13.6, 5.7$ Hz, 1H), 4.88 (dd, $J = 13.6, 8.6$ Hz, 1H), 3.82 (s, 3H), 4.21 (dd, $J =$

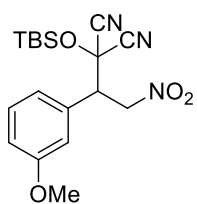
8.6, 5.7 Hz, 1H), 25.2 (s, 9H), 0.38 (s, 3H); 0.33 (s, 3H); ^{13}C NMR (CDCl_3 , 100 MHz) δ

161.0 (s), 130.6 (d), 121.9 (s), 114.8 (d), 113.8 (s), 113.3 (s), 74.3 (t), 67.0 (s), 55.3 (q),

52.7 (d), 25.2 (q), 18.1 (s), -4.72 (q), -4.74 (q); HPLC: R_t 8.57 min (major), 7.08 min

(minor); $[\alpha]^{25}_D = +8.1$ ($c = 1.0$, CHCl_3); HRMS ESI: Exact mass calcd for

$\text{C}_{18}\text{H}_{25}\text{N}_3\text{O}_4\text{SiNa}$ $[\text{M}+\text{Na}]^+$, 398.1506. Found 398.1509.



2-((tert-Butyldimethylsilyl)oxy)-2-(1-(3-methoxyphenyl)-2-

nitroethyl)malononitrile (4.28f): Following the general procedure for

the enantioselective addition of MAC to β -nitrostyrenes, **4.8f** was

isolated as a white solid (43.3 mg, 69% yield, 87% *ee.*). $R_f = 0.36$ (20% EtOAc/Hex). mp

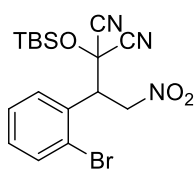
77-80 $^\circ\text{C}$; IR (solid) 2958, 2931, 2860, 2243, 1559, 1259, 1136 cm^{-1} ; ^1H NMR (CDCl_3 ,

400 MHz) δ 7.34 (t, $J = 8.0$ Hz, 1H), 7.04-6.91 (m, 3H), 5.04 (dd, $J = 13.8, 5.8$ Hz, 1H),

4.90 (dd, $J = 13.8, 8.3$ Hz, 1H), 4.22 (dd, $J = 8.3, 5.8$ Hz, 1H), 3.82 (s, 3H), 0.94 (s, 9H),

0.38 (s, 3H), 0.33 (s, 3H); ^{13}C NMR (CDCl_3 , 100 MHz) δ 160.1 (s), 131.6 (d), 130.4 (d),

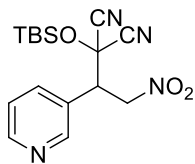
121.3 (d), 115.7 (d), 115.3 (d), 113.7 (s), 113.3 (s), 74.2 (t), 66.7 (s), 55.4 (q), 53.2 (d), 25.2 (q), 18.1 (s), -4.71 (q), -4.75 (q); HPLC: R_t 7.44 min (major), 6.50 min (minor); $[\alpha]_D^{25} = +7.0$ ($c = 0.96$, CHCl_3); HRMS ESI: Exact mass calcd for $\text{C}_{18}\text{H}_{25}\text{N}_3\text{O}_4\text{SiNa}$ $[\text{M}+\text{Na}]^+$, 398.1506. Found 398.1509.



2-(1-(2-Bromophenyl)-2-nitroethyl)-2-((tert-

butyldimethylsilyl)oxy)malononitrile (4.28g): Following the general procedure for the enantioselective addition of MAC to β -nitrostyrenes,

4.8g was isolated as a yellow oil (50.2 mg, 90% yield, 85% *ee*). $R_f = 0.44$ (20% EtOAc/Hex). IR (thin film) 2932, 2859, 2244, 1567, 1376, 1136 cm^{-1} ; ^1H NMR (CDCl_3 , 400 MHz) δ 7.72 (dd, $J = 8.0, 1.2$ Hz, 1H), 7.49 (dd, $J = 7.8, 1.6$ Hz, 1H), 7.40 (td, $J = 7.6, 1.2$ Hz, 1H), 7.30 (td, $J = 8.0, 1.6$ Hz, 1H), 5.15 (dd, $J = 9.0, 5.2$ Hz, 1H), 5.06 (dd, $J = 13.7, 5.2$ Hz, 1H), 4.89 (dd, $J = 13.7, 9.0$ Hz, 1H), 0.94 (s, 9H), 0.40 (s, 3H), 0.33 (s, 3H); ^{13}C NMR (CDCl_3 , 100 MHz) δ 134.4 (d), 131.5 (d), 130.4 (s), 128.4 (d), 128.2 (d), 127.4 (s), 113.3 (s), 113.2 (s), 74.3 (t), 65.5 (s), 50.5 (d), 25.2 (q), 18.1 (s), -4.65 (q), -4.70 (q); HPLC: R_t 6.13 min (major), 5.32 min (minor); $[\alpha]_D^{25} = +29.0$ ($c = 1.0$, CHCl_3); HRMS ESI: Exact mass calcd for $\text{C}_{17}\text{H}_{22}\text{BrN}_3\text{O}_3\text{SiNa}$ $[\text{M}+\text{Na}]^+$, 446.0506. Found 446.0508.

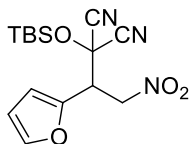


2-((tert-Butyldimethylsilyl)oxy)-2-(2-nitro-1-(pyridin-3-

yl)ethyl)malononitrile (4.28h): Following the general procedure for the enantioselective addition of MAC to β -nitrostyrenes, **4.8h** was purified

by SiO_2 (25%, 50%, 100% EtOAc/hexanes) and isolated as a brown oil (45.0 mg, 65% yield, 50% *ee*). IR (thin film) 2927, 2854, 2212, 1715, 1375, 1104 cm^{-1} ; ^1H NMR (CDCl_3 , 400 MHz) δ 8.62 (dd, $J = 4.8, 1.6$ Hz, 1H), 8.60 (d, $J = 2.2$ Hz, 1H), 7.68 (dt, J

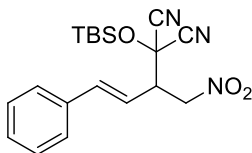
=8.0, 2.1 Hz, 1H), 7.30 (ddd, $J = 8.0, 4.8, 0.6$ Hz, 1H), 5.01 (dd, $J = 13.9, 5.3$ Hz, 1H), 4.85 (dd, $J = 13.9, 9.1$ Hz, 1H), 4.20 (dd, $J = 9.1, 5.3$ Hz, 1H), 0.84 (s, 9H), 0.28 (s, 3H), 0.22 (s, 3H); ^{13}C NMR (CDCl_3 , 100 MHz) δ 151.6 (d), 150.7 (d), 136.5 (d), 126.5 (s), 123.9 (d), 113.3 (s), 112.9 (s), 73.5 (t), 66.1 (s), 51.2 (d), 25.2 (q), 18.1 (s), -4.73 (q), -4.78 (q); HPLC: R_t 3.42 min (major), 4.01 min (minor). $[\alpha]_D^{25} = -44.1$ ($c = 0.54$, CHCl_3)



2-((tert-Butyldimethylsilyl)oxy)-2-(1-(furan-2-yl)-2-

nitroethyl)malononitrile (4.28i): Following the general procedure for the enantioselective addition of MAC to β -nitrostyrenes, **4.8j** was

isolated as a pale-yellow oil (52.1 mg, 72% yield, 87% *ee*). $R_f = 0.28$ (20% EtOAc/Hex). IR (thin film) 2931, 2860, 2237, 1565, 1375, 1261, 1136 cm^{-1} ; ^1H NMR (CDCl_3 , 400 MHz) δ 7.50 (dd, $J = 1.8, 0.6$ Hz, 1H), 6.60 (d, $J = 3.4$ Hz, 1H), 6.45 (dd, $J = 3.4, 1.8$ Hz, 1H), 4.97 (d, $J = 6.3$ Hz, 1H), 4.95 (d, $J = 7.4$ Hz, 1H), 4.47 (dd, $J = 7.4, 6.3$ Hz, 1H), 0.92 (s, 9H), 0.38 (s, 3H), 0.34 (s, 3H); ^{13}C NMR (CDCl_3 , 100 MHz) δ 144.6 (d), 143.7 (s), 113.5 (s), 113.0 (s), 112.3 (d), 111.3 (d), 72.6 (t), 65.5 (s), 47.8 (d), 25.1 (q), 18.0 (s), -4.76 (q), -4.79 (q); HPLC: R_t 6.04 min (major), 5.17 min (minor); $[\alpha]_D^{25} = -5.6$ ($c = 1.0$, CHCl_3); HRMS ESI: Exact mass calcd for $\text{C}_{15}\text{H}_{21}\text{N}_3\text{O}_4\text{SiNa}$ $[\text{M}+\text{Na}]^+$, 358.1193. Found 358.1195.

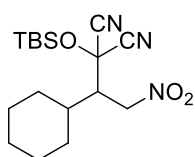


(E)-2-((tert-Butyldimethylsilyl)oxy)-2-(1-nitro-4-phenylbut-3-en-2-yl)malononitrile (4.28j): Following the general procedure for

the enantioselective addition of MAC to β -nitrostyrenes, **4.8i** was

isolated as a yellow oil (63.0 mg, 99% yield, 76% *ee*). $R_f = 0.43$ (20% EtOAc/Hex). IR (thin film) 2930, 2860, 2240, 1561, 1376, 1135 cm^{-1} ; ^1H NMR (CDCl_3 , 400 MHz) δ 7.37 (m, 5H), 6.87 (d, $J = 15.7$ Hz, 1H), 6.00 (dd, $J = 15.7, 9.4$ Hz, 1H), 4.85 (dd, $J = 10.3, 5.1$

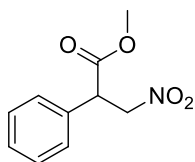
Hz, 1H), 4.59 (dd, $J = 13.0, 8.7$ Hz, 1H), 3.85 (ddd, $J = 9.1, 8.9, 5.1$ Hz, 1H), 0.95 (s, 9H), 0.41 (s, 3H), 0.39 (s, 3H); ^{13}C NMR (CDCl_3 , 100 MHz) δ 141.0 (d), 134.8 (s), 129.3 (d), 128.8 (d), 127.1 (d), 116.8 (d), 113.7 (s), 113.2 (s), 74.3 (t), 66.0 (s), 52.0 (d), 25.2 (q), 18.1 (s), -4.65 (q), -4.68 (q); HPLC: R_t 6.27 min (major), 5.66 min (minor); $[\alpha]_D^{25} = -3.2$ ($c = 1.0$, CHCl_3); HRMS ESI: Exact mass calcd for $\text{C}_{19}\text{H}_{25}\text{N}_3\text{O}_3\text{SiNa}$ $[\text{M}+\text{Na}]^+$, 394.1557. Found 394.1559.



2-((tert-Butyldimethylsilyl)oxy)-2-(1-cyclohexyl-2-

nitroethyl)malononitrile (4.28k): Following the general procedure for the enantioselective addition of MAC to β -nitrostyrenes, **4.8k** was

separated on a ACCQ Prep HP125, Phenomenex Prodigy 5 micron ODS(3) 100 Å, water/acetonitrile gradient. **4.8k** was isolated as a colorless oil (31.9 mg, 47% yield, 67% *ee*). $R_f = 0.51$ (20% EtOAc/Hex). IR (thin film) 2969, 2930, 2860, 1563, 1377, 1157 cm^{-1} ; ^1H NMR (CDCl_3 , 400 MHz) δ 4.60 (dd, $J = 14.5, 6.8$ Hz, 1H), 4.53 (dd, $J = 14.5, 4.5$ Hz, 1H), 3.08 (ddd, $J = 7.3, 4.3, 3.2$ Hz, 1H), 2.04-0.97 (m, 10H), 0.90 (s, 9H), 0.42 (s, 9H), 0.36 (s, 3H); ^{13}C NMR (CDCl_3 , 100 MHz) δ 114.4 (s), 114.1 (s), 72.0 (t), 66.0 (s), 52.6 (d), 37.9 (d), 32.5 (t), 28.2 (t), 26.4 (t), 26.0 (t), 25.7 (t), 25.1 (q), 18.0 (s), -4.64 (q), -4.75 (q); HPLC: R_t 4.24 min (major), 4.58 min (minor); HRMS ESI: Exact mass calcd for $\text{C}_{17}\text{H}_{29}\text{N}_3\text{O}_3\text{SiNa}$ $[\text{M}+\text{Na}]^+$, 372.187039. Found 372.186843.



Methyl 3-nitro-2-phenylpropanoate (4.44): To a 20 mL vial, **4.34a**

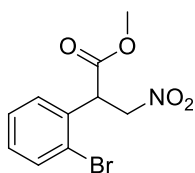
(50 mg, 0.14 mmol) was dissolved in THF (0.15 M). The reaction was

left to cool at -25 °C for 10 minutes before HF·Pyr in THF (1.35 eq, 0.6

M) was added dropwise. The reaction stirred for 2 hours before MeOH (0.16M) was

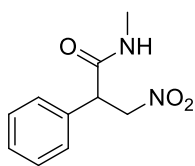
added followed by TEA in MeOH (3 eq, 0.98 M) 10 minutes later. The reaction stirred an

additional 10 minutes before warming to 0 °C and quenching with 5 mL 1 N HCl. The reaction was extracted 2x with Et₂O. The combined organic layers were collected, dried over Na₂SO₄, filtered through Celite and concentrated. Purification on SiO₂ (5-10-20% EtOAc/hexanes) yielded a pale yellow oil (20.4 mg, 64% yield). Characterization data matched that found at the following reference.¹⁶⁴



Methyl 2-(2-bromophenyl)-3-nitropropanoate (4.45): To a 20 mL vial, **4.34a** (50 mg, 0.14 mmol) was dissolved in THF (0.15 M). The

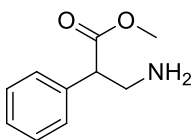
reaction was left to cool at -25 °C for 10 minutes before HF·Pyr in THF (1.35 eq, 0.6M) was added dropwise. The reaction stirred for 2 hours before MeOH (0.16M) was added followed by TEA in MeOH (3 eq, 0.98 M) 10 minutes later. The reaction stirred an additional 10 minutes before warming to 0 °C and quenching with 5 mL 1 N HCl. The reaction was extracted 2x with Et₂O. The combined organic layers were collected, dried over Na₂SO₄, filtered through Celite and concentrated. Purification on SiO₂ (5-10-20% EtOAc/hexanes) yielded a yellow oil (17.8 mg 59% yield); IR (thin film)¹H NMR (CDCl₃, 400 MHz) δ 7.63 (m, 1H), 7.32 (m, 1H), 7.22 (m, 2H), 5.01 (m, 2H), 4.57 (m, 1H), 3.77 (s, 3H); ¹³C NMR (CDCl₃, 100 MHz) δ: 170.7 (s), 133.8 (d), 133.0 (s), 130.2 (d), 129.2 (d), 128.3 (d), 124.4 (s), 74.4 (t), 53.1 (q), 48.0 (d)



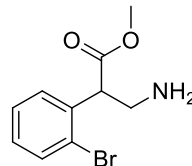
N-Methyl-3-nitro-2-phenylpropanamide (4.46): To a 10 mL round bottom flask under N₂, **4.63** was dissolved in THF. MeNH₂ (4 eq, .578 mmol) was added and the reaction cooled to -25 °C for 10 minutes

before TBAF (1.2 eq, .173 mmol) was added dropwise. The reaction was left to stir for 2 hours before being quenched with NH₄Cl and extracted three times with Et₂O. The organic layers were collected, dried over Na₂SO₄, filtered through Celite and

concentrated. Purification on SiO₂ (25-50-100% EtOAc/hexanes) provided an orange solid (8.3 mg, 94% yield). $R_f = 0.07$ (20% EtOAc/Hex). mp 90-93 °C; IR (thin film) 3306, 2909, 1648, 1543 cm⁻¹; ¹H NMR (CDCl₃, 400 MHz) δ : 7.40-7.25 (m, 5H), 5.68 (s, 1H), 5.22 (dd, $J = 14.2, 8.4$ Hz, 1H), 4.55 (dd, $J = 14.2, 6.3$ Hz, 1H), 4.28 (dd, $J = 8.4, 6.3$ Hz, 1H), 2.77 (d, $J = 4.8$ Hz, 1H); ¹³C NMR (CDCl₃, 100 MHz) δ 170.2 (s), 134.6 (s), 129.5 (d), 128.7 (d), 128.1 (d), 76.3 (t), 50.0 (s), 26.7 (q). HRMS ESI: Exact mass calcd for C₁₀H₁₂N₂O₃Na [M+Na]⁺, 231.074013. Found 231.073962.



Methyl 3-amino-2-phenylpropanoate (4.47): To a 10 mL flame dried round bottom flask, **4.65** (245 mg, 1.2 mmol) was added and dissolved in EtOH (1.2 mL). Pd/C (10% by weight, 0.2 eq) was weighed out and added to the stirring reaction. A full H₂ balloon was added and used to purge the reaction before it was refilled and attached. The reaction stirred 18 h before being filtered through Celite and washed with EtOAc. The reaction was concentrated to provide a yellow oil that did not need purification (167 mg, 80% yield). Characterization data can be found at the provided reference.¹⁶⁵



Methyl 3-amino-2-(2-bromophenyl)propanoate (4.47): To a 10 mL flame dried round bottom flask, **4.65** (105 mg, 0.36 mmol) was added and dissolved in EtOH (1.2 mL). Pd/C (10% by weight, 0.2 eq) was weighed out and added to the stirring reaction. A full H₂ balloon was added and used to purge the reaction before it was refilled and attached. The reaction stirred 18 h before being filtered through Celite and washed with EtOAc. The reaction was concentrated to furnish an orange oil that did not require further purification (160 mg, 75% yield). IR (thin film) 3029, 1731, 1550, 1375 cm⁻¹; ¹H NMR (CDCl₃, 400 MHz) δ 7.41-7.23 (m, 3H),

7.28 (d, $J = 2.0$ Hz, 1H), 5.11 (dd, $J = 14.6, 9.9$ Hz, 1H), 4.55 (dd, $J = 14.6, 5.1$ Hz, 1H), 4.45 (dd, $J = 9.9, 5.1$ Hz, 1H), 3.74 (s, 3H), 1.74 (br s, NH₂, 2H); ¹³C NMR (CDCl₃, 100 MHz) δ : 171.1 (s), 133.2 (s), 129.4 (d, 2C), 128.8 (d), 127.9 (d, 2C), 75.8 (t), 52.9 (d), 48.7 (q).

CHAPTER V - CONCLUSION

Presented in this dissertation is an overarching theme of using noncovalent interactions to manipulate organic reactions for the synthesis of natural product synthons and the binding of natural products with enzymes. In the first project, a method was established to convert esters to ethers in a two-step process. The first step was a DIBAL-H reduction followed with a TMS protection to form a stable acetal. It was monitored using ReactIR enabling the time to drastically decrease to currently set literature precedent, as well as to determine the exact number of equivalents of DIBAL-H necessary for each substrate. Additionally, this reaction did not require further purification of the acetal with crude yields mainly above 80%. The reduction of the acetal to ether was also carried out successfully with a broad range of substrates. The intermediate is an oxonium ion and in cases where the yield was lower, a reaction bifurcation with a competing oxonium ion was identified which led to the formation of byproducts including a symmetric ether. In total 13 esters were successfully converted to the ether product.

The second project involved the synthesis of trisubstituted biaryl quinolines for the inhibition of HIV-1 integrase. These substrates bind noncovalently in the hydrophobic pocket of the allosteric site of HIV-1 integrase, causing enzyme multimerization and rendering it unable to function. The work focused on developing a short synthetic strategy that provided a late stage derivatization. A structure activity relationship at the 4-position of the quinoline was initiated to probe the noncovalent interactions in the hydrophobic pocket of the enzyme. The total synthesis of these quinolines was completed in 8 steps starting with 2-methyl-4-hydroxyquinoline. Highlights include the ability to

scale to as much as 25 g and requiring no purifications within many initial steps of the synthesis. Late stage derivatization utilized a Suzuki coupling with various aromatic boronic acids to install the 4-position probe, followed by saponification of the ester side group to produce the acetic acid side chain. Out of 36 compounds that were synthesized, the best substrates contained a para-chlorophenyl group as well as a benzodioxane derivative which resulted in multimerization inhibitions of 0.10 μ M and 0.08 μ M, respectively.

The third and final project honed in on the importance of the manipulation of noncovalent interactions in organic synthesis via the utilization of squaramide organocatalysts for organic transformations. This class of organocatalysts rely on noncovalent interactions, such as hydrogen bonding, π - π , and π -H stacking interactions to initiate the reaction and provide enantioselectivity. Using these organocatalysts, a new reaction was identified to synthesize nitroolefins via a Michael addition of masked acyl cyanides (MAC) to β -nitrostyrenes achieving yields of 50-99% and enantioselectivities in of 50-88%. This class of compounds as natural product synthons is apparent in their ability to access chiral indolines, β -lactams, and β -amino acids. This strategy also highlights the use of MAC as a versatile acyl anion equivalent that can be activated and added in an enantiopure fashion using organocatalysts.

Overall, it has been shown that noncovalent interactions should always be considered when developing new reaction methodologies, as they are of vital importance in reaction mechanisms. Noncovalent interactions are a key factor in organic synthesis, and if used correctly, can provide the necessary momentum to a reaction to produce a single product, as well as producing the product in an enantioselective fashion.

Noncovalent interactions are also a key factor in binding and inhibition of enzymes, and the synthesis of small molecules for their inhibitory purposes must be designed with noncovalent interactions in mind.

APPENDIX A

Supplementary data (NMR, IR, MS, and Elemental Analysis) for Chapter 2 compounds is provided in the supporting text titled “Supplementary Spectral Data”.

APPENDIX B

Supplementary data (NMR, IR, MS, and Elemental Analysis) for Chapter 3 compounds is provided in the supporting text titled “Supplementary Spectral Data”.

APPENDIX C

Supplementary data (NMR, IR, MS, and Elemental Analysis) for Chapter 4 compounds is provided in the supporting text titled “Supplementary Spectral Data”.

References

1. Chen, J. J.; Wang, S. W.; Hsiao, H. Y.; Lee, M. S.; Ju, Y. M.; Kuo, Y. H.; Lee, T. H., Aliphatic phenolic ethers from *Trichobotrys effusa*. *J. Nat. Prod.* **2014**, 77 (5), 1097-101.
2. Teranishi, T.; Kuwahara, S., Stereoselective approach to the DEF ring system of terpendole E. *Tetrahedron Lett.* **2014**, 55 (8), 1486-1487.
3. Jung, Y.-S.; Kim, D. H.; Hwang, J. Y.; Yun, N. Y.; Lee, Y.-H.; Han, S. B.; Hwang, B. Y.; Lee, M. S.; Jeong, H.-S.; Hong, J. T., Anti-inflammatory effect of tricin 4'-O-(threo- β -guaiacylglyceryl) ether, a novel flavonolignan compound isolated from *Njavara* on in RAW264.7 cells and in ear mice edema. *Toxicol. Appl. Pharmacol.* **2014**, 277 (1), 67-76.
4. Williamson, A. W., XXII.-On etherification. *Quarterly Journal of the Chemical Society of London* **1852**, 4 (3), 229-239.
5. H. Sagitani, M. O., K. Itoh, Characteristics of poly(oxytetramethylene) poly(glyceryl)alkyl ether nonionic surfactants as emulsifiers. *J. Soc. Cosmet. Chem.* **1987**, 38, 419-433.
6. Forrest, J. E.; Richard, R.; Heacock, R. A., Colour reactions of some aromatic ethers found in essential oils1. *J. Chromatogr. A* **1972**, 65 (2), 439-444.
7. Campbell, W. E.; George, P., New phenolic ethers from essential oils of some rutaceae. *Phytochemistry* **1982**, 21 (6), 1455-1456.
8. Oae, S., The Formation of Phenolic Ethers by the Acid-catalyzed Condensation of Phenols and Alcohols. *Bull. Chem. Soc. Jpn.* **1966**, 39, 611-614.
9. Chengyuan Liang, Z. T., Lan Wang, Gennian Mao, Weidong Qian, Huihui Song, One-pot three-component synthesis of new oxindoles through a tandem etherification-coupling sequence ignited by tungstophosphoric acid. *J. Chem. Pharm. Res.* **2014**, 6 (4), 941-949.
10. Vincent Tran, T. G. M., Lewis Acid Catalyzed Intramolecular Condensation of Ynol Ether-Acetals. Synthesis of Alkoxy cycloalkene Carboxylates. *Org. Lett.* **2012**, 14 (23), 6100-6103.
11. Paul, S.; Gupta, M., Zinc-catalyzed Williamson ether synthesis in the absence of base. *Tetrahedron Lett.* **2004**, 45 (48), 8825-8829.
12. Mochalov, S. S.; Fedotov, A. N.; Trofimova, E. V.; Zefirov, N. S., Hydrochloric acid as an efficient catalyst for intermolecular condensation of alcohols. A simple and highly efficient synthesis of unsymmetrical ethers from benzylic alcohols and alkanols. *Russ. J. Org. Chem.* **2015**, 51 (9), 1217-1231.
13. Herbert C. Brown, J. T. K., Min-Hon Rei, Kerry L. Thompson, Solvomercuration-Demercuration. 11. Alkoxymercuration-Demercuration of Representative Alkenes in Alcohol Solvents with the Mercuric Salts Acetate, Trifluoroacetate, Nitrate, and Methanesulfonate. *J. Org. Chem.* **1984**, 49, 2551-2557.
14. Alfred Hassner, V. A., Direct Room Temperature Esterification of Carboxylic Acids. *Tetrahedron Lett.* **1978**, 46, 4475-4478.

15. Dhaon, M. K.; Olsen, R. K.; Ramasamy, K., Esterification of N-protected α -amino acids with alcohol/carbodiimide/4-(dimethylamino)pyridine. Racemization of aspartic and glutamic acid derivatives. *J. Org. Chem.* **1982**, *47* (10), 1962-5.
16. Hosangadi, B. D.; Dave, R. H., An efficient general method for esterification of aromatic carboxylic acids. *Tetrahedron Lett.* **1996**, *37* (35), 6375-6378.
17. Sivagurunathan, K.; Raja Mohamed Kamil, S.; Syed Shafi, S.; Liakth Ali Khan, F.; Ragavan, R. V., Efficient one-pot selective reduction of esters in β -ketoesters using LiHMDS and lithium aluminium hydride. *Tetrahedron Lett.* **2011**, *52* (11), 1205-1207.
18. Brown, M. S.; Rapoport, H., The Reduction of Esters with Sodium Borohydride 1. *J. Org. Chem.* **1963**, *28* (11), 3261-3263.
19. Jun-Cai Feng, B. L., Li Dai, Xiao-Liang Yang, Shu-Jiang Tu, Microwave assisted solid reaction: Reduction of Esters to Alcohols by Potassium Borohydride-Lithium chloride. *Synth. Commun.* **2001**, *31* (12), 1875-1877.
20. Enzo Santaniello, P. G., Piero Sozzani, Reduction of Esters to Alcohols by means of Sodium Borohydride in Polyethylene Glycols. *J Org Chem* **1980**, *46*, 4584-4585.
21. Tetsuo Ohta, M. K., Keisuke Kusui, Tsugumi Michibata, Mami Nobutomo, Isao Furukawa, Rhodium-Catalyzed Reduction of Esters to Alcohols Using Diphenylsilane. *Tetrahedron Lett.* **1999**, *40*, 6963-6966.
22. Scott C. Berk, K. A. K., Stephen L. Buchwald, A Catalytic Method for the Reduction of Esters to Alcohols. *J. Am. Chem. Soc.* **1991**, *113*, 5093-5095.
23. Das, S.; Moller, K.; Junge, K.; Beller, M., Zinc-catalyzed chemoselective reduction of esters to alcohols. *Chemistry* **2011**, *17* (27), 7414-7.
24. L. I. Zakharkin, I. M. K., Reduction of Esters of Carboxylic Acids into Aldehydes with Diisobutylaluminium Hydride. *Tetrahedron Lett.* **1962**, *14*, 619-620.
25. Min Jung Chae, J. I. S., Duk Keun An, Chemoselective Reduction of Esters to Aldehydes by Potassium Diisobutyl-t-Butoxyaluminium Hydride (PDBBA). *Bull. Korean. Chem. Soc.* **2007**, *28* (12), 2517.
26. Kim, M. S.; Choi, Y. M.; An, D. K., Lithium diisobutyl-t-butoxyaluminum hydride, a new and efficient reducing agent for the conversion of esters to aldehydes. *Tetrahedron Lett.* **2007**, *48* (29), 5061-5064.
27. Song, J. I.; An, D. K., New Method for Synthesis of Aldehydes from Esters by Sodium Diisobutyl-t-butoxyaluminum Hydride. *Chem. Lett.* **2007**, *36* (7), 886-887.
28. Shin, W. K.; Kang, D.; An, D. K., Partial Reduction of Esters to Aldehydes Using a Novel Modified Red-Al Reducing Agent. *Bull. Korean. Chem. Soc.* **2014**, *35* (7), 2169-2171.
29. Steven L. Baxter, J. S. B., New Conversion of Esters to Ethers and Its Application to the Preparation of Furano-18-crown-6. *J. Org. Chem.* **1981**, *46*, 831-832.
30. Michihisa Yato, K. H., Akihiko Ishida, Reduction of carboxylic esters to ethers with triethyl silane in the combined use of titanium tetrachloride and trimethylsilyl trifluoromethanesulfonate. *Tetrahedron* **2001**, *57*, 5353-5359.
31. Marcus C. Hansen, X. V., Stephen L. Buschwald, Convenient Two-Step Conversion of Lactones into Cyclic Ethers. *J. Org. Chem.* **1998**, *63*, 2360-2361.
32. Das, S.; Li, Y.; Junge, K.; Beller, M., Synthesis of ethers from esters via Fe-catalyzed hydrosilylation. *Chem. Commun. (Camb)* **2012**, *48* (87), 10742-4.

33. Sakai, N.; Moriya, T.; Fujii, K.; Konakahara, T., Direct Reduction of Esters to Ethers with an Indium(III) Bromide/Triethylsilane Catalytic System. *Synthesis* **2008**, 2008 (21), 3533-3536.
34. Doo Ok Jang, S. H. S., Dae Hyan Cho, Conversion of Esters and Lactones to Ethers *via* Thionoesters and Thionolactones Using Reductive Radical Desulfurization. *Tetrahedron* **1999**, 55, 3479-3488.
35. Pettit, G. R.; Kasturi, T. R., Steroids and related natural products. II. Method for the direct conversion of esters to ethers. *J. Org. Chem.* **1960**, 25, 875-6.
36. George R. Pettit, T. R. K., Steroids and related products. VIII. Synthesis of oxa steroids. *J. Org. Chem.* **1961**, 26, 4557-4563.
37. George R. Pettit, D. M. P., Steroids and related natural products. XI. Reduction of esters to ethers. *J. Org. Chem.* **1962**, 27, 2127-2130.
38. Ranjender S. Varma, D. K., Microwave-Accelerated Solvent -Free Synthesis of Thioketones, Thiolactones, Thioamides, Thionoesters, and Thioflavonoids. *Org. Lett.* **1999**, 1 (5), 697-700.
39. Doo Ok Jang, S. H. S., Organotin Hydride Catalyzed Radical Desulfurization of Thionoesters and Thionolactones. *Synlett* **2000**, 6, 811-812.
40. Nicolaou, K. C.; Sato, M.; Theodorakis, E. A.; Miller, N. D., Conversion of thionoesters and thionolactones to ethers; a general and efficient radical desulfurization. *J. Chem. Soc., Chem. Commun.* **1995**, (15), 1583-5.
41. Sakai, N.; Usui, Y.; Moriya, T.; Ikeda, R.; Konakahara, T., One-Pot Sequential Synthesis of Ethers from an Aliphatic Carboxylic Acid and an Alcohol by Indium-Catalyzed Deoxygenation of an Ester. *Eur. J. Org. Chem.* **2012**, 2012 (24), 4603-4608.
42. Tsurugi, J.; Nakao, R.; Fukumoto, T., γ -Induced reduction with trichlorosilane. Dialkyl ether from alkyl aliphatic carboxylate. *J. Am. Chem. Soc.* **1969**, 91 (16), 4587-8.
43. Nicholas A. Morra, B. L. P., Reduction of Esters to Ethers Utilizing the Powerful Lewis Acid BF₂OTf.OEt₂. *Synthesis* **2008**, 4 (511-514), 511.
44. Yato, M.; Homma, K.; Ishida, A., Reduction of carboxylic esters to ethers with triethyl silane in the combined use of titanium tetrachloride and trimethylsilyl trifluoromethanesulfonate. *Tetrahedron* **2001**, 57 (25), 5353-5359.
45. Boussonnière, A.; Bénateau, R.; Lebreton, J.; Dénès, F., Aluminum Acetals in Organic Synthesis. *Eur. J. Org. Chem.* **2013**, 2013 (35), 7853-7866.
46. Vilas H. Dahanukar, S. D. R., General Synthesis of *r*-Acetoxy Ethers from Esters by DIBALH Reduction and Acetylation. *J. Org. Chem.* **1996**, 61, 8317-8320.
47. David J. Kopecky, S. D. R., Improved procedure for the reductive acethylation of acyclic esters and a new synthesis of ethers *J. Org. Chem.* **2000**, 65, 191-198.
48. Scott d. Rychnovsky, B. M. B., enantioselective reduction of esters synthesis of optically active alpha acetoxy ethers. *Tetrahedron Lett.* **2000**, 41, 3593-3596.
49. Scott D. Rychnovsky, J. C., Diastereoselective Additions of Nucleophiles to α -Acetoxy Ethers Using the α -(Trimethylsilyl)benzyl Auxiliary. *Org. Lett.* **2003**, 5 (13), 2367-2370.
50. Burns, N. Z.; Witten, M. R.; Jacobsen, E. N., Dual Catalysis in Enantioselective Oxidopyrylium-Based [5 + 2] Cycloadditions. *J. Am. Chem. Soc.* **2011**, 133 (37), 14578-14581.

51. Reisman, S. E.; Doyle, A. G.; Jacobsen, E. N., Enantioselective Thiourea-Catalyzed Additions to Oxocarbenium Ions. *J. Am. Chem. Soc.* **2008**, *130* (23), 7198-7199.
52. Luan, Y.; Barbato, K. S.; Moquist, P. N.; Kodama, T.; Schaus, S. E., Enantioselective Synthesis of 1,2-Dihydronaphthalene-1-carbaldehydes by Addition of Boronates to Isochromene Acetals Catalyzed by Tartaric Acid. *J. Am. Chem. Soc.* **2015**, *137* (9), 3233-3236.
53. Moquist, P. N.; Kodama, T.; Schaus, S. E., Enantioselective Addition of Boronates to Chromene Acetals Catalyzed by a Chiral Bronsted Acid/Lewis Acid System. *Angew. Chem., Int. Ed.* **2010**, *49* (39), 7096-7100, S7096/1-S7096/69.
54. Hsiao, C.-C.; Liao, H.-H.; Sugiono, E.; Atodiresei, I.; Rueping, M., Shedding Light on Organocatalysis-Light-Assisted Asymmetric Ion-Pair Catalysis for the Enantioselective Hydrogenation of Pirylium Ions. *Chem. - Eur. J.* **2013**, *19* (30), 9775-9779.
55. Rueping, M.; Volla, C. M. R.; Atodiresei, I., Catalytic Asymmetric Addition of Aldehydes to Oxocarbenium Ions: A Dual Catalytic System for the Synthesis of Chromenes. *Org. Lett.* **2012**, *14* (17), 4642-4645.
56. Maity, P.; Srinivas, H. D.; Watson, M. P., Copper-catalyzed enantioselective additions to oxocarbenium ions: alkynylation of isochroman acetals. *J. Am. Chem. Soc.* **2011**, *133* (43), 17142-17145.
57. Wittkamp, B., Recent Advances in Organic Chemistry: A Review of Recently Reported Applications Using *In Situ* Spectroscopy. Inc., M.-T. A., Ed. Mettler-Toledo AutoChem Inc.: 2012.
58. Ki Bum Hong, M. G. D., Jeffery N. Johnson, On the Nature of Rate Acceleration in the Synthesis and Fragmentation of Triazolines by Bronstead Acid: Secondary Catalysis by Water (Hydronium Triflate). *J. Am. Chem. Soc.* **2008**, *130*, 2323-2328.
59. Dalibor Sames, Y. L., Lynn DeYoung, Robin Polt, Preparation of Monosilyl Acetals from Esters via *i*Bu₂AlH reduction and Trapping with N-(Trimethylsilyl)imidazole. Addition of Allyltrimethylsilane to Yield Homoallylic Alcohols or Ethers. *J. Org. Chem.* **1995**, *60*, 2153-2159.
60. Taylor, R. R. R.; Batey, R. A., A Hetero Diels-Alder Approach to the Synthesis of Chromans (3,4-Dihydrobenzopyrans) Using Oxonium Ion Chemistry: The Oxa-Povarov Reaction. *J. Org. Chem.* **2013**, *78* (4), 1404-1420.
61. Taylor, R. R. R.; Batey, R. A., A Hetero Diels-Alder Approach to the Synthesis of Chromans (3,4-Dihydrobenzopyrans) Using Oxonium Ion Chemistry: The Oxa-Povarov Reaction. *J. Org. Chem.* **2013**, *78* (4), 1404-1420.
62. Alison Hart, S. A. K., Tyler Harless, John A. Hood, Michael Tagert, Julie A. Pigza, An efficient method for the reductive conversion of acyclic esters to ethers via a TMS-protected acetal. *Tetrahedron Lett.* **2017**, *58*, 3024-3027.
63. Sassaman, M. B.; Kotian, K. D.; Prakash, G. K. S.; Olah, G. A., General ether synthesis under mild acid-free conditions. Trimethylsilyl iodide catalyzed reductive coupling of carbonyl compounds with trialkylsilanes to symmetrical ethers and reductive condensation with alkoxysilanes to unsymmetrical ethers. *J. Org. Chem.* **1987**, *52* (19), 4314-4319.

64. Ess, D. H.; Wheeler, S. E.; Iafe, R. G.; Xu, L.; Celebi-Olçüm, N.; Houk, K. N., Bifurcations on potential energy surfaces of organic reactions. *Angew. Chem. Int. Ed. Engl.* **2008**, *47* (40), 7592-7601.
65. Sakai, N.; Kawana, K.; Ikeda, R.; Nakaike, Y.; Konakahara, T., InBr₃-Catalyzed Deoxygenation of Carboxylic Acids with a Hydrosilane: Reductive Conversion of Aliphatic or Aromatic Carboxylic Acids to Primary Alcohols or Diphenylmethanes. *Eur. J. Org. Chem.* **2011**, *2011* (17), 3178-3183.
66. Morra, N. A.; Pagenkopf, B. L., Reduction of Esters to Ethers Utilizing the Powerful Lewis Acid BF₂OTf·OEt₂. *Synthesis* **2008**, *2008* (04), 511-514.
67. Greber, G., Vogel's textbook of practical organic chemistry (5th ed.), revised by Brian S. Furniss, Antony J. Hannaford, Peter W. G. Smith, and Austin R. Tatchell, John Wiley & Sons, New York, 1514 pp. price: \$84.95. *J. Polym. Sci. A: Polymer Chemistry* **1991**, *29* (8), 1223-1223.
68. Pangborn, A. B.; Giardello, M. A.; Grubbs, R. H.; Rosen, R. K.; Timmers, F. J., Safe and Convenient Procedure for Solvent Purification. *Organometallics* **1996**, *15* (5), 1518-1520.
69. Hoyer, T. R.; Hanson, P. R.; Vyvyan, J. R., A Practical Guide to First-Order Multiplet Analysis in ¹H NMR Spectroscopy. *J. Org. Chem.* **1994**, *59* (15), 4096-4103.
70. Ren, L.; Wang, L.; Lv, Y.; Li, G.; Gao, S., An Effective Method for the Construction of Esters Using Cs₂CO₃ as Oxygen Source. *Org. Lett.* **2015**, *17* (21), 5172-5175.
71. Chen, F.-K.; Ke, C.-S., Direct Esterification of Carboxylic Acids with Alcohols Catalyzed by Iron(III) Acetylacetonate Complex AU - Weng, Shiue-Shien. *Synth. Commun.* **2013**, *43* (19), 2615-2621.
72. Pramanik, S.; Reddy, R. R.; Ghorai, P., Intramolecular Rearrangement of α -Azidoperoxides: An Efficient Synthesis of tert-Butyl Esters. *Org. Lett.* **2015**, *17* (6), 1393-1396.
73. Xu, J.-X.; Wu, X.-F., Palladium-Catalyzed Decarboxylative Carbonylative Transformation of Benzyl Aryl Carbonates: Direct Synthesis of Aryl 2-Arylacetates. *Org. Lett.* **2018**, *20* (18), 5938-5941.
74. Yu, W.; Yang, S.; Xiong, F.; Fan, T.; Feng, Y.; Huang, Y.; Fu, J.; Wang, T., Palladium-catalyzed carbonylation of benzylic ammonium salts to amides and esters via C–N bond activation. *Org. Biomol. Chem.* **2018**, *16* (17), 3099-3103.
75. Vico Solano, M.; González Miera, G.; Pascanu, V.; Inge, A. K.; Martín-Matute, B., Versatile Heterogeneous Palladium Catalysts for Diverse Carbonylation Reactions under Atmospheric Carbon Monoxide Pressure. *Chem. Cat. Chem.* **2018**, *10* (5), 1089-1095.
76. Magens, S.; Ertelt, M.; Jatsch, A.; Plietker, B., A Nucleophilic Fe Catalyst for Transesterifications under Neutral Conditions. *Org. Lett.* **2008**, *10* (1), 53-56.
77. Lee, Y. H.; Morandi, B., Ether Synthesis through Reductive Cross-Coupling of Ketones with Alcohols Using Me₂SiHCl as both Reductant and Lewis Acid. *Synlett* **2017**, *28* (18), 2425-2428.
78. Ferrand, L.; Tang, Y.; Aubert, C.; Fensterbank, L.; Mouriès-Mansuy, V.; Petit, M.; Amatore, M., Niobium-Catalyzed Intramolecular Addition of O–H and N–H Bonds to Alkenes: A Tool for Hydrofunctionalization. *Org. Lett.* **2017**, *19* (8), 2062-2065.

79. Hosokawa, S.; Toya, M.; Noda, A.; Morita, M.; Ogawa, T.; Motoyama, Y., Catalytic Silane-Reduction of Carboxylic Esters and Lactones: Selective Synthetic Methods to Aldehydes, Lactols, and Ethers via Silyl Acetal Intermediates. *Chem. Select* **2018**, 3 (11), 2958-2961.
80. HIV Basics: Global Statistics. Overview: Data & Trends: .
81. HIV/AIDS. <http://www.who.int/news-room/fact-sheets/detail/hiv-aids>.
82. Gao, F.; Bailes, E.; Robertson, D. L.; Chen, Y.; Rodenburg, C. M.; Michael, S. F.; Cummins, L. B.; Arthur, L. O.; Peeters, M.; Shaw, G. M.; Sharp, P. M.; Hahn, B. H., Origin of HIV-1 in the chimpanzee *Pan troglodytes troglodytes*. *Nature* **1999**, 397 (6718), 436-441.
83. Patel, P.; Borkowf, C. B.; Brooks, J. T.; Lasry, A.; Lansky, A.; Mermin, J., Estimating per-act HIV transmission risk: a systematic review. *AIDS (London, England)* **2014**, 28 (10), 1509-1519.
84. Organization, W. H. Substance Abuse. <https://afro.who.int/health-topics/substance-abuse>.
85. Unicef HIV and AIDS Overview. https://www.unicef.org/esaro/5482_HIV_AIDS.html.
86. Tan, I. L.; McArthur, J. C., HIV-associated neurological disorders: a guide to pharmacotherapy. *CNS Drugs* **2012**, 26 (2), 123-134.
87. Barré-Sinoussi, F.; Ross, A. L.; Delfraissy, J.-F., Past, present and future: 30 years of HIV research. *Nat. Rev. Microbiol.* **2013**, 11, 877.
88. Quashie, P. K.; Mesplede, T.; Wainberg, M. A., Evolution of HIV integrase resistance mutations. *Curr. Opin. Infect. Dis.* **2013**, 26 (1), 43-49.
89. Engelman, A.; Cherepanov, P., The structural biology of HIV-1: mechanistic and therapeutic insights. *Nat. Rev. Microbiol.* **2012**, 10 (4), 279-290.
90. Goldgur, Y.; Dyda, F.; Hickman, A. B.; Jenkins, T. M.; Craigie, R.; Davies, D. R., Three new structures of the core domain of HIV-1 integrase: an active site that binds magnesium. *Proc. Natl. Acad. Sci.* **1998**, 95 (16), 9150-9154.
91. Lesbats, P.; Engelman, A. N.; Cherepanov, P., Retroviral DNA Integration. *Chem. Rev. (Washington, DC, U. S.)* **2016**, 116 (20), 12730-12757.
92. Engelman, A.; Craigie, R., Identification of conserved amino acid residues critical for human immunodeficiency virus type 1 integrase function in vitro. *J. Virol.* **1992**, 66 (11), 6361-9.
93. Cai, M.; Zheng, R.; Caffrey, M.; Craigie, R.; Clore, G. M.; Gronenborn, A. M., Solution structure of the N-terminal zinc binding domain of HIV-1 integrase. *Nat. Struct. Biol.* **1997**, 4 (7), 567-577.
94. van Gent, D. C.; Vink, C.; Groeneger, A. A.; Plasterk, R. H., Complementation between HIV integrase proteins mutated in different domains. *The EMBO Journal* **1993**, 12 (8), 3261-3267.
95. Davies, T. K. C. D. R., Structure and Function of HIV-1 Integrase. *Curr. Top. Med. Chem.* **2004**, 4, 956-977.
96. Cherepanov, P.; Devroe, E.; Silver, P. A.; Engelman, A., Identification of an Evolutionarily Conserved Domain in Human Lens Epithelium-derived Growth Factor/Transcriptional Co-activator p75 (LEDGF/p75) That Binds HIV-1 Integrase. *J. Biol. Chem.* **2004**, 279 (47), 48883-48892.

97. Cherepanov, P.; Ambrosio, A. L. B.; Rahman, S.; Ellenberger, T.; Engelman, A., Structural basis for the recognition between HIV-1 integrase and transcriptional coactivator p75. *Proc. Natl. Acad. Sci.* **2005**, *102* (48), 17308-17313.
98. McKee, C. J.; Kessl, J. J.; Shkriabai, N.; Dar, M. J.; Engelman, A.; Kvaratskhelia, M., Dynamic Modulation of HIV-1 Integrase Structure and Function by Cellular Lens Epithelium-derived Growth Factor (LEDGF) Protein. *J. Biol. Chem.* **2008**, *283* (46), 31802-31812.
99. Di Santo, R., Inhibiting the HIV Integration Process: Past, Present, and the Future. *J. Med. Chem.* **2014**, *57* (3), 539-566.
100. Engelman, A.; Kessl, J. J.; Kvaratskhelia, M., Allosteric inhibition of HIV-1 integrase activity. *Curr. Opin. Chem. Biol.* **2013**, *17* (3), 339-345.
101. Christ, F.; Shaw, S.; Demeulemeester, J.; Desimmie, B. A.; Marchand, A.; Butler, S.; Smets, W.; Chaltin, P.; Westby, M.; Debyser, Z.; Pickford, C., Small-molecule inhibitors of the LEDGF/p75 binding site of integrase block HIV replication and modulate integrase multimerization. *Antimicrob. Agents Chemother.* **2012**, *56* (8), 4365-4374.
102. Tsiang, M.; Jones, G. S.; Niedziela-Majka, A.; Kan, E.; Lansdon, E. B.; Huang, W.; Hung, M.; Samuel, D.; Novikov, N.; Xu, Y.; Mitchell, M.; Guo, H.; Babaglu, K.; Liu, X.; Geleziunas, R.; Sakowicz, R., New Class of HIV-1 Integrase (IN) Inhibitors with a Dual Mode of Action. *J. Biol. Chem.* **2012**, *287* (25), 21189-21203.
103. Fader, L. D.; Malenfant, E.; Parisien, M.; Carson, R.; Bilodeau, F.; Landry, S.; Pesant, M.; Brochu, C.; Morin, S.; Chabot, C.; Halmos, T.; Bousquet, Y.; Bailey, M. D.; Kawai, S. H.; Coulombe, R.; LaPlante, S.; Jakalian, A.; Bhardwaj, P. K.; Wernic, D.; Schroeder, P.; Amad, M. a.; Edwards, P.; Garneau, M.; Duan, J.; Cordingley, M.; Bethell, R.; Mason, S. W.; Bos, M.; Bonneau, P.; Poupert, M.-A.; Faucher, A.-M.; Simoneau, B.; Fenwick, C.; Yoakim, C.; Tsantrizos, Y., Discovery of BI 224436, a Ncatalytic Site Integrase Inhibitor (NCINI) of HIV-1. *ACS Med. Chem. Lett.* **2014**, *5* (4), 422-427.
104. Vitaku, E.; Smith, D. T.; Njardarson, J. T., Analysis of the Structural Diversity, Substitution Patterns, and Frequency of Nitrogen Heterocycles among U.S. FDA Approved Pharmaceuticals. *J. Med. Chem.* **2014**, *57* (24), 10257-10274.
105. H., S. Z., Synthesis of quinolines. *Ber. Dtsch. Chem. Ges.* **1880**, *13*, 2086-2087.
106. Ciamician, G. L.; Dennstedt, M., Action of chloroform on potassium-pyrroline. *Ber. Dtsch. Chem. Ges.* **1881**, *14*, 1153-63.
107. Combes, A., Action of phenylhydrazine and hydroxylamine on acetylacetone. *Bull. Soc. Chim. Fr.* **1888**, *48*, 471.
108. Minisci, F.; Galli, R.; Malatesta, V.; Caronna, T., Nucleophilic character of alkyl radicals. II. Selective alkylation of pyridine, quinoline, and acridine by hydroperoxides and oxaziranes. *Tetrahedron* **1970**, *26* (17), 4083-91.
109. Pfitzinger, W., Quinoline-derivatives from isatinic acid. *J. Prakt. Chem.* **1886**, *33* (2), 100.
110. Conrad, M.; Limpach, L., Syntheses of quinoline-derivatives by means of ethyl acetoacetate. γ -Hydroxyquinaldine. *Ber. Dtsch. Chem. Ges.* **1887**, *20*, 944-59.
111. Doebner, O.; von Miller, W., A homologue of quinoline. *Ber. Dtsch. Chem. Ges.* **1881**, *14*, 2812-7.

112. Friedlaender, P.; Gohring, C. F., Preparation of substituted quinolines. *Ber. Dtsch. Chem. Ges.* **1883**, *16*, 1833-9.
113. Willumstad, T. P.; Boudreau, P. D.; Danheiser, R. L., Synthesis of Highly Substituted Quinolines via a Tandem Ynamide Benzannulation/Iodocyclization Strategy. *J. Org. Chem.* **2015**, *80* (23), 11794-11805.
114. Huang, Q.; Hunter, J. A.; Larock, R. C., Synthesis of Substituted Isoquinolines by Electrophilic Cyclization of Iminoalkynes. *J. Org. Chem.* **2002**, *67* (10), 3437-3444.
115. Wu, K.; Huang, Z.; Liu, C.; Zhang, H.; Lei, A., Aerobic C–N bond activation: a simple strategy to construct pyridines and quinolines. *Chem. Commun.* **2015**, *51* (12), 2286-2289.
116. Li, Y.; Zhou, X.; Wu, Z.; Cao, J.; Ma, C.; He, Y.; Huang, G., Metal free synthesis of 2,4-diarylquinoline derivatives with enamides and imines. *RSC Adv.* **2015**, *5* (107), 88214-88217.
117. Yu, Z.-H.; Zheng, H.-F.; Yuan, W.; Tang, Z.-L.; Zhang, A.-D.; Shi, D.-Q., An unexpected one-pot synthesis of multi-substituted quinolines via a cascade reaction of Michael/Staudinger/aza-Wittig/aromatization of ortho-azido- β -nitro-styrenes with various carbonyl compounds. *Tetrahedron* **2013**, *69* (38), 8137-8141.
118. Jentsch, N. G.; Hume, J. D.; Crull, E. B.; Beauti, S. M.; Pham, A. H.; Pigza, J. A.; Kessler, J. J.; Donahue, M. G., Quinolines from the cyclocondensation of isatoic anhydride with ethyl acetoacetate: preparation of ethyl 4-hydroxy-2-methylquinoline-3-carboxylate and derivatives. *Beilstein J. Org. Chem.* **2018**, *14*, 2529-2536.
119. Fandrick, K. R.; Li, W.; Zhang, Y.; Tang, W.; Gao, J.; Rodriguez, S.; Patel, N. D.; Reeves, D. C.; Wu, J. P.; Sanyal, S.; Gonnella, N.; Qu, B.; Haddad, N.; Lorenz, J. C.; Sidhu, K.; Wang, J.; Ma, S.; Grinberg, N.; Lee, H.; Tsantrizos, Y.; Poupart, M. A.; Busacca, C. A.; Yee, N. K.; Lu, B. Z.; Senanayake, C. H., Concise and Practical Asymmetric Synthesis of a Challenging Atropisomeric HIV Integrase Inhibitor. *Angew. Chem. Int. Ed.* **2015**, *54* (24), 7144-7148.
120. Garcia, M. B.; Grilli, S.; Lunazzi, L.; Mazzanti, A.; Orelli, L. R., Conformational Studies by Dynamic NMR. 84.1 Structure, Conformation, and Stereodynamics of the Atropisomers of N-Aryl-tetrahydropyrimidines. *J. Org. Chem.* **2001**, *66* (20), 6679-6684.
121. Pretsch, E. B., P.; Badertscher, M., *Structure Determination of Organic Compounds*. 4th ed.; Springer: 2009; p 433.
122. Kessler, J. J.; Sharma, A.; Kvaratskhelia, M., Methods for the Analyses of Inhibitor-Induced Aberrant Multimerization of HIV-1 Integrase. *Methods Mol. Biol.* **2016**, *1354* (HIV Protocols), 149-164.
123. Kessler, J. J.; Li, M.; Ignatov, M.; Shkriabai, N.; Eidahl, J. O.; Feng, L.; Musier-Forsyth, K.; Craigie, R.; Kvaratskhelia, M., FRET analysis reveals distinct conformations of IN tetramers in the presence of viral DNA or LEDGF/p75. *Nucleic Acids Res.* **2011**, *39* (20), 9009-9022.
124. Imai, Y. N.; Inoue, Y.; Nakanishi, I.; Kitaura, K., Cl– π interactions in protein–ligand complexes. *Protein Sci.* **2008**, *17* (7), 1129-1137.
125. Jentsch, N. G.; Hart, A. P.; Hume, J. D.; Sun, J.; McNeely, K. A.; Lama, C.; Pigza, J. A.; Donahue, M. G.; Kessler, J. J., Synthesis and Evaluation of Aryl Quinolines as HIV-1 Integrase Multimerization Inhibitors. *ACS Med. Chem. Lett.* **2018**, *9* (10), 1007-1012.

126. Jentsch, N. G. Synthetic and Theoretical Studies for Cyclization Reactions to Form C-C and C-N Bonds. Dissertation, University of Southern Mississippi, 2018.
127. Wang, A.; Li, J.; Zhang, T., Heterogeneous single-atom catalysis. *Nat Rev. Chem.* **2018**, 2 (6), 65-81.
128. Munnik, P.; de Jongh, P. E.; de Jong, K. P., Recent Developments in the Synthesis of Supported Catalysts. *Chem. Rev.* **2015**, 115 (14), 6687-6718.
129. Liu, L.; Corma, A., Metal Catalysts for Heterogeneous Catalysis: From Single Atoms to Nanoclusters and Nanoparticles. *Chem. Rev.* **2018**, 118 (10), 4981-5079.
130. Krische, M. J., Asymmetric Organocatalysis. From Biomimetic Concepts to Applications in Asymmetric Synthesis. By Albrecht Berkessel and Harald Gröger. *Angew. Chem. Int. Ed* **2005**, 44 (28), 4285-4286.
131. MacMillan, D. W. C., The advent and development of organocatalysis. *Nature* **2008**, 455, 304.
132. Sigman, M. S.; Jacobsen, E. N., Schiff Base Catalysts for the Asymmetric Strecker Reaction Identified and Optimized from Parallel Synthetic Libraries. *J. Am. Chem. Soc.* **1998**, 120 (19), 4901-4902.
133. Wenzel, A. G.; Jacobsen, E. N., Asymmetric Catalytic Mannich Reactions Catalyzed by Urea Derivatives: Enantioselective Synthesis of β -Aryl- β -Amino Acids. *J. Am. Chem. Soc.* **2002**, 124 (44), 12964-12965.
134. Liao, Y.-H.; Chen, W.-B.; Wu, Z.-J.; Du, X.-L.; Cun, L.-F.; Zhang, X.-M.; Yuan, W.-C., Organocatalytic Asymmetric Michael Addition of Pyrazolin-5-ones to Nitroolefins with Bifunctional Thiourea: Stereocontrolled Construction of Contiguous Quaternary and Tertiary Stereocenters. *Adv. Synth. & Catal.* **2010**, 352 (5), 827-832.
135. Li, F.; Sun, L.; Teng, Y.; Yu, P.; Zhao, J. C.-G.; Ma, J.-A., Highly Diastereo- and Enantioselective Organocatalytic One-Pot Sequential 1,4-Addition/De-aromative-Fluorination Transformation. *Chem. Eur. J.* **2012**, 18 (45), 14255-14260.
136. Rombola, M.; Sumaria, C. S.; Montgomery, T. D.; Rawal, V. H., Development of Chiral, Bifunctional Thiosquaramides: Enantioselective Michael Additions of Barbituric Acids to Nitroalkenes. *J. Am. Chem. Soc.* **2017**, 139 (15), 5297-5300.
137. Otevrel, J.; Bobal, P., Diamine-Tethered Bis(thiourea) Organocatalyst for Asymmetric Henry Reaction. *J. Org. Chem.* **2017**, 82 (16), 8342-8358.
138. Reisman, S. E.; Doyle, A. G.; Jacobsen, E. N., Enantioselective Thiourea-Catalyzed Additions to Oxocarbenium Ions. *J. Am. Chem. Soc.* **2008**, 130 (23), 7198-7199.
139. Malerich, J. P.; Hagihara, K.; Rawal, V. H., Chiral Squaramide Derivatives are Excellent Hydrogen Bond Donor Catalysts. *J. Am. Chem. Soc.* **2008**, 130 (44), 14416-14417.
140. Konishi, H.; Lam, T. Y.; Malerich, J. P.; Rawal, V. H., Enantioselective α -Amination of 1,3-Dicarbonyl Compounds Using Squaramide Derivatives as Hydrogen Bonding Catalysts. *Org. Lett.* **2010**, 12 (9), 2028-2031.
141. Li, J.-H.; Du, D.-M., Squaramide-catalysed enantioselective Michael addition of pyrazolin-5-ones to nitroalkenes. *Org. Biomol. Chem.* **2013**, 11 (36), 6215-6223.
142. Yang, K. S.; Nibbs, A. E.; Türkmen, Y. E.; Rawal, V. H., Squaramide-Catalyzed Enantioselective Michael Addition of Masked Acyl Cyanides to Substituted Enones. *J. Am. Chem. Soc.* **2013**, 135 (43), 16050-16053.

143. Reddy, R. R.; Gudup, S. S.; Ghorai, P., Organocatalytic, Enantioselective Synthesis of Cyclohexadienone Containing Hindered Spirocyclic Ethers through an Oxidative Dearomatization/Oxa-Michael Addition Sequence. *Angew. Chem. Int. Ed* **2016**, 55 (48), 15115-15119.
144. Hazra, G.; Maity, S.; Bhowmick, S.; Ghorai, P., Organocatalytic, enantioselective synthesis of benzoxaboroles via Wittig/oxa-Michael reaction Cascade of α -formyl boronic acids. *Chem. Sci.* **2017**, 8 (4), 3026-3030.
145. Li, Y.; He, C. Q.; Gao, F.-X.; Li, Z.; Xue, X.-S.; Li, X.; Houk, K. N.; Cheng, J.-P., Design and Applications of N-tert-Butyl Sulfinyl Squaramide Catalysts. *Org. Lett.* **2017**, 19 (7), 1926-1929.
146. Qian, Y.; Ma, G.; Lv, A.; Zhu, H.-L.; Zhao, J.; Rawal, V. H., Squaramide-catalyzed enantioselective Friedel–Crafts reaction of indoles with imines. *Chem. Commun.* **2010**, 46 (17), 3004-3006.
147. Song, H.-L.; Yuan, K.; Wu, X.-Y., Chiral phosphine-squaramides as enantioselective catalysts for the intramolecular Morita–Baylis–Hillman reaction. *Chem. Commun.* **2011**, 47 (3), 1012-1014.
148. Hamza, A.; Schubert, G.; Soos, T.; Papai, I., Theoretical studies on the bifunctionality of chiral thiourea-based organocatalysts: competing routes to C-C bond formation. *J. Am. Chem. Soc.* **2006**, 128 (40), 13151-60.
149. Ni, X.; Li, X.; Wang, Z.; Cheng, J.-P., Squaramide Equilibrium Acidities in DMSO. *Org. Lett.* **2014**, 16 (6), 1786-1789.
150. Jakab, G.; Tancon, C.; Zhang, Z.; Lippert, K. M.; Schreiner, P. R., (Thio)urea Organocatalyst Equilibrium Acidities in DMSO. *Org. Lett.* **2012**, 14 (7), 1724-1727.
151. Andrés, J. M.; Losada, J.; Maestro, A.; Rodríguez-Ferrer, P.; Pedrosa, R., Supported and Unsupported Chiral Squaramides as Organocatalysts for Stereoselective Michael Additions: Synthesis of Enantiopure Chromenes and Spirochromanes. *J. Org. Chem.* **2017**, 82 (16), 8444-8454.
152. Zhu, Y.; Malerich, J. P.; Rawal, V. H., Squaramide-Catalyzed Enantioselective Michael Addition of Diphenyl Phosphite to Nitroalkenes. *Angew. Chem. Int. Ed.* **2010**, 49 (1), 153-156.
153. Wang, H.; Wang, Y.; Song, H.; Zhou, Z.; Tang, C., Bifunctional Squaramide-Catalyzed One-Pot Sequential Michael Addition/Dearomative Bromination: Convenient Access to Optically Active Brominated Pyrazol-5(4H)-ones with Adjacent Quaternary and Tertiary Stereocenters. *Eur. J. Org. Chem.* **2013**, 2013 (22), 4844-4851.
154. Yang, K. S.; Rawal, V. H., Synthesis of α -Amino Acid Derivatives and Peptides via Enantioselective Addition of Masked Acyl Cyanides to Imines. *J. Am. Chem. Soc.* **2014**, 136 (46), 16148-16151.
155. Zhao, K.; Zhi, Y.; Wang, A.; Enders, D., Synthesis of Malononitrile-Substituted Diarylmethines via 1,6-Addition of Masked Acyl Cyanides to para-Quinone Methides. *Synthesis* **2018**, 50 (04), 872-880.
156. Worrall, D. E., Nirtostyrene. *Org. Synth.* **1929**, 9 (66), 1.
157. Quan, X.-J.; Ren, Z.-H.; Wang, Y.-Y.; Guan, Z.-H., p-Toluenesulfonic Acid Mediated 1,3-Dipolar Cycloaddition of Nitroolefins with NaN_3 for Synthesis of 4-Aryl-NH-1,2,3-triazoles. *Org. Lett.* **2014**, 16 (21), 5728-5731.

158. Chen, H.; Han, X.; Qin, N.; Wei, L.; Yang, Y.; Rao, L.; Chi, B.; Feng, L.; Ren, Y.; Wan, J., Synthesis and biological evaluation of novel inhibitors against 1,3,8-trihydroxynaphthalene reductase from *Magnaporthe grisea*. *Bioorg. Med. Chem.* **2016**, *24* (6), 1225-1230.
159. Li, X.; Deng, H.; Zhang, B.; Li, J.; Zhang, L.; Luo, S.; Cheng, J.-P., Physical Organic Study of Structure–Activity–Enantioselectivity Relationships in Asymmetric Bifunctional Thiourea Catalysis: Hints for the Design of New Organocatalysts. *Chem. Eur. J.* **2010**, *16* (2), 450-455.
160. Martin, N. J. A.; Cheng, X.; List, B., Organocatalytic Asymmetric Transferhydrogenation of β -Nitroacrylates: Accessing β 2-Amino Acids. *J. Am. Chem. Soc.* **2008**, *130* (42), 13862-13863.
161. Nicewicz, D. A.; Yates, C. M.; Johnson, J. S., Catalytic Asymmetric Acylation of (Silyloxy)nitrile Anions. *Angew. Chem. Int. Ed.* **2004**, *43* (20), 2652-2655.
162. Viswanathan, R.; Prabhakaran, E. N.; Plotkin, M. A.; Johnston, J. N., Free Radical-Mediated Aryl Amination and Its Use in a Convergent [3 + 2] Strategy for Enantioselective Indoline α -Amino Acid Synthesis. *J. Am. Chem. Soc.* **2003**, *125* (1), 163-168.
163. Hume, J. D.; Pigza, J. A., Acetylmalononitrile. *Org. Synth.* **2019**, *manuscript in preparation*.
164. Li, S.; Xiao, T.; Li, D.; Zhang, X., First Iridium-Catalyzed Highly Enantioselective Hydrogenation of β -Nitroacrylates. *Org. Lett.* **2015**, *17* (15), 3782-3785.
165. Ram, S.; Ehrenkaufer, R. E., A Facile Synthesis of α -Amino Esters via Reduction of α -Nitro Esters Using Ammonium Formate as a Catalytic Hydrogen Transfer Agent. *Synthesis* **1986**, (02), 133-135.
-